UNIVERZITA KARLOVA V PRAZE

Přírodovědecká fakulta

Studijní program: Biologie

Studijní obor: Buněčná a vývojová biologie

Bc. Ondřej Vaňátko

Identification of changes in membrane properties of astrocytes in a mouse model of amyotrophic lateral sclerosis

Identifikace změn membránových vlastností astrocytů u myšího modelu amyotrofické laterální sklerózy

Diplomová práce

Vedoucí diplomové práce: Mgr. Jana Turečková, Ph.D.

Praha, 2020

Prohlášení:

Prohlašuji, že jsem závěrečnou práci zpracoval samostatně a že jsem uvedl všechny použité informační zdroje a literaturu. Tato práce ani její podstatná část nebyla předložena k získání jiného nebo stejného akademického titulu.

V Praze, 10. srpna 2020

Podpis:

Poděkování

Rád bych poděkoval mojí školitelce Mgr. Janě Turečkové, Ph.D. za odborné vedení při vypracování diplomové práce, trpělivost, připomínky, cenné rady a vždy pozitivní přístup. Dále bych chtěl poděkovat Ing. Miroslavě Anděrové, CSc. za její odborné rady a připomínky a také všem členům Laboratoře buněčné neurofyziologie za jejich cenné rady, milý kolektiv a příjemné pracovní prostředí. Jmenovitě bych chtěl poděkovat našim laborantkám Markétě Hemerové a Heleně Pavlíkové za pomoc s genotypizací a imunohistochemickými experimenty. Velký dík take patří mé rodině a přátelům za podporu a motivaci během studia.

Abstract

Amyotrophic lateral sclerosis (ALS) is a progressive neurological disorder of the central nervous system characterized by loss of motor neurons and voluntary muscle degeneration. Astrocytes play a major role in regulation of the disease onset and progression due to their intimate association with neurons. Regulation of ionic homeostasis is one of their key functions and its failure has been linked to several neurological diseases. The aim of this thesis was to explore differences in membrane properties of astrocytes in ALS. To fulfill this aim, a double transgenic mouse strain with ALS-like phenotype and a specific expression of enhanced green fluorescent protein in astrocytes was generated. To phenotype this strain, two sensorimotor tests, wire grid hang test and rotarod test, were conducted. Immunohistochemistry was used to characterize the strain on a cellular level and to explore changes of specific ion channels. Functional properties of astrocytes were explored using the patch clamp technique. The double transgenic strain has the characteristic ALS-like phenotype and is comparable to the original strain with differences in symptom onset and progression between models and sexes. On the cellular level, there are characteristic ALS features, specifically loss of motor neurons and astrogliosis. Mutant cells have higher input resistance and lower membrane capacitance compared to controls, but we observed no changes in membrane potential. Mutants have lower incidence of inwardly rectifying K^+ currents and higher amplitude of delayed outwardly rectifying K^+ currents compared to controls. We also observed decreased immunostaining of Kir4.1 channel subunit in the brain of mutant mice compared to controls.

Key words: amyotrophic lateral sclerosis; astrocytes; membrane properties; electrophysiology; patch clamp; immunohistochemistry; wire grid hang; rotarod

Abstrakt

Amyotrofická laterální skleróza (ALS) je progresivní neurodegenerativní onemocnění nervové soustavy. Toto onemocnění je charakteristické ztrátou motorických neuronů a odumíráním kosterního svalstva. Astrocyty hrají roli v regulaci nástupu a progresi onemocnění díky jejich asociaci s neurony. Jednou z klíčových funkcí astrocytů je regulace iontové homeostázy. Deregulace tohoto procesu je spojená s řadou neurologických onemocnění. Cílem této práce bylo prozkoumat rozdíly v membránových vlastnostech astrocytů v ALS. Za tímto účelem jsme vygenerovali dvojitě-transgenní myší model s fenotypem podobným průběhu ALS a specifickou expresí zeleného fluorescenčního proteinu v astrocytech. K charakterizaci fenotypu tohoto modelu jsme použili dva sensorimotorické testy: wire grid hang test a rotarod test. Pomocí imunohistochemických metod jsme dále charakterizovali tento model na buněčné úrovni a prozkoumali expresi konkrétního iontového kanálu. Elektrofyziologické vlastnosti astrocytů jsme charakterizovali pomocí metody terčíkového zámku. Námi vygenerovaný dvojitě-transgenní model má charakteristický ALS fenotyp na úrovni celého organismu a je srovnatelný s původním ALS modelem, nicméně s rozdíly v nástupu a průběhu onemocnění. Tento model má charakteristický ALS fenotyp také na buněčné úrovni, kde dochází ke ztrátě motorických neuronů a rozvoji astrogliózy. Mutantní astrocyty mají vyšší vstupní odpor a nižší membránovou kapacitanci než kontrolní astrocyty, ale neliší se v membránovém potenciálu. Mutantní astrocyty mají nižší incidenci dovnitř usměrněných K^+ proudů a vyšší amplitudu opožděných vně usměrněných K^+ proudů v porovnání s kontrolními astrocyty. Také jsme pozorovali redukci v barvení kanálové podjednotky Kir4.1 v mozku mutantních myší v porovnání s kontrolami.

Klíčová slova: amyotrofická laterální skleróza; astrocyty; membránové vlastnosti; elektrofyziologie; metoda terčíkového zámku; imunohistochemie; wire grid hang; rotarod

Table of contents

Abbreviations

aCSF	artificial cerebrospinal fluid
ALDH1L1	aldehyde dehydrogenase 1L1
ALS	amyotrophic lateral sclerosis
ATP	adenosine triphosphate
AQP4	aquaporin 4
Best1	bestrophin1
CK1δ	casein kinase 1 delta
ClC-2/4/5	chloride channel protein 2/4/5
CNS	central nervous system
CTRL	control
Cx	connexin
C9ORF72	chromosome 9 open reading frame 72
DAPI	4',6-diamidino-2-phenylindole
DNA	2'-deoxyribonucleic acid
EAAT1/2	excitatory amino acid transporter 1/2
E_k	equilibrium potential
ER	endoplasmic reticulum
fALS	familial amyotrophic lateral sclerosis
FUS	fused in sarcoma
GABA	γ-aminobutyric acid
GEF	guanine nucleotide exchange factor
GFAP	glial fibrillary acidic protein
GLAST	glutamate aspartate transporter
GLT-1	glutamate transporter 1
HCN	hyperpolarization-activated cyclic nucleotide-gated channels
ICS	intracellular recording solution
$InsP_3R$	inositol 1,4,5-trisphosphate receptor
KCC1	K^+/Cl^- cotransporter 1
K_A	fast activating and inactivating current or A-type K^+ current
K_{DR}	delayed outwardly rectifying K^+ current
K_{IR}	inwardly rectifying K^+ current
Kir	inwardly rectifying K^+ channel

K_v	voltage-gated K^+ channel
K_{2P}	two-pore domain K^+ channel
MCT1	monocarboxylate transporter 1
mSOD1	mutated superoxide dismutase 1
NBC	sodium-bicarbonate cotransporter
NDRG2	N-myc downstream-regulated gene 2
NeuN	neuronal nuclei
NHE-1	sodium-proton antiporter 1
NKCC1	$Na^+/K^+/2Cl^-$ cotransporter 1
OPC	oligodendrocyte precursor cell
PBS	phosphate-buffered saline
PCR	polymerase chain reaction
PFA	paraformaldehyde
PTB	pentobarbital
P-loop	pore loop
RMP	resting membrane potential
RNA	ribonucleic acid
ROS	reactive oxygen species
RyR	ryanodine receptor channel
sALS	sporadic amyotrophic lateral sclerosis
SOD1	superoxide dismutase 1
S100β	S100 calcium-binding protein β
TDP-43	transactive response DNA-binding protein 43
TALK	alkaline-sensitive K^+ channel
TASK	acid-sensitive K^+ channel
THIK	halothane-inhibited K^+ channel
TREK	lipid-sensitive mechano-gated K^+ channel
TRESK	fatty acid inhibited calcium activated K^+ channel
TRP	transient potential receptor channel
TWIK	weak inwardly rectifying K^+ channel
VRAC	volume-regulated anion channel

1 Introduction

Amyotrophic lateral sclerosis (ALS) is a progressive neurological disorder of the central nervous system (CNS) characterized by the loss of motor neurons. Research focus in the last three decades has shifted from neurons to glial cells. Being the most abundant glial cell type in the CNS, astrocytes perform variety of different functions. These include regulation of extracellular ionic homeostasis and clearance of excessive potassium from the synaptic cleft. The goal of this thesis is to explore the changes in electrophysiological properties of astrocytes in the pathology of amyotrophic lateral sclerosis.

2 Amyotrophic lateral sclerosis

Amyotrophic lateral sclerosis was first described by Jean-Martin Charcot in 1869 (hence the original name for ALS – Charcot's disease). ALS is also known as Lou Gehrig's disease (named after Henry Louis Gehrig, a professional American baseball player who died to ALS in 1941) or Motor Neuron Disease. However, the term "motor neuron diseases" also stands for a group of neurodegenerative diseases of which amyotrophic lateral sclerosis is the most common one. Hallmark of ALS is the loss of both upper and lower motor neurons in the brain cortex, brain stem and spinal cord. Loss of motor neurons results in skeletal muscle denervation and degeneration. This eventually leads to death due to failure of respiratory muscles. In majority of cases, life expectancy varies from 3 to 5 years after disease onset.

ALS is usually classified as sporadic (sALS) or familial (fALS). About 10 % of individuals affected by ALS have at least one family member diagnosed with ALS and are defined as having familial ALS. Sporadic form occurs without a family history and accounts for about 90 % of all ALS cases. However, up 10 % of sALS cases are linked to a mutation of specific gene and/or have a genetic background (reviewed by Chen et al. 2013).

Global incidence of ALS is estimated to be between 1-2 people per 100 000, while the prevalence of ALS is about 5 people per 100 000, however these numbers vary slightly between sexes, different populations, nationalities and ages. Men are more likely to develop ALS. Risk of ALS development increases with age, most cases are diagnosed between the ages 50 and 70 (reviewed by Longinetti and Fang 2019). Though ALS

is relatively rare in human population, it is a disease with fast progression and 100% mortality.

Though described more than 150 years ago, treatment options are still very limited and are mostly based on symptom management, respiratory support and increasing the quality of life. Only two drugs are currently approved for the treatment of ALS: Riluzole and Edaravone. Riluzole was believed to act on glutamate receptors (Doble 1996), however recent study has described its role in regulation of trans-active response DNA-binding protein 43 (TDP-43) via inhibition of casein kinase 1 delta (CK1δ; Bissaro et al. 2018). Edaravone is believed to be an antioxidant (Yamamoto et al. 1996; Pérez-González and Galano 2011; Jami et al. 2015), though its mechanism of function is not fully understood. However, these drugs provide only mild benefits in terms of increasing life expectancy. Therefore, ALS patients mostly rely on supportive care and symptomatic treatment (reviewed by Ng et al. 2017).

Research directions mostly comprise clinical trials of new disease-modifying agents. In the past, vast majority of the tested compounds were shown not to affect the disease progression. In the last years however, several compounds have been shown to have clinical efficacy and it is possible that some of these drugs will be approved for treatment of ALS in the near future (reviewed by Filipi et al. 2020). Other therapeutic approach are cell-based therapies. Most of the trials again suffered from being underpowered and failed to show the clinical efficacy (reviewed by Goutman et al. 2019) with the exception of NurOwn, a mesenchymal stem cell therapy (Petrou et al. 2016; Gothelf et al. 2017) which is currently being evaluated in a large-scale Phase III trial (trial ID#: NCT03280056). More recently, several trials explored and discovered possible benefits of gene therapies in the treatment of fALS, including Tofersen (T. M. Miller et al. 2013), miQure (Martier et al. 2019) and VM202 (Sufit et al. 2017).

2.1 Genetics

Mechanisms responsible for causing the sporadic form of ALS have not yet been identified, however multiple risk factors have been suggested, including smoking, military service and exposure to heavy metals (reviewed by Nowicka et al. 2019). Variety of genetic factors have been shown to directly cause or contribute to ALS onset and progression. Though a lot of genes associated with ALS were discovered, the mechanisms which ultimately lead to motor neuron degeneration remain elusive. Mechanisms and

pathways suggested to be dysregulated in ALS include glutamate excitotoxicity, protein misfolding and aggregation, mitochondrial dysfunction, oxidative stress, cellular transport, activation of microglia and astrocytes, neuroinflammation and disruption in axonal and cytoskeletal dynamics. Recently, research focus shifted towards alterations in genes involved in RNA metabolism, such as *TARDBP* and *FUS*, which are often mutated in ALS (reviewed by Mejzini et al. 2019). Genes most frequently associated with ALS are presented in **Table 1**.

In humans, the gene that encodes for a protein superoxide dismutase 1 is *SOD1*. Mutations in *SOD1* were the first directly associated with ALS (Rosen et al. 1993) and are responsible for approximately 20 % of familial ALS cases. SOD1 can be found in cytoplasm and intermembrane space of the mitochondria. It catalyses the conversion of dangerous superoxide radical into oxygen and hydrogen peroxide and thus reduces the amount of reactive oxygen species in the cell. Though it was initially believed that the ALS phenotype is caused by the loss of enzymatic activity, later studies have shown that the SOD1 toxicity is rather gain-of-function and is independent of the dismutase activity (Bruijn et al. 1998). Still, *SOD1* mutations result in increased oxidative stress and mitochondrial dysfunction. The precise mechanism through which mutant SOD1 (mSOD1) promotes motor neuron degeneration is still unknown. Mutations in this protein result in improper folding, which propagates in a prion-like manner, leading to formation of ubiquitinated inclusion bodies in the cytoplasm (Bruijn et al. 1998). Mutated SOD1 induces motor neuron degeneration via non-cell-autonomous pathways, as expression of mSOD1 specifically in motor neurons is not sufficient to cause the disease onset (Yamanaka et al. 2008a). However, mSOD1 induces motor neuron degeneration when specifically expressed in astrocytes (Yamanaka et al. 2008b). In line with these findings, delay in the disease onset and/or progression was observed when the *mSOD1* was selectively downregulated or silenced in astrocytes (L. Wang, Gutmann, and Roos 2011), microglia (Boillée et al. 2006) or oligodendrocytes (S. H. Kang et al. 2013), further supporting the idea of non-cell-mediated toxicity. Mutations in *SOD1* are believed to induce toxicity via various mechanisms, including excitotoxicity, endoplasmic reticulum (ER) stress, increased production of reactive oxygen species (ROS), impaired axonal transport and mitochondrial dysfunction (reviewed by Hayashi, Homma, and Ichijo 2016).

FUS is a gene that encodes for fused in sarcoma protein (FUS), which is a DNA/RNA-binding protein. Mutations in *FUS* are responsible for approximately 5% of fALS cases. FUS protein plays a role in nucleocytoplasmic transport (Zinszner et al. 1997), regulation of gene expression (reviewed by Ratti and Buratti 2016), formation of paraspeckles (Hennig et al. 2015) and DNA damage response (Mastrocola et al. 2013; W. Y. Wang et al. 2013). Mechanism by which FUS promotes ALS in currently unknown. Mutations in *FUS* are associated with translocation of FUS from nucleus to the cytoplasm, which can lead to aberrant aggregation and impaired stress granule function (Vance et al. 2009; 2013). However, there is still debate whether FUS promotes ALS by the loss of its RNA-binding function (Shelkovnikova et al. 2013; Robinson et al. 2015) or by its increased accumulation in the cytoplasm (Scekic-Zahirovic et al. 2016; Sharma et al. 2016).

TARDBP is a gene that encodes for a protein TDP-43, which is a DNA/RNA-binding protein that is localized both in the cytoplasm and the nucleus (Ayala et al. 2008). Mutations in *TARDBP* are responsible for approximately 5 % of familial ALS cases. TDP-43 function shares a lot of similarities with FUS protein. Same as FUS, TDP-43 plays a role in regulation of gene expression (Tollervey et al. 2011; reviewed by Ratti and Buratti 2016) and DNA damage response (Mitra et al. 2019). Expression of TDP-43 is strictly regulated and disruptions in TDP-43 homeostasis lead to various cellular and organism deficits. Knockout of *TARDBP* is lethal both in embryonic development (L. S. Wu et al. 2010) and adult mice (Chiang et al. 2010) and overexpression of TDP-43 leads to neurodegenerative phenotype (Stallings et al. 2010; Xu et al. 2011). Similar to FUS, mutated TDP-43 can also form aggregates in the cytoplasm, as TDP-43 redistribution and ubiquitinated cytoplasmic occlusion are present in familial TARDBP-ALS (T. Arai et al. 2006; Neumann et al. 2006). TDP-43 is also sometimes present in cytoplasmic aggregates in sALS (Takeuchi et al. 2016).

Table 1. The genetics of ALS (*Taylor, Brown and Cleveland* 2017; edited)

Locus	Gene	Protein	Protein function	Mutations	Proportion of ALS	
					Familial	Sporadic
21q22.1	*SOD1*	Cu–Zn superoxide dismutase	Superoxide dismutase	>150	20%	2%
2p13	*DCTN1*	Dynactin subunit 1	Component of dynein motor complex	10	1%	<1%
14q11	*ANG*	Angiogenin	Ribonuclease	>10	<1%	<1%
q36	*TARDBP*	TDP-43	RNA-binding protein	>40	5%	<1%
16p11.2	*FUS*	FUS	RNA-binding protein	>40	5%	<1%
9p13.3	*VCP*	Transitional endoplasmic reticulum ATPase	Ubiquitin segregase	5	1–2%	<1%
10p15-p14	*OPTN*	Optineurin	Autophagy adaptor	1	4%	<1%
9p21-22	*C9orf72*	C9orf72	Possible guanine nucleotide exchange factor	Intronic GGGGCC repeat	25%	10%
Xp11.23-Xp13.1	*UBQLN2*	Ubiquilin 2	Autophagy adaptor	5	<1%	<1%
5q35	*SQSTM1*	Sequestosome 1	Autophagy adaptor	10	<1%	?
17p13.2	*PFN1*	Profilin-1	Actin-binding protein	5	<1%	<1%
12q13.1	*HNRNPA1*	hnRNP A1	RNA-binding protein	3	<1%	<1%
5q31.2	*MATR3*	Matrin 3	RNA-binding protein	4	<1%	<1%
2q36.1	*TUBA4A*	Tubulin α-4A chain	Microtubule subunit	7	<1%	<1%
22q11.23	*CHCHD10*	Coiled-coil-helix-coiled-coil-helix domain-containing protein 10	Mitochondrial protein of unknown function	2	<1%	<1%
12q14.1	*TBK1*	Serine/threonine-protein kinase TBK1	Regulates autophagy and inflammation	10	?	?

C9ORF72 is a gene that encodes for a protein chromosome 9 open reading frame 72 (C9ORF72). Its function was only recently discovered, and it is believed to be a guanine nucleotide exchange factor (GEF), likely having a role in endosomal trafficking (Farg et al. 2014), autophagy (Webster et al. 2016) and regulation of the immune system (Burberry et al. 2016). Unlike mutations in other genes associated with ALS, mutations in *C9ORF72* are intronic expansions of hexanucleotide repeat GGGGCC (Renton et al. 2011). While there are usually only few copies of these expansions in healthy individuals, they appear in orders of hundreds or thousands in ALS patients. Mutated C9ORF72 accumulates in the nucleus in structures called RNA foci, sequestering RNA-binding proteins and generally affect RNA processing. At the same time, non-ATG translation of the repeats results in production of dipeptide chains that form inclusion bodies in the cytoplasm (reviewed by Todd and Petrucelli 2016). Mutations in *C9ORF72* are responsible for approximately 20 % of familial ALS cases and, interestingly, up to 10 % of sporadic ALS cases.

2.2 Animal models

Mice with SOD1-G93A mutation were the first ALS model, in which glycine on position 93 was substituted by alanine (Gurney et al. 1994). This mouse model is the most widely used model for the study of ALS. It is characterized by the 4-fold increase expression of mutant human *SOD1* (*hSOD1*) under the control of human *SOD1* promoter, which induces an ALS-like phenotype similar to that in humans. Mice with this mutation face relatively fast phenotypic progression, with the lifespan of approximately 19 to 23 weeks. Unlike in human ALS cases, hSOD1-G93A in mice always results first in the loss of spinal cord motor neurons. On the phenotype level, this is represented by the paralysis of the hind limbs, while function of the front limbs remains relatively unaffected until later stages (Gurney et al. 1994; Chiu et al. 1995; Wooley et al. 2005).

Besides mouse model carrying SOD1 mutations, many rodent models with variety of mutations in different genes were produced. These represent mostly models with mutations in genes described in chapter 2.1: *FUS*, *TARDBP* and *C9ORF72*. While mouse models are the ones most commonly used in ALS studies, other models also exist, including *Danio rerio*, *Drosophila melanogaster*, *Caenorhabditis elegans* and various cell cultures. Each model has its own advantages and disadvantages (reviewed by Gois et al. 2020).

2.3 Molecular mechanisms

The degeneration and death of motor neurons in the CNS is the hallmark of ALS. Their degeneration results in denervation of skeletal muscle and muscle atrophy, which ultimately leads to death of the patient due to the dysfunction of respiratory muscles. Surprisingly, neurons innervating bowel, bladder and extraocular muscles are usually spared until the late stages of the disease (Nübling et al. 2014; McLoon et al. 2014). Common feature of ALS in humans is the presence of ubiquitinated inclusions in neurons with TDP-43 as the major component (Neumann et al. 2006). Other processes dysregulated in neurons include mitochondrial dysfunction and oxidative stress, endoplasmic reticulum stress, protein misfolding and impaired axonal transport (reviewed by Robberecht and Philips 2013).

On the cellular level, motor neuron degeneration results from disrupted interplay between neurons and glial cells, but specific mechanisms of this process are yet to be elucidated (**Figure 1**). Generally speaking, activation of microglia (microgliosis) leads to activation of astrocytes (astrogliosis) via the production of soluble cellular factors Astrogliosis includes increased proliferation, changes in morphology and altered gene expression profile. Similar to microglia, activated astrocytes can acquire either neurotrophic A2 or cytotoxic A1 phenotype, depending on the activating factors and state of the disease (Liddelow et al. 2017). Loss of oligodendrocytes is accompanied by increased proliferation of oligodendrocyte precursor cells (OPCs), however those appear to be dysfunctional both in terms of myelination and trophic support. As myelinating oligodendrocytes allow saltatory conduction and also provide trophic support for neurons, loss of these functions directly contributes to the motor neuron death (Y. Lee et al. 2012; Toomey and Mitchell 2016; Philips et al. 2013). The reason why ALS does not affect other neuronal subtypes besides motor neurons is unknown.

Though motor neurons are the primary cell type affected in ALS, other cell types unquestionably contribute to the induction and progression of this disease. In last decade, the attention turned towards glia cells, namely astrocytes, as these cells provide numerous homeostatic functions, which are essential for proper neuronal functioning. Their failure in maintaining CNS homeostasis might trigger the disease or contribute to its progression. Evidence for their involvement in ALS came from studies on genetic models, in which the motor neuron-specific expression of mutant genes does not result in loss of motor

neurons (Pramatarova et al. 2001; Lino, Schneider, and Caroni 2002). In addition, astrocytes derived both from mice models and human ALS patients are directly toxic to motor neurons (Nagai et al. 2007; Haidet-Phillips et al. 2011). Activated ALS astrocytes likely induce death of motor neurons by the combined action of several mechanisms. These include altered synaptic function and glutamate uptake (Howland et al. 2002; Pardo et al. 2006; Gibb et al. 2007; Van Damme et al. 2007), impaired trophic support (Ferraiuolo et al. 2011), production of soluble factors directly toxic to neurons (Hensley et al. 2006; Haidet-Phillips et al. 2011) and induction of necroptosis (Re et al. 2014). In addition, activated astrocytes may also directly cause the death of oligodendrocytes (Liddelow et al. 2017), which contributes to motor neuron death.

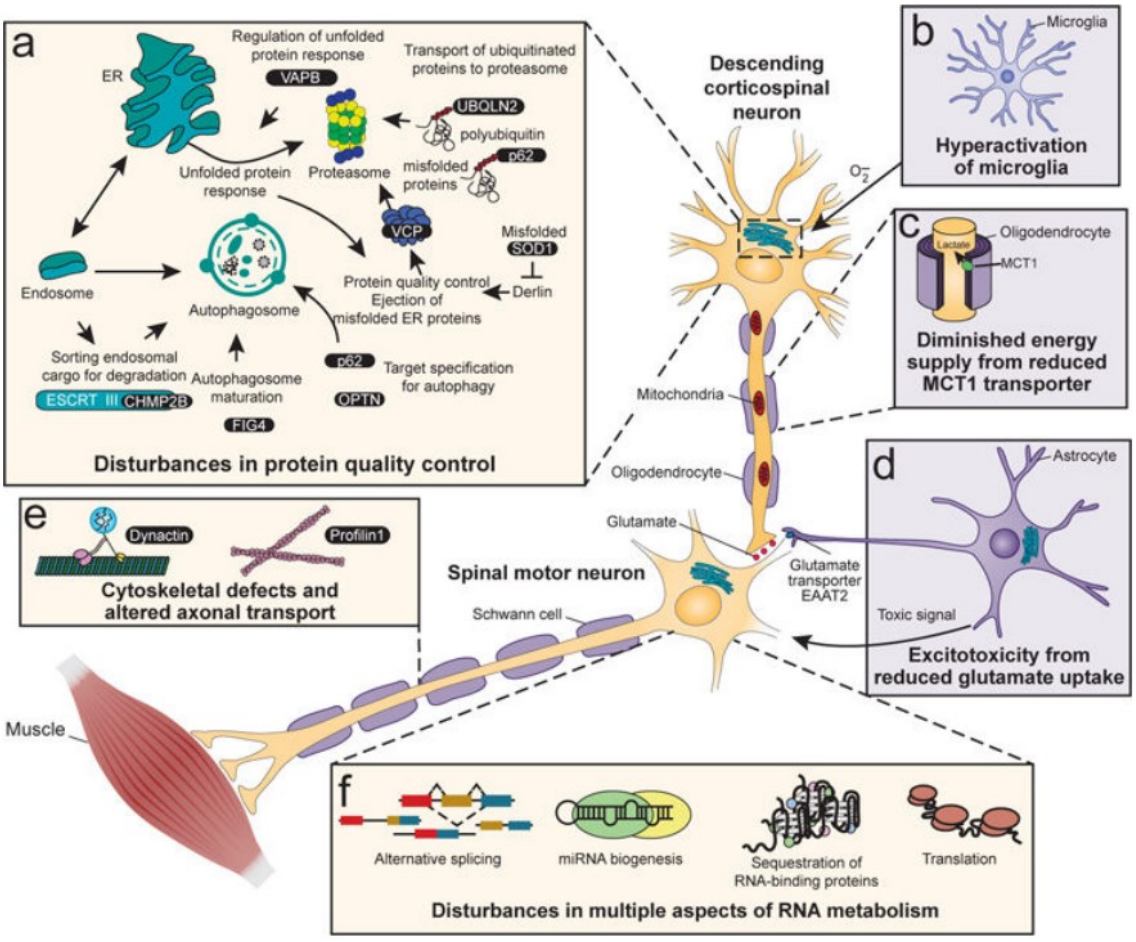

Fig. 1. Schematic representation of the main cellular processes disrupted in ALS. Major processes dysregulated in ALS pathology include disrupted protein quality control (a), activation of microglia (b), loss of trophic support (c), glutamate excitotoxicity (d), cytoskeletal defects (e) and altered RNA metabolism (f)(*Taylor, Brown, and Cleveland* 2017; edited).

3 Astrocytes

Astrocytes are the most abundant glial cell type in the CNS. They are characterized by morphological, molecular, and functional heterogeneity, depending on the location in the CNS. Because astrocytes fulfil various important roles in the CNS, their dysfunction has been linked to various pathological states and neurodegenerative diseases such as stroke, epilepsy, Alzheimer's disease, Huntington's disease, Parkinson's disease or Down's syndrome (reviewed by Pekny et al. 2016; Dossi, Vasile, and Rouach 2018). They are also the primary source of brain tumors (Furnari et al. 2007). As this thesis focuses on ALS-related changes in astrocyte electrophysiology, following chapters will primarily cover functions of astrocytic channels and transporters which underlie astrocyte electrophysiological properties, and will also cover astrocytic functions related to this topic.

3.1 Morphology and structure

Historically, astrocytes have been divided into two main groups based on their distinct morphology: protoplasmic and fibrous astrocytes (R. H. Miller and Raff 1984). Protoplasmic astrocytes are found in the gray matter in high densities and exhibit relatively short and highly branched processes. In healthy brain, protoplasmic astrocytes branches form "domains" that are mutually exclusive with other protoplasmic astrocytes and overlap only in the most distal processes. They always contact at least one capillary with their processes, forming a perivascular endfeet. In mice, their processes can contact tens of thousands of synapses; however this number increases greatly with evolutionary complexity of the organism. In humans, the number of synapses found in a single astrocyte domain is predicted to be up to 2 million synapses (Bushong et al. 2002; Oberheim et al. 2006; Wilhelmsson et al. 2006). Fibrous astrocytes on the other hand are found predominantly in the white matter in relatively low densities and have long, less branched processes. They form several perivascular and/or subpial endfeet and also extend processes to the nodes of Ranvier. Unlike protoplasmic astrocytes, fibrous astrocytes show high degree of overlap (Oberheim et al. 2009). Additionally, specific subtypes of astrocytes can be found in the human brains, like inter-laminar or varicosity projection astrocytes (Oberheim et al. 2009).

Astrocytes are interconnected with each other in a structure called syncytium (Kuffler, Nicholls, and Orkand 1966). In syncytium, astrocytes are functionally coupled

by gap junctions which are formed by hemichannels. Each hemichannel is formed by 2 connexons, while each connexon is a hexamer of connexin proteins. Connexins are predominantly found in astrocyte-astrocyte connections are connexin-30 (Cx30) and connexin-43 (Cx43; J. E. Rash et al. 2001). A feature of hemichannels is their permeability to molecules of to 1 kDa such as water, ions, second messengers, nucleotides, metabolites and possibly RNA (Valiunas et al. 2005). This is important for spatial buffering of K^+ ions and propagation of Ca^{2+} waves. Astrocytes also form hemichannels with oligodendrocytes and ependymal cells (John E. Rash et al. 1997; Kamasawa et al. 2005).

3.2 Astrocyte identification

Astrocytes express various molecules that are typically used for their identification. Most reliable marker for labeling of astrocytes is an enzyme aldehyde dehydrogenase 1L1 (ALDH1L1). This protein is specifically expressed in astrocytes and is present in most of the astrocyte subpopulations (Cahoy et al. 2008). Other widely used markers for identification of astrocytes are N-myc downstream-regulated gene 2 (NDRG2; Flügge et al. 2014), excitatory amino acid transporters 1 and 2 (EAAT1/2; Schmitt et al. 1997; Williams et al. 2005), S100 calcium-binding protein β (S100β; Ogata and Kosaka 2002) and glutamine synthetase (Anlauf and Derouiche 2013). Less often, other markers such as aquaporin 4 (AQP4), Cx30 and Cx43 (Nagy et al. 1999; Erlend A. Nagelhus and Ottersen 2013) are employed. The oldest and the most commonly used marker for astrocyte identification is glial fibrillary acidic protein (GFAP), which has also been used to identify astrocytes in this thesis (**Figure 2**; L. F. Eng et al. 1971).

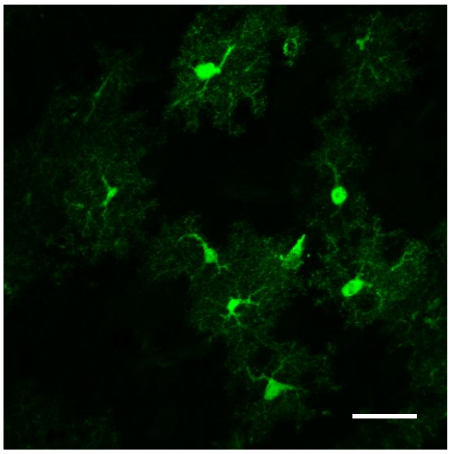

Fig. 2. $GFAP^+$ astrocytes expressing enhanced green fluorescent protein (eGFP); Bar: 30 µm

3.3 Astrocytic functions

Astrocytes are closely associated with neurons, particularly at the synapses. Together with pre- and post-synaptic neuron, astrocytes are part of a structure called tripartite synapse (reviewed by Araque et al. 1999). Here, they are important for integration and modulation of synaptic transmission and maintenance of the functional synapse. Perisynaptic astrocytic processes contain various neurotransmitter receptors, channels and transporters. Synaptic activity leads to activation of astrocytic receptors resulting in intracellular [Na^+] and [Ca^{2+}] increase, which ultimately regulates the function of various effector molecules. Astrocytes are essential for maintenance of synaptic homeostasis, especially the extracellular concentration of neurotransmitters like glutamate, γ-aminobutyric acid (GABA) and adenosine triphosphate (ATP), and K^+ (Barbour, Brew, and Attwell 1988; Rothstein et al. 1996; Erecińska et al. 1996; J. Yang, Li, and Shen 2005).

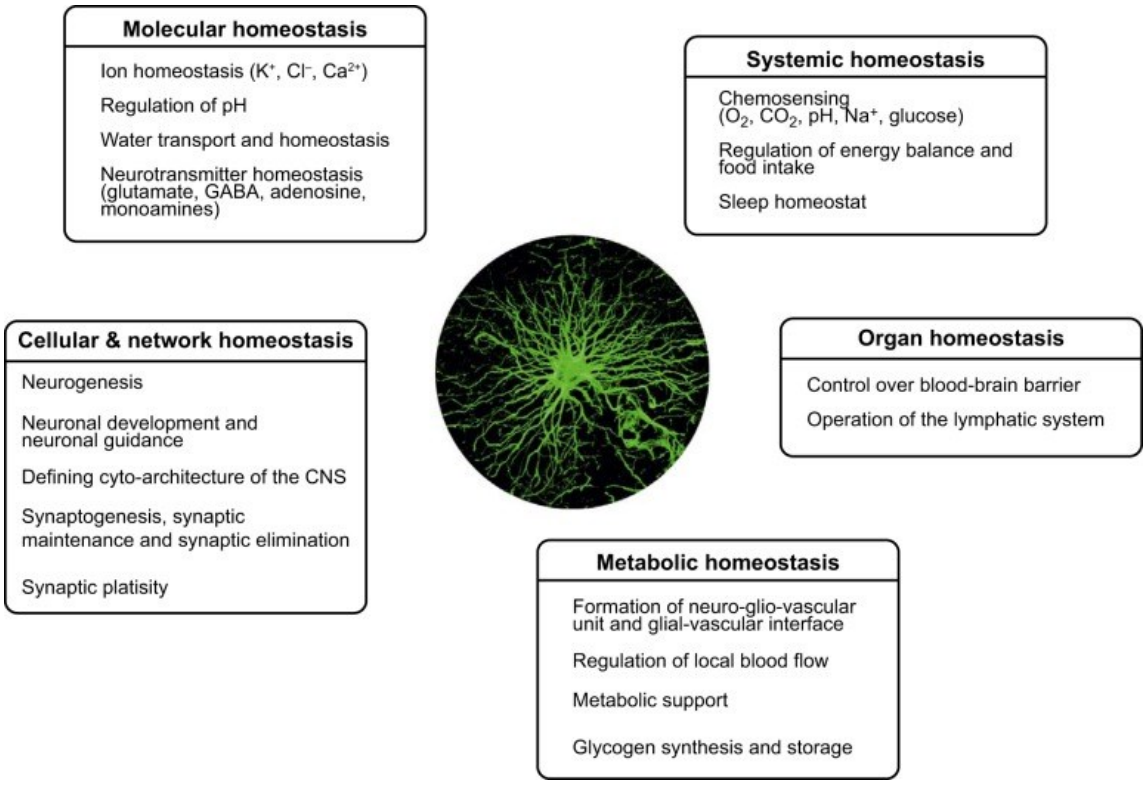

Fig. 3. Overview of astrocyte functions in the healthy CNS (*Verkhratsky and Nedergaard* 2018).

Astrocytes provide essential structural integrity of the nervous system. In developing nervous system, astrocytes are essential for the proper formation of neuronal circuitry, as they are important for neuron migration and guidance of axonal growth (reviewed by Allen and Lyons 2018). Together with endothelial cells and pericytes, astrocytes contribute to formation and function of blood-brain barrier (reviewed by Obermeier, Daneman, and Ransohoff 2013) and play role in regulation of the blood flow as well (Girouard et al. 2010; Marina et al. 2020). After brain injury, astrocyte contribute to the formation of glial scar, which serves to isolate the damaged tissue from the rest of the nervous system. Though it is generally accepted that glial scar impairs axonal regrowth and regeneration (reviewed by Bradbury and Burnside 2019), some studies have shown supportive role of astrocytes in tissue repair (Anderson et al. 2016).

Another important aspect of astrocyte function is nutrition, as they serve as brain glycogen storage (Cataldo and Broadwell 1986). Moreover, astrocytes use monocarboxylate transporter 1 (MCT1) to release lactate which is subsequently taken up by neurons, where it serves as a metabolic substrate; this process is called "neuron-astrocyte lactate shuttle" (Pellerin and Magistretti 1994; Qu et al. 2000). As MCT1 is a lactate/H^+ cotransporter, it also contributes to the decrease of extracellular pH. Finally, astrocytes produce trophic factors essential for the neuron survival and development (Gomes et al. 1999; Dezonne et al. 2013). Overview of astrocyte functions in the CNS is presented in **Figure 3**.

3.3.1 Synaptic homeostasis and maintenance

Glutamate uptake, which is provided by astrocytes is an essential function for maintaining synaptic transmission. Glutamate is taken up from the synaptic cleft by astrocytes via the action of glutamate transporters EAAT1 (glutamate aspartate transporter – GLAST – in mice) and EAAT2 (glutamate transporter 1 – GLT-1 – in mice) (Chaudhry et al. 1995; Lehre et al. 1995). In astrocytes, glutamate is converted to glutamine and transported back to neurons, where it is hydrolyzed to glutamate, as neurons are incapable of *de novo* glutamate synthesis (Yu et al. 1983). This is known as the glutamate-glutamine cycle (reviewed by Bak, Schousboe, and Waagepetersen 2006). Under pathological conditions, insufficient clearing of glutamate from synaptic cleft leads to its accumulation and results in glutamate excitotoxicity. High glutamate

levels overactivate neuronal glutamate receptors, which results in intracellular [Ca^{2+}] elevation and activation of intracellular processes ultimately leading to the neuronal damage or death (Rothstein et al. 1996). Similar to glutamate, astrocyte also participate in GABA-glutamine cycle on inhibitory synapses (reviewed by Bak, Schousboe, and Waagepetersen 2006).

Increased [K^+] in the synaptic cleft leads to more frequent depolarization of the post-synaptic neuron membrane, which interferes with normal signal transmission (reviewed by Kofuji and Newman 2004). Excess K^+ is taken up by astrocytes by the action of several transport systems: Na^+/K^+ ATPase (Kala et al. 2000), inwardly rectifying K^+ channel 4.1 (Kir4.1 channel; Kucheryavykh et al. 2007), K^+/Cl^- cotransporter KCC1 (Ringel and Plesnila 2008) and $Na^+/K^+/2Cl^-$ cotransporter NKCC1 (Yan, Dempsey, and Sun 2001). K^+ is distributed through astrocytic syncytium and subsequently released into the interstitium or perivascular space. This is known as K^+ spatial buffering (**Figure 4)** To maintain electroneutrality during the K^+ transport, these changes are accompanied by the transport of Cl^-. Intracellular [Cl^-] is maintained mostly by NKCC1, which is a transporter that translocates two Cl^- together with one Na^+ and K^+ to the inside of the cell. Importantly, most transport mechanisms are accompanied by the function of water channels called aquaporins. Most notable aquaporin found in astrocytes is AQP4 (E. A. Nagelhus, Mathiisen, and Ottersen 2004). Aquaporins are essential for maintenance of cell volume and osmotic homeostasis (Nielsen et al. 1997). In addition, astrocytes regulate synaptic pH via the function of sodium-proton antiporter 1 (NHE-1; Ma and Haddad 1997) and sodium-bicarbonate cotransporter 1 (NBC1; Deitmer 1989).

Astrocytes are essential for the synaptic maintenance also from the developmental point of view. During ontogenesis, they have been shown to play a role in synaptogenesis (Kucukdereli et al. 2011; Diniz et al. 2012; 2014), synaptic stability (H. Nishida and Okabe 2007) and synaptic pruning (Stevens et al. 2007). Defects in synaptic development connected to astrocyte dysfunction are a feature found in several neurodegenerative diseases such as Rett syndrome or Down syndrome (reviewed by Blanco-Suárez, Caldwell, and Allen 2017).

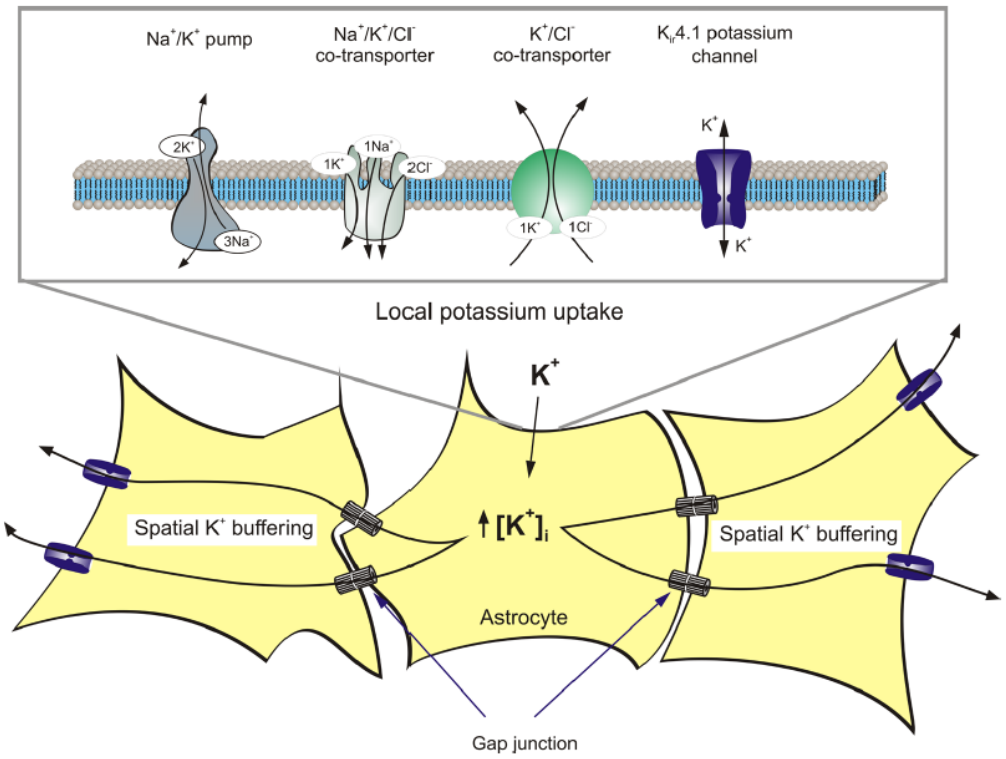

Fig. 4. Schematic representation of K^+ spatial buffering. Extracellular K^+ is taken up from the extracellular space into the astrocyte by the function of several membrane proteins including Na^+/K^+ pump, $Na^+/K^+/2Cl^-$ cotransporter NKCC1, K^+/Cl^- cotransporter KCC1 and Kir4.1 channel. Potassium is then spread through the syncytium via gap junctions and subsequently released into the interstitium. (*Verkhratsky and Parpura* 2015; edited).

3.4 Astrocyte electrophysiology

Astrocytes exhibit specific electrophysiological properties which differ both among and between specific regions of the brain. They are electrically non-excitable cells, as they do not generate action potentials. However, they actively respond to stimulation by changes in intracellular concentration of ions, most notably Na^+ and Ca^{2+}. Concentrations of major ions in the astrocyte cytoplasm are as follows: 120-140 K^+ [mM], 15-20 Na^+ [mM], 50-100 Ca^{2+} [nM], 30-60 Cl^- [mM] and 63 H^+ [nM]. As astrocytes are characterized by large passive K^+ conductance, they mostly show a linear current-voltage (I-V) relationship.

It is universally accepted that astrocytes maintain highly negative resting membrane potential (RMP) approximately between -80 and -90 mV, which is close to the equilibrium potential (E_k) predicted by the Goldman-Hodgkin-Katz equation for K^+ (E_k = -96 mV). However, past studies have reported inconsistent results regarding this topic. In earlier studies, astrocytic RMP varied between -25 and -90 mV. These studies

also showed bimodal distribution with peaks around -68 and -42 mV (McKhann, D'Ambrosio, and Janigro 1997). Other studies had reported relatively uniform highly negative astrocytic RMP varying between -75 and -100 mV (Chvátal et al. 1995; 1997; Adermark and Lovinger 2008; Mishima and Hirase 2010). Though this fact may possibly reflect astrocyte heterogeneity across the CNS, it is likely that it rather reflects different methodological approaches.

Based on literature, astrocytes exhibit two types of pattern: a complex pattern typical for immature cells and a passive current pattern which is characteristic for mature astrocytes (Schools, Zhou, and Kimelberg 2006; M. Zhou, Schools, and Kimelberg 2006). Complex current pattern is characterized by the presence of fast activating and inactivating current (A-type K^+ current, K_A) and delayed outwardly rectifying K^+ (K_{DR}) currents, inwardly rectifying K^+ (K_{IR}) current as well as fast activating tetrodoxin-sensitive Na^+ currents. On the other hand, passive current pattern is represented mostly by time- and voltage-independent K^+ currents together with small K_{IR} currents. Presence of these two types differs both among and within the different brain structures. In addition, incidence of these currents in astrocytes changes both during the prenatal and postnatal development (Nixdorf-Bergweiler, Albrecht, and Heinemann 1994; M. Zhou, Schools, and Kimelberg 2006).

3.4.1 Astrocyte potassium channels

Potassium channels are the most diverse and most widely distributed family of ion channels. They are the most abundant channels found in astrocytes (**Figure 5**). Three major classes will be discussed in greater detail: inwardly rectifying K^+ channels, two-pore domain K^+ channels and voltage gated K^+ channels.

3.4.1.1 Inwardly Rectifying K^+ channels

Potassium inwardly rectifying (Kir) channels are a group of channels which are characterized by their ability to conduct K^+ ions better in the inward direction than in the outward direction. Their primary function is maintaining the cell RMP close to E_k for K^+. This is possible due to the fact that Kir channels have a high probability of staying open at negative transmembrane potentials. Kir channels have an important role in various tissues such as brain, heart, kidney and retina. In electrically excitable cells they can modulate cell excitability and its ability of potential repolarization (reviewed by Hibino et al. 2010).

There are currently 15 known members of the Kir family members which are divided into 7 subfamilies (Kir1.x – Kir7.x). These subfamilies can by further divided in four groups: classical K^+ channels (Kir2.x), G-protein-gated K^+ channels (Kir3.x), ATP-sensitive K^+ channels (Kir6.x) and K^+ transport channels (Kir1.x, Kir4.x, Kir5.x, Kir7.x). In addition, Kir channels can be divided into weak (Kir1.x, Kir6.x), intermediate (Kir4.x) or strong (Kir2.x, Kir3.x) rectifying channels, based on the channel sensitivity to blocking by intracellular Mg^{2+}. In the membrane they exist as homotetramers or heterotetramers. Heterotetramerization generally occurs between members of the same subfamily, however exceptions exist, such as assembly of Kir4.1/4.2 with Kir5.1 (Tanemoto et al. 2000; Pessia et al. 2001; Hibino et al. 2004). Each subunit consists of two transmembrane segments M1 and M2, a pore loop (P-loop), an N-terminal cytoplasmic domain and a C-terminal cytoplasmic domain (M. Nishida and MacKinnon 2002; Kuo et al. 2003). Similar to other K^+ channels, the P-loop functions as an ion selectivity filter (Heginbotham et al. 1994). However, in contrast to voltage gated K^+ channels, Kir channels lack the voltage-sensing transmembrane segments.

In astrocytes, the most predominant form of inwardly rectifying K^+ channels are channels formed of Kir4.1 and Kir5.1 subunits (Li, Head, and Timpe 2001; Olsen et al. 2006; Lichter-Konecki et al. 2008). These can occur either as Kir4.1 homomers or Kir4.1/5.1 heteromers. These two form are distinguishable by their different sensitivity to intracellular pH and rectification strength (Cui et al. 2001). In astrocytes, Kir4.1/5.1 heteromers are predominantly found in the endfeet surrounding blood vessels, while both heteromers and homomers are present on the synaptic processes. However, both forms are differentially expressed in different regions of the brain (Higashi et al. 2001; Hibino et al. 2004). Other Kir channels expressed by some astrocytes include Kir2.1, 2.2 and 2.3 (Murata et al. 2016), and Kir6.2 (Cahoy et al. 2008). Recently, an expression of Kir7.1 subunit in astrocytes was reported (Papanikolaou, Lewis, and Butt 2019). In astrocytes, Kir channels are functionally co-localized in noncaveolar detergent resistant microdomains with water channels AQP4, as these are also highly expressed in astrocytes (E. A. Nagelhus, Mathiisen, and Ottersen 2004; Hibino and Kurachi 2007). Moreover, Kir4.1 can possibly be functionally coupled with glutamate transporters EAAT1 and EAAT2, as knockdown and knockout of *KCNJ10* (Kir4.1 gene) resulted in impaired glutamate uptake (Djukic et al. 2007; Kucheryavykh et al. 2007).

3.4.1.2 Two-pore domain K^+ channels

Two-pore domain K^+ (K_{2P}) channels are the most recently discovered group of K^+ channels responsible for the generation of background leak K^+ currents (Ketchum et al. 1995). Hallmark of K_{2P} channels is the presence of two pore-forming domains called P-loops. Structurally, K_{2P} channel subunits forms dimers in the membrane (in contrast to Kir channels forming tetramers), while each subunit consists of four transmembrane domains, two P-loops, smaller N-terminal and larger C-terminal intracellular domains (Brohawn, Del Mármol, and MacKinnon 2012; A. N. Miller and Long 2012). In humans, there are currently 15 known members of this family of channels which can be divided into 6 functional subfamilies: weak inwardly rectifying (TWIK) channels, acid sensitive (TASK) channels, lipid-sensitive mechano-gated (TREK) channels, halothane inhibited (THIK) channels, alkaline sensitive (TALK) channels and the fatty acid inhibited calcium activated (TRESK) channel. K2P subunits form homodimers in the cell membrane, however they have been observed to form heterodimers as well, like TWIK-1/TASK-1 and TWIK-1/TASK-3 dimers in cerebellum neurons (Plant et al. 2012), TWIK-1/TREK-1 dimers in astrocytes (Mi Hwang et al. 2014; Levitz et al. 2016) or TRESK/TREK-2 dimers in primary somatosensory neurons (Lengyel et al. 2020).

K_{2P} channels show time- and voltage-independent K^+ conductance which is consistent with Goldman-Hodgkin-Katz rectification. They allow both influx and efflux of K^+ across the cell membrane. Under physiological conditions they allow greater efflux of K^+ than influx which is essential for the maintenance of RMP. K_{2P} have therefore significant physiological function. Regulation of K2P channels occurs at different levels. Function of K_{2P} can be modulated by various agents such as volatile anesthetics, anti-depressants and neuroprotective agents, amino acids, lipids, G-proteins, phosphorylation, changes in pH, temperature and mechanical stress (reviewed by Feliciangeli et al. 2015). K_{2P} can also be subject to alternate splicing (Han, Kang, and Kim 2003; Rinné et al. 2014).

Concerning K_{2P} channels, astrocytes have been shown to express TWIK-1 and TREK-1 (Kindler et al. 2000; Cahoy et al. 2008), TREK-2 (Gnatenco et al. 2002) and TASK-1 subunits (Chu et al. 2010); however, expression of specific subunits differs between astrocytes from different brain regions. K_{2P} channels are responsible for the passive K^+ conductance in mature astrocytes, as knockdown of TWIK-1 and TREK-1

results in reduction, but not in complete loss of passive K^+ conductance (Mi Hwang et al. 2014). This suggests that while TWIK-1 and TREK-1 are responsible for the majority of passive K^+ conductance, other K_{2P} channels likely contribute to it as well (Gnatenco et al. 2002; Chu et al. 2010).

3.4.1.3 Voltage-gated K^+ channels

Voltage-gated K^+ (K_v) channels represent heterogeneous family of K^+ channels that are activated by changes in transmembrane potential. In humans, there are currently 40 known members (called α subunits) divided into 12 classes (K_vα1-12) based on their amino sequence homology, which can be further divided into functional subgroups based on a distinct gating mechanisms. Each K_v channel consists of four pore-forming subunits forming either a homotetramere on heterotetramere. Each subunit has four voltage-sensing transmembrane segments (S1-4), two transmembrane segments (S5, S6), a P-loop, an N-terminus cytoplasmic domain and a C-terminus cytoplasmic domain. In addition, K_v channels can be associated with beta subunits, which are auxiliary subunits that can modulate the channel function. For a comprehensive review see Abbott (2020).

K_v channels play specific roles in different cells. They are highly selective for K^+ (Heginbotham et al. 1994; Lemasurier, Heginbotham, and Miller 2001), which is essential for membrane repolarization after an action potential and maintaining the cell RMP in neurons. Consequently, they are important for regulation of firing threshold and duration of action potentials and the firing rates (Gabel and Nisenbaum 1998; Glazebrook et al. 2002; Begum et al. 2016). Apart from the excitability control, K_v channels have been shown to play a role in exocytosis (Singer-Lahat et al. 2007; Feinshreiber et al. 2010), apoptosis (Redman et al. 2007; Hu et al. 2008) and proliferation (Kotecha and Schlichter 1999; Jiménez-Pérez et al. 2016). K_v channels dysregulation or dysfunction is associated with many neurological disorders (reviewed by Shah and Aizenman 2014).

Astrocytes have been reported to express various K_v channels (Cahoy et al. 2008). Similar to K_{2P} channels, function of astrocytic K_v channels is only poorly understood, as their activation occurs around values positive to -40 mV, which is in contrast with proposed RMP of astrocytes. K_v channels have been predicted to regulate Ca^{2+} influx in neonatal rat cortical astrocytes, though this study did not specify the type of K_v channels involved (K. C. Wu et al. 2015).

3.4.1.4 Other potassium channels

Different type of K^+ channel present in astrocytes is calcium-activated K^+ channel $K_{Ca}3.1$ (Longden et al. 2011). Neuronal activity induces increase in intracellular Ca^{2+} concentration that spreads through the astrocytic syncytium. In astrocyte endfeet, Ca^{2+} activates big conductance K^+ channels, leading to release of K^+ into perivascular space. This leads to uptake of K^+ by Kir channels of smooth muscle cells which results in vasodilatation (Filosa et al. 2006; Girouard et al. 2010).

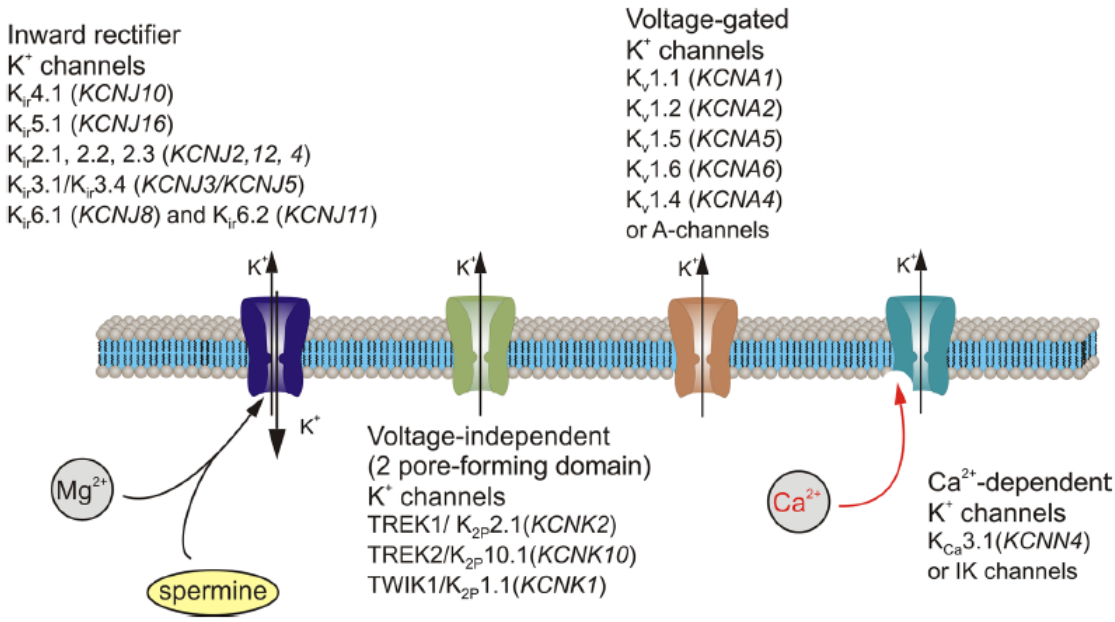

Fig. 5. Astrocyte K^+ channels. Astrocytes express inwardly rectifying K^+ (Kir) channels, two-pore domain K^+ (K_{2P}) channels, voltage-gated K^+ (K_v) channels and calcium-activated K^+ channels (*Verkhratsky and Parpura* 2015).

3.4.2 Astrocyte chloride channels

In addition to having a strong K^+ conductance, astrocytes express various different Na^+, Ca^{2+} and Cl^- channels. Of these, Cl^- channels are the most notable, because Cl^- is important in regulation of K^+ spatial buffering, as it is responsible for maintaining electroneutrality of the process. Three Cl^- channels most commonly found in astrocytes are briefly discussed.

Chloride channel protein 2 (ClC-2) is a slowly rectifying voltage-gated Cl^- channel that is activated at negative potentials during membrane hyperpolarization. Besides being expressed in astrocytic endfeet surrounding blood vessels (Sík, Smith, and

Freund 2000), ClC-2 is widely expressed in many different tissues throughout the body (Thiemann et al. 1992). In the CNS, ClC-2 is believed to have a role in regulation of excitability in GABAergic neurons (Rinke, Artmann, and Stein 2010; Ratté and Prescott 2011).

Another Cl^- channel found in astrocytes is bestrophin1 (Best1). Best1 is a calcium-activated Cl^- channel that is also permeable for some neurotransmitters, including glutamate and GABA (S. Lee et al. 2010; H. Park et al. 2013). On the neuronal synapses, Best1 regulate glutamate (via interaction with TREK-1) and GABA release from astrocytes (D. H. Woo et al. 2012; J. Woo et al. 2018).

Volume regulated anion channel (VRAC) is an outwardly rectifying Cl^- channel that is also permeable to small osmolytes like glutamate or ATP (Kimelberg et al. 1990; Pasantes-Morales et al. 1994). In plays a major role in the process of regulatory volume decrease, which is an important function in astrocytes, as astrocytes tend to increase cellular volume both under physiological and pathological conditions (reviewed by Mongin 2016).

3.4.3 Other astrocyte channels

Other ion channels are also present in astrocytic membranes, though these are usually typical for other cell types. They are either expressed in low numbers, under specific conditions (pathology, development) and are usually relatively understudied.

One of these channels is voltage-gated Na^+ channels (Na_v). However, there are inconsistencies in evidence of expression of specific subunits of these channels between studies *in vitro* and *in situ*. Because these channels are present in astrocyte membranes in very low densities, they mediate only relatively small currents (Chvátal et al. 1995). Physiological function of Na_v channels in astrocytes is currently unknown. One suggested function for these channels is maintaining function of Na^+/K^+ pump (Sontheimer et al. 1994).

Calcium channels in astrocytes are represented mostly by intracellular ryanodine receptor channels (RyRs), specifically those regulated by inositol 1,4,5-trisphosphate, called inositol 1,4,5-trisphosphate receptors ($InsP_3Rs$). Predominant type of these channels found in astrocytes is $InsP_3R2$. These channels are responsible for release of Ca^{2+} from endoplasmic reticulum. While presence of other types of Ca^{2+} channels has

been reported, it was mostly at the mRNA and/or in *in vitro* studies, and contribution of these channels to astrocyte Ca^{2+} signaling remains largely unexplored (for a review on Ca^{2+} signaling see Verkhratsky, Rodríguez, and Parpura 2012).

Another family of channels present in astrocytes are transient potential receptor (TRP) channels. TRP channels are associated with highly diverse physiological functions, specifically different kinds of sensory sensing and regulation of volume and osmotic pressure, muscle contraction and blood pressure. TRP channels and non-selectively permeable to cations such as Ca^{2+}, Na^{+} and Mg^{2+}. They are divided into 10 families based on their physiological properties. Astrocytes have been shown to express several types of TRPC (C = "canonical") channels, TRPA1 (A = "ankyrin") and TRPV (V= "vanilloid") channels TRPV1 and TRPV4 (reviewed by Verkhratsky, Reyes, and Parpura 2014). These channels are important for intracellular [Ca^{2+}] maintenance. Most notably, TRPV4 are found at perisynaptic processes, where they interact with AQP4. Together with VRAC channels, TRPV4-AQP4 complexes are essential for regulatory volume decrease (Benfenati et al. 2011).

Last notable channels present in astrocytes are hyperpolarization activated cyclic nucleotide-gated (HCN) channels. There are four channels (HCN1-4) with small differences in voltage-dependence and kinetics. HCN channels are permeable for Na^{+} and K^{+}, but under physiological conditions predominantly carry depolarizing inward Na^{+} current (Biel et al. 2009). Expression of these channels in astrocytes was reported only in reactive astrocytes after ischemia (Honsa et al. 2014). Similarly, another group recently reported presence of HCN1 and HCN2 in reactive astrocytes after transient ischemia induction in gerbils (J. H. Park et al. 2019).

4 Materials and Methods

4.1 Materials

4.1.1 Chemicals

- saline (Ardeapharma, Sevetin, Czech Republic)
- heparin (Zentiva, Prague, Czech Republic)
- sucrose (10%, 20%, 30%; Sigma-Aldrich, St. Louis, MO, USA)
- paraformaldehyde (PFA; Sigma-Aldrich, St. Louis, MO, USA)
- pentobarbital (PTB; 100 mg/kg, i.p.; Sigma-Aldrich, St. Louis, MO, USA)
- phosphate-buffered saline (PBS; Sigma-Aldrich, St. Louis, MO, USA)
- Chemiblocker (Merck Millipore, Billerica, MA, USA)
- Triton X-100 (Sigma-Aldrich, St. Louis, MO, USA)
- 4′,6-diamidino-2-phenylindole (DAPI; Invitrogen, Carlsbad, CA, USA)
- SYBR Safe DNA Gel Stain (Invitrogen, Carlsbad, CA, USA)

4.1.2 Solutions

- Recording artificial cerebrospinal fluid (r-aCSF) containing (in mmol): 122 NaCl, 3 KCl, 1,5 $CaCl_2$, 1,3 $MgCl_2$, 1,25 Na_2HPO_4, 28 $NaHCO_3$ and 10 D-glucose (osmolality 300 ± 3 mmol/kg).
- Isolation artificial cerebrospinal fluid (i-aCSF) containing (in mmol): 110 NMDG-Cl, 2,5 KCl, 0,5 $CaCl_2$, 7 $MgCl_2$, 1,25 Na_2HPO_4, 24,5 $NaHCO_3$ and 20 D-glucose (osmolality 290 ± 3 mmol/kg).
- Intracellular recording solution (ICS) containing (in mmol): 130 KCl; 0.5 $CaCl_2$; 2 $MgCl_2$; 5 EGTA; 10 HEPES; pH 7,2

Note: all chemicals used for preparation of solutions were purchased from Sigma-Aldrich.

4.1.3 Lab equipment

- Behavioral testing
    - plastic cage (25 x 15 x 60 cm; homemade)
    - Mouse Rotarod 47650 (Ugo Basile, Comerio, Italy)
- Immunohistochemistry
    - cryostat (Zeiss Hyrax C50, Zeiss, Germany)
    - confocal microscope (Olympus FV10i, Olympus, Tokyo, Japan)
- Patch clamp recordings
    - automated vibrating microtome (Leica VT1200S; Leica Microsystems, Wetzlar, Germany)
    - P-97 or P-1000 Flaming/Brown micropipette puller (Sutter Instruments, Novato, CA, USA)
    - recording equipment
        - upright Axioscop microscope (Zeiss, Gottingen, Germany)
        - electronic micromanipulators (Luigs & Neumann, Ratingen, Germany)
        - AxioCam HR digital camera (Zeiss, Gottingen, Germany)
        - EPC-9 amplifier
    - software
        - PatchMaster (HEKA Elektronik, Lambrecht/Pfalz, Germany)
        - FitMaster (HEKA Elektronik, Lambrecht/Pfalz, Germany)
- Data analysis and processing
    - GraphPad Prism 8.4.3 (GraphPad Software, San Diego, CA, USA)
    - CorelDRAW Graphics Home & Student Suite 2019 (Corel Corporation, Ottawa, Canada)
    - ImageJ (open source)

4.1.4 Animals

Four mouse strains were used in this work:

1) C57BL/6J strain – default wild type strain (JAX Laboratory, #000664).
2) B6.Cg-Tg(SOD1*G93A)1Gur/J (C57BL/6J background, further referred to as "**C57Bl6-SOD1**") strain in which the expression of mutated human copper-zinc superoxide dismutase 1 (SOD1) is controlled by a human SOD1 promoter (JAX Laboratory, #004435). In this strain, overexpression of mutated SOD1 induces ALS-like phenotype (Gurney et al. 1994; Tu et al. 1996; Wooley et al. 2005).
3) FVB-GFAP/eGFP strain (FVB background) in which the enhanced green fluorescent protein (eGFP) is expressed under the control of the promoter for human glial fibrillary acidic protein (GFAP) and thus relatively specifically (see chapter 2.5.1) expressed in astrocytes (obtained from Nolte et al 2001).
4) GFAP/eGFP(SOD1*G93A) strain (mixed background; further referred to as "**mbGFAP-SOD1**" strain). This strain was produced by cross-breeding the Bl6-SOD1 strain with the FVB-GFAP/eGFP strain.

In total, four groups of mice entered the experiments (see **Figure 6** for details). First two groups were mice from the C57Bl6-SOD1 strain either carrying the *mSOD1* (further referred to as "**Bl6-SOD1**" mice) and carrying the wild type SOD1 (further referred to as "**Bl6-CTRL**" mice). The other two groups were mice from the mbGFAP-SOD1 strain carrying the *mSOD1* (further referred to as "**GFAP-SOD1**" mice) and carrying the wild type SOD1 (further referred to as "**GFAP-CTRL**" mice). All four groups were used in the behavioral testing. GFAP-CTRL and GFAP-SOD1 mice were used for immunohistochemistry experiments and patch clamp recordings.

Mice were housed in standard breeding cages at a constant temperature of 21 ± 1 °C and relative humidity of 30 % with a 12:12 dark/light cycle. Food and water were available *ad libitum*. All procedures involving the use of laboratory animals were performed in accordance with the European Communities Council Directive 24 November 1986 (86/609/EEC) and animal care guidelines approved by the Animal Care Committee of Institute of Experimental Medicine, Czech Academy of Sciences (approval number 40/2019). All efforts were made to minimize both the suffering and the number of animals used.

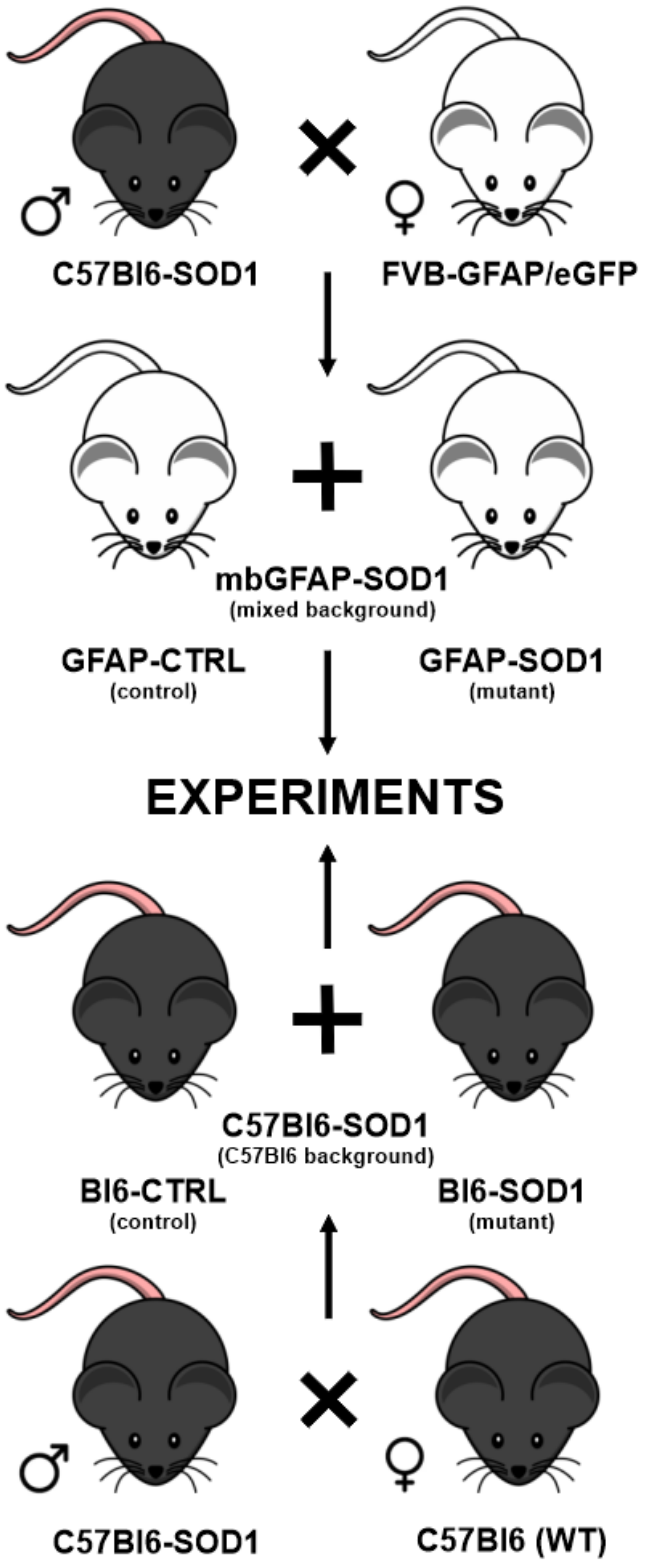

Fig. 6. Generation and breeding of mice used in the experiments. Male C57Bl6-SOD1 mice were crossed with FVB-GFAP/eGFP females to produce mbGFAP-SOD1 mice (GFAP-CTRL and GFAP-SOD1) (**UPPER PART**). Male C57Bl6-SOD1 mice were bred with C57Bl6 females to produce Bl6-CTRL and Bl6-SOD1 mice. GFAP-CTRL, GFAP-SOD1, Bl6-CTRL and Bl6-SOD1 mice were used in the experiments (**LOWER PART**).

4.2 Methods

4.2.1 PCR genotyping

To validate the SOD1 mutation, PCR of tail genomic DNA was used. The primers used are listed in **Table 2**. DNA extraction from mice tail biopsies and PCR amplification was performed using REDExtract-N-AmpTM Tissue PCR Kit (Sigma-Aldrich, St. Louis, MO, USA). PCR products were separated on 1.5% agarose and visualized with SYBR Safe DNA Gel Stain (Molecular Probes, Invitrogen, Carlsbad, CA, USA).

Table 2. Sequence of primers used for PCR genotyping

Primer type	**Sequence 5' -> 3'**
Transgene forward	CAT CAG CCC TAA TCC ATC TGA
Transgene reverse	CGC GAC TAA CAA TCA AAG TGA
Internal positive control forward	CTA GGC CAC AGA ATT GAA AGA TCT
Internal positive control reverse	GTA GGT GGA AAT TCT AGC ATC ATC C

4.2.2 Behavioral tests

To assess muscle strength, function and coordination over time, two sensorimotor tests were conducted (**Figure 7**): a modified wire grid hang test (Hosaka et al., 2002; Carlson et al., 2010) and the Rota-rod test (Deacon, 2013; Oliván et al., 2015). In addition, measuring of weight was conducted together with the wire grid hang test as an additional parameter of disease progression. Testing consisted of a single three-attempt session every week beginning at P30, for a period of 10 weeks. Prior to experiment, all animals performed a training for both tests at the age of P30 (a single three-trial session for wire grid hang; three single-trial sessions at 5, 10 and 15 rpm for rotarod).

Fig. 7. Behavioral tests. Wire grid hang (left) and rotarod test (right)

4.2.2.1 The wire grid hang test

A steel grid was placed on a top of a plastic cage filled with a soft bedding made of wood chips (the cage should be at least 35 cm high; in this case a 60 cm high cage was used). The animal was placed on the top of the steel grid and the grid was inverted. Mouse was then suspended upside-down. The animal had three attempts to remain on the grid for a maximum of 180 s per attempt, or the latency to fall was recorded.

4.2.2.2 The Rota-rod test

The animal was placed on a stationary rod facing against the direction of rotation. The rod then started rotating at a constant speed of 15 rpm. The animals had three attempts to remain on the rotarod for a maximum of 180 s per attempt, or the latency to fall was recorded.

4.2.3 Immunohistochemistry

Animals at the age of P30 (1 month; 1M) or P90 (3 months; 3M) were anesthetized with intraperitoneal injection of PTB (100 mg/kg) and transcardially perfused with 20 ml of pre-cooled saline containing heparin (2500 IU/100ml) followed by solution of 4% PFA in 0.1 M phosphate-buffered saline (PBS). After swift decapitation, the brains were dissected out and post-fixed overnight in PFA and subsequently treated with sucrose gradient (10%, 20%, 30% sucrose in 0.01M PBS [pH 7.4]) for the purpose of cryoprotection. Brains were then coronally sliced using a cryostat (Zeiss Hyrax C50,

Zeiss, Germany). The slices (thickness 30 μm) were initially washed in PBS and treated with a blocking solution containing: 5% Chemiblocker (Millipore, Billerica, MA, USA) and 0.2% Triton X-100 (Sigma-Aldrich, St. Louis, MO, USA) in PBS for 1 hour. Afterwards the slices were incubated with the primary antibodies diluted in blocking solution at 4°C overnight followed by a treatment with the appropriate secondary antibodies applied for 2 hrs at 4 °C. Antibodies used for immunohistochemistry are listed in **Table 3**. To visualize cell nuclei, the slices were incubated with 300nM 4′,6-diamidino-2-phenylindole (DAPI; Invitrogen, Carlsbad, CA, USA) in PBS for 5min at room temperature. An Olympus FV10i confocal microscope was used for immunochemical analyses.

Table 3. Primary and secondary antibodies used for immunohistochemistry

Antigen	Dilution	Isotype	Manufacturer	Sec. antibody
NeuN	1:100	mouse monoclonal IgG	Merck Millipore (MAB377)	GAM 594 1:200
Kir4.1	1:400	guinea pig polyclonal IgG	Alomone Labs (AGP-012)	GAGP-Cy3 1:400

GAM 594: goat anti-mouse IgG conjugated with Alexa Fluor 594 (Invitrogen);
GAGP-Cy3: goat anti-guinea pig IgG conjugated with Cy3 (Chemicon).

4.2.4 Preparation of acute brain slices

Animals at the age of P30 (1M) were anesthetized with intraperitoneal injection of PTB (100 mg/kg), transcardially perfused with pre-cooled isolation artificial cerebrospinal fluid (i-aCSF). After swift decapitation, the brains were dissected out, glued to a small agarose block and transferred to a slicing chamber filled with cold i-aCSF (4 °C). Acute coronal slices (thickness 220 μm) were prepared using an automated vibrating microtome (Leica VT1200S; Leica Microsystems, Wetzlar, Germany). After obtaining enough slices, these were transferred to a recovery chamber filled with preheated i-aCSF (34 °C) and incubated for 30 minutes. Afterwards the slices were transferred to a holding chamber filled with recording aCSF (r-aCSF), where they were incubated for at least 30 minutes until used for recording. Both i-aCSF and r-aCSF had pH adjusted to 7.4 by saturating with carbogen (95% O_2/5% CO_2) during all phases of isolation.

4.2.5 Patch clamp recordings

All recordings were performed in slices acutely isolated from the brain. Single brain slice was transferred to the recording chamber with recording setup (see 4.1.3), always prior to the recording. All recordings were performed at room temperature in r-aCSF which was continuously saturated with 5% CO_2 to sustain a pH of 7,4. Recording capillaries with a tip resistance of 9 – 12 MΩ were produced from borosilicate capillaries using either P-97 or P-1000 flaming/brown micropipette puller. Recording capillaries were filled with intracellular recording solution. All data were measured with a 10 kHz sample frequency using an EPC9 amplifier. Recordings were controlled by the PatchMaster software, analysis was performed using the FitMaster software.

All recordings were performed in the whole-cell configuration. Astrocytes were identified by the presence of eGFP using blue light. Current patterns were obtained by clamping the membrane from the holding potential of -70 mV to values ranging from -160 to 40 mV in 10 mV steps, pulse duration was 50 ms. To isolate K_{IR} and K_{DR} current components, a voltage step from -70 to -60 mV was used to subtract time- and voltage-independent currents (see Chvátal 1995, Anděrová 2006). The amplitudes of K_{IR} currents were measured at -160 mV at the end of the pulse. To activate K_{DR} currents only, the cells were held at -50 mV, and the amplitude of K_{DR} current was measured at 40 mV, at the end of the pulse.

Membrane potential (V_M) was obtained by switching the EPC-9 amplifier to the current clamp mode. Membrane input resistance (IR) was calculated from the FitMaster software from the current value at 40 ms after the onset of the depolarizing pulse from -70 to -60 mV. Membrane capacitance (C_M) was acquired automatically by PatchMaster using the Lock-In protocol. Current densities were calculated by dividing the maximum current amplitudes by the C_M, which indicates the cell size.

4.2.6 Data analysis

Data are presented as mean or mean ± standard error of mean (S.E.M.) for n cells or animals unless stated otherwise. Repeated measures two-way ANOVA with Holm-Sidak's multiple comparison correction was used to analyze differences between groups in behavioral tests. Student's t-test, Welch's t-test or Mann-Whitney test was used to analyze differences between groups in patch clamp recordings. D'Agostino-Pearson normality test was used to assess normal distribution of a sample set, and an F-test was used to assess variances between two sample sets. Values of */#/§ ($p < 0.05$) were considered significant, **/## ($p < 0.01$) very significant and ***/### ($p < 0.001$) extremely significant.

5 Aims of the study

This study focuses on the phenotypic characterization of the double transgenic mbGFAP-SOD1 model on the whole-organism and cellular level. It also focuses on the electrophysiological properties of astrocytes in the motor cortex, layers V/VI. Measurements will be performed *in situ* in acutely isolated brain slices from mice at the age of 1M (which is considered a pre-symptomatic phase in this model), using the whole-cell patch clamp technique.

Hypothesis 1: In order to visualize astrocytes in ALS mouse model, we planned to crossbreed the C57Bl6-SOD1 strain with the FVB-GFAP/eGFP strain and we supposed that there will be no phenotypic differences between the newly generated mouse strain and the original C57Bl6-SOD1 model.

Aim 1: Generation of double transgenic animals in order to visualize astrocytes in ALS mouse model:

- phenotype assessment of the double transgenic mbGFAP-SOD1 strain with the use of behavioral tests, specifically:
    i. confirm the presence of ALS-like phenotype in this strain
    ii. comparison of mbGFAP-SOD1 and the original Bl6-SOD1 model
    iii. comparison of differences between sexes
- immunohistochemical analysis of the double transgenic mbGFAP-SOD1 mouse model:
    - confirm the presence of ALS-like phenotype on cellular level

Hypothesis 2: Since the astrocytes participate in K^+ homeostasis, we expect that their membrane properties, namely K^+ conductance, may be altered already in early stages of ALS progression.

Aim 2: Elucidation of astrocytic membrane properties in the motor cortex :

- electrophysiological analysis of astrocytes from GFAP-SOD1 mice and comparison with astrocytes from GFAP-CTRL mice
    i. analysis of basic electrophysiological parameters
    ii. analysis of ionic current patterns
- immunohistochemical analysis of ion channel expression

6 Results

6.1 Generation of double transgenic strain

We successfully crossbred the C57Bl6-SOD1 strain with the FVB-GFAP/eGFP strain and generated a double transgenic mbGFAP-SOD1 model. As female hemizygotes are poor breeders, and rarely produce more than one litter before the onset of disease, male hemizygous carriers have been bred with female non-carriers. Both male and female mice were used in all experiments. To validate the presence of mSOD1 in the offspring, PCR of tail genomic DNA was used. The expected results for SOD1 mutants were two DNA bands: transgene (236 bp) and internal positive standard (324 bp; **Figure 8**).

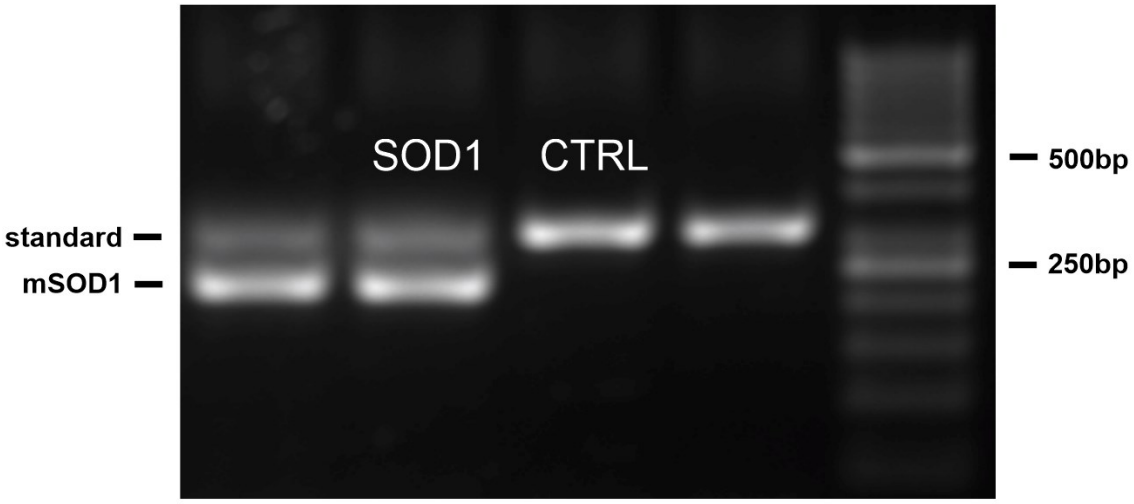

Fig. 8. PCR of tail genomic DNA isolated from the mbGFAP-SOD1 mice.

6.1.1 Behavioral tests

To characterize the original C57Bl6-SOD1 strain and to confirm that newly generated mbGFAP-SOD1 transgenic mice carry the ALS-like phenotype, we have performed two different sensorimotor tests: the wire grid hang test and the rotarod test. In addition, weight measurements were conducted always prior to the wire hang grid test. In total, n = 115 mice completed the testing. Mice were separated into 8 groups based on strain, sex and presence of mSOD1 (**Table 4**). There were n = 16-17 individuals in the mutant groups and n = 12 individuals in the control groups. If the mouse were considered uncompliant after three weeks, they were removed from both tests (n = 3).

Table 4 - List of animals used for behavioral testing

GROUPS		mice (n)
Bl6-CTRL	**male**	12
	female	12
Bl6-SOD1	**male**	17
	female	17
GFAP-CTRL	**male**	12
	female	12
GFAP-SOD1	**male**	17
	female	16

6.1.1.1 General aspects, behavior

Based on our observation, both GFAP-CTRL and GFAP-SOD1 mice seemed to be bigger and more active than their Bl6 counterparts. Otherwise, no substantial differences were observed. Around the 10^{th} to 12^{th} week of age, first clinical signs of motor dysfunction in mutants became apparent. Specifically, mutant mice showed slight trembling in the hind limbs when suspended by the tail (hindlimb extension reflex). These trembles gradually worsened over time; however, no objective measurement was applied. Control mice never displayed these symptoms.

6.1.1.2 The wire grid hang test

We examined the effect of the mSOD1 on neuromuscular strength measured by the mouse ability to hold on a wire grid from 5^{th} to 14^{th} week of age. First, we examined differences between mutants and their corresponding controls to see whether there are any differences and changes over time. Both mutants and controls showed similar performance within the first three weeks of testing, however from the 8^{th} week of age onwards, mutant mice showed progressive decline in neuromuscular strength when compared to controls. This was true both for the Bl6-SOD1 (**Figure 9**) and GFAP-SOD1 (**Figure 10**) mice and also for both sexes. For Bl6-SOD1 males and females, differences in performance became statistically significant at the 8^{th} and 10^{th} week of age, respectively, and continued until the end of the experiment, at the 14^{th} week of age. Similar results were obtained for GFAP-SOD1 mice; differences in males and females became statistically significant in the 9^{th} and 8^{th} week of age, respectively.

Except for some Bl6-SOD1 females (n = 7), all mutants failed to hold on to the inverted grid for full 180 seconds at the 14th week of age. Starting at the 11th week, few individuals (n = 2) failed to hang on the grid at all. At the 14th week of age, n = 10 individuals were not capable of holding on to the grid; this was especially true for GFAP-SOD1 females. We further focused on the performance of the mutants only.

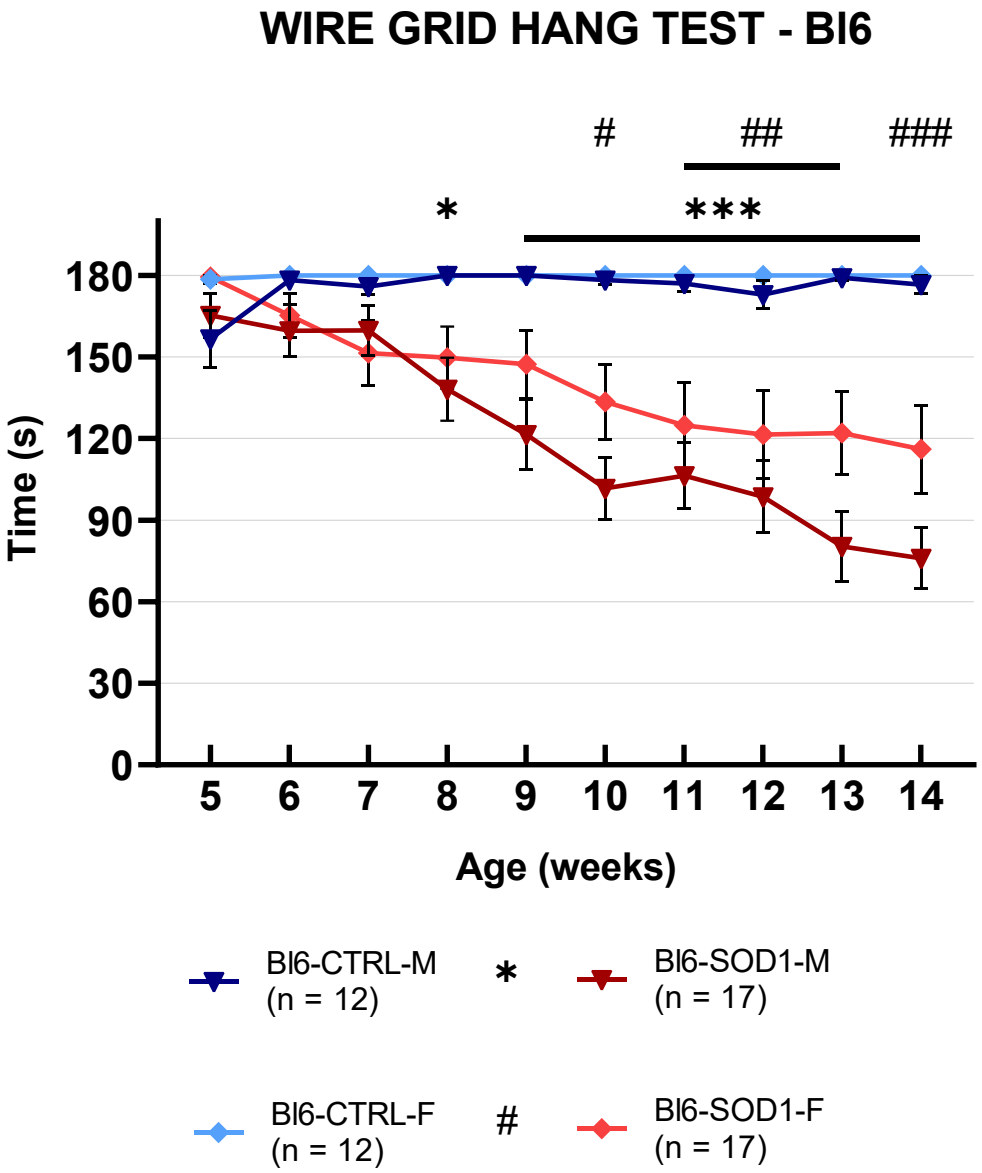

Fig. 9. Time-dependent changes in wire grid hang test performance of Bl6 mice. On average, Bl6-CTRL mice (both male and female) were able to maintain a 180-second wire grid hang duration throughout the study, while Bl6-SOD1 mice became unable to maintain wire grid hang duration from 8th week of age onwards. * indicates significant differences between males, # indicates significant differences between females

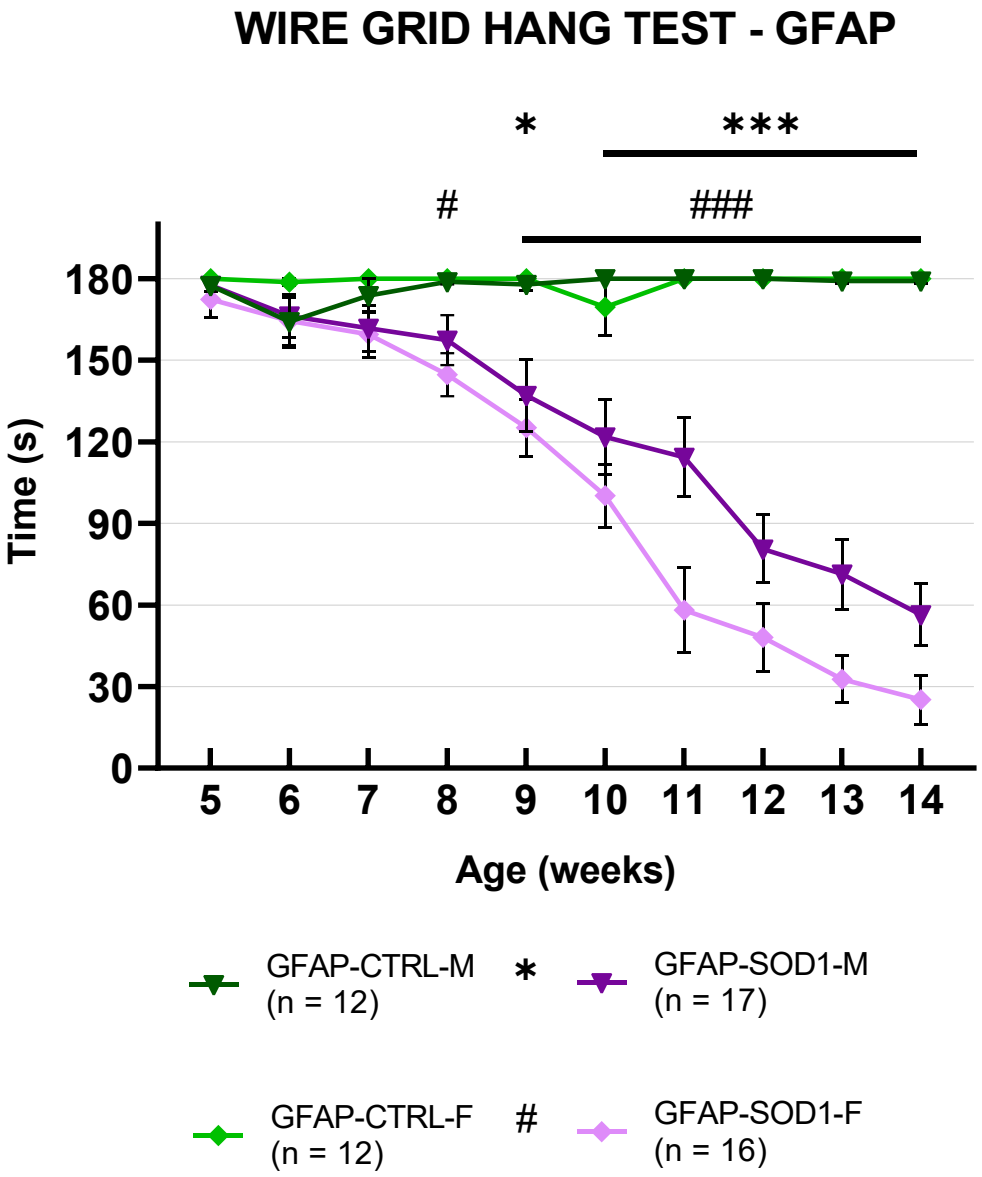

Fig. 10 Time-dependent changes in wire grid hang test performance of GFAP mice. On average, GFAP-CTRL mice (both male and female) were able to maintain a 180-second wire grid hang duration throughout the study, while GFAP-SOD1 mice became unable to maintain wire grid hang duration from 8th week of age onwards. * indicates significant differences between males, # indicates significant differences between females

The mutants showed different rates of decline. Relatively mildest decline in neuromuscular strength was observed in Bl6-SOD1 females, followed by Bl6-SOD1 males, GFAP-SOD1 males and GFAP-SOD1 females, which showed the fastest decline (**Figure 11**).

6.1.1.2.1 The effect of gender on wire grid hang test performance

Both Bl6-SOD1 males and females showed similar rates of performance decline over time. Differences in the performance of Bl6-SOD1 males and females were not statistically significant at any given timepoint. At the 14th week of age, the average performance value of males was 76 ± 11.24 s, the average performance value of the females was 116.06 ± 16.18 s. The mean difference was 40.06 s.

Both GFAP-SOD1 males and females showed similar rates of performance decline over time. A sharp drop in performance of males observed at the 12th week of age was observed also in females one week earlier (11th week of age). Differences in the performance of GFAP-SOD1 males and females were not statistically significant with the exception of the difference observed at 11th week of age. At 14th week of age, the average performance value of males was 56.41 ± 11.4 s, the average performance value of females was 25.19 ± 9.11 s. The mean difference was 31.22 s.

6.1.1.2.2 The effect of strain on wire grid hang test performance

Bl6-SOD1 and GFAP-SOD1 males showed comparable decline in performance over time with no statistically significant differences. There was only mild decline in performance over the first three to four weeks. Afterwards, we observed slightly faster decline in both strains. The sharp drop in performance observed in GFAP-SOD1 males was not observed in Bl6-SOD1 males.

The biggest difference was observed when comparing the decline in performance between females from both strains. GFAP-SOD1 females showed strikingly faster decline than their Bl6-SOD1 counterparts. The differences were statistically significant from the 11th week of age onwards. Similarly to males, there was no sharp drop in performance of Bl6-SOD1 females when compared to GFAP-SOD1 females. At 14th week of age, the difference in performance value between both strains was 90.87 s.

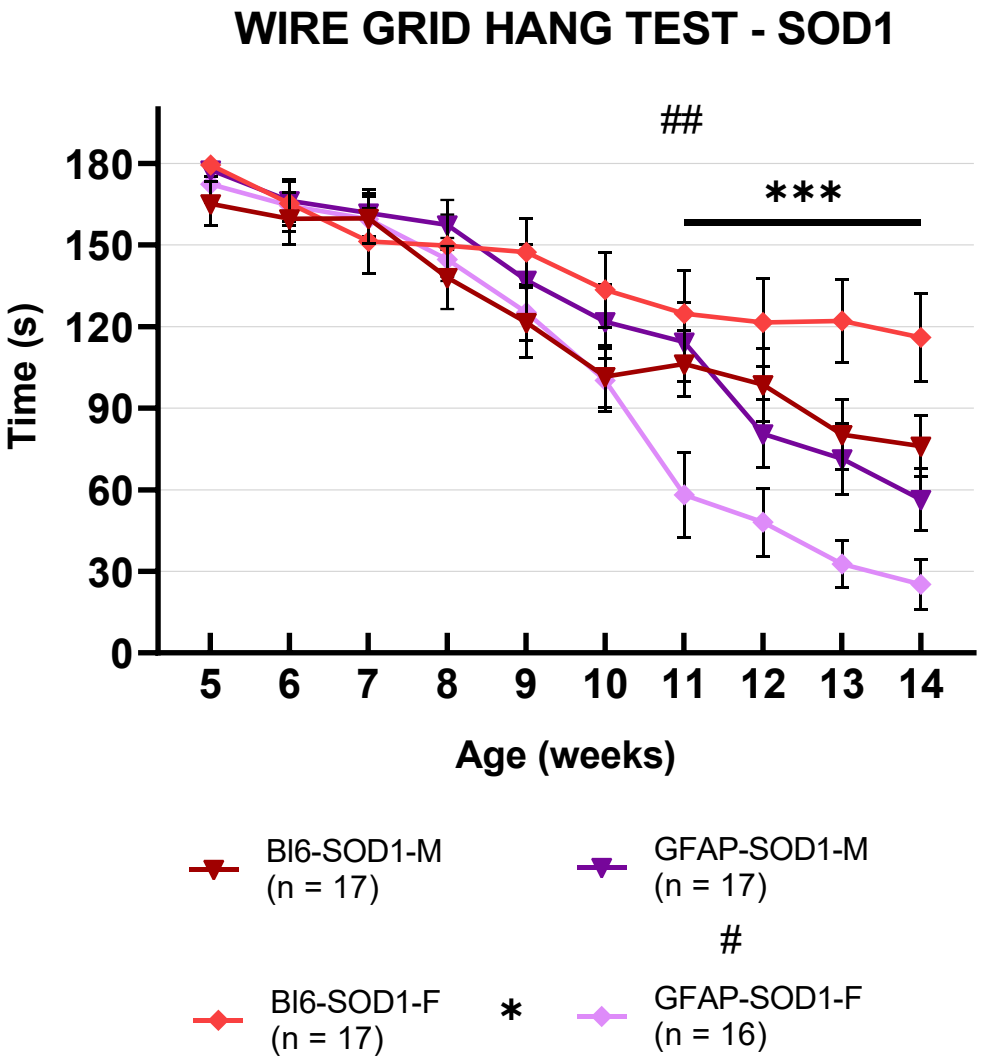

Fig. 11 Time-dependent changes in wire grid hang test performance of SOD1 mice. On average, all four groups of SOD1 mice were not able to maintain a 180-second wire grid hang duration throughout the study. Differences in performance occurred between the Bl6-SOD1 and GFAP-SOD1 females (11^{th} week of age onwards) and between GFAP-SOD1 males and females (11^{th} week of age). * indicates significant differences between females, # indicates significant differences between GFAP-SOD1 males and females

6.1.1.3 The rotarod test

We examined the effect of mSOD1 on motor coordination, strength and balance, measured by the ability to endure on a constantly rotating ridged cylinder from 5th to 14th week of age. First, we examined differences between mutants and their corresponding controls to see whether there are any differences and changes over time. Both the mutants and the controls showed similar performance up to the 11th week of age. First visible differences were observed from the 12th week of age onward when both Bl6-SOD1 (**Figure 12**) and GFAP-SOD1 (**Figure 13**) mutants showed a decline in the performance compared to controls. However, this was not true for Bl6-SOD1 females, which were able to stay on the rotarod for the maximal amount of time up to the 14th week of age. For Bl6-SOD1 males, the differences in performance were statistically significant from 13th week of age onwards. For GFAP-SOD1 males and females, the differences were significant from 13th and 12th week of age, respectively. Note that first statistically significant differences between mutants and controls were observed four to five weeks later than in the wire hang test.

From the 12th week onwards, few individuals (n = 2) failed to remain on the rotarod at all. This number further increased up to the last week of testing (n = 7). Similar to wire grid hang test, this was especially true for the GFAP-SOD1 females.

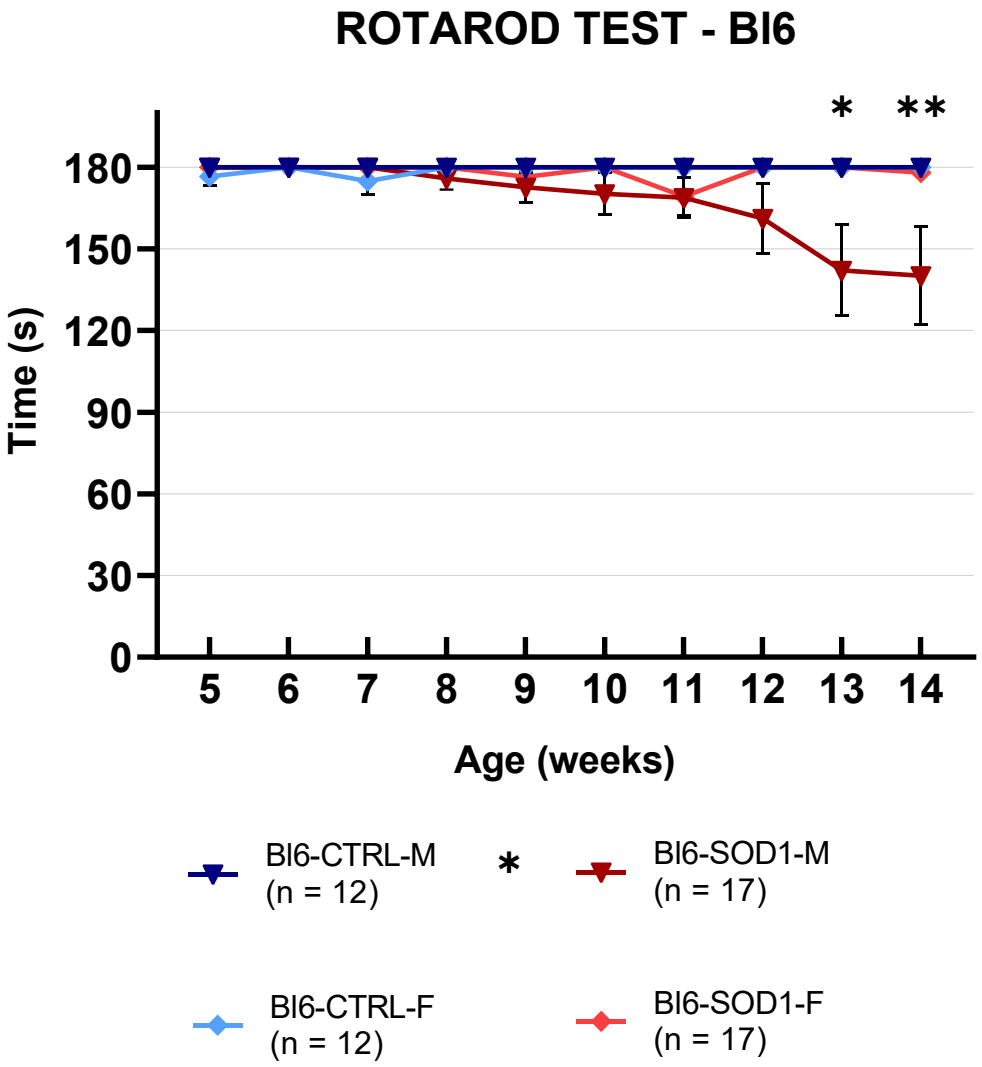

Fig. 12. Time-dependent changes in rotarod test performance of Bl6 mice. On average, Bl6-CTRL mice (both male and female) and Bl6-SOD1 females were able to maintain a 180-second rotarod duration throughout the study, while Bl6-SOD1 males became unable to maintain the duration from 13th week of age onwards. * indicates significant differences between males

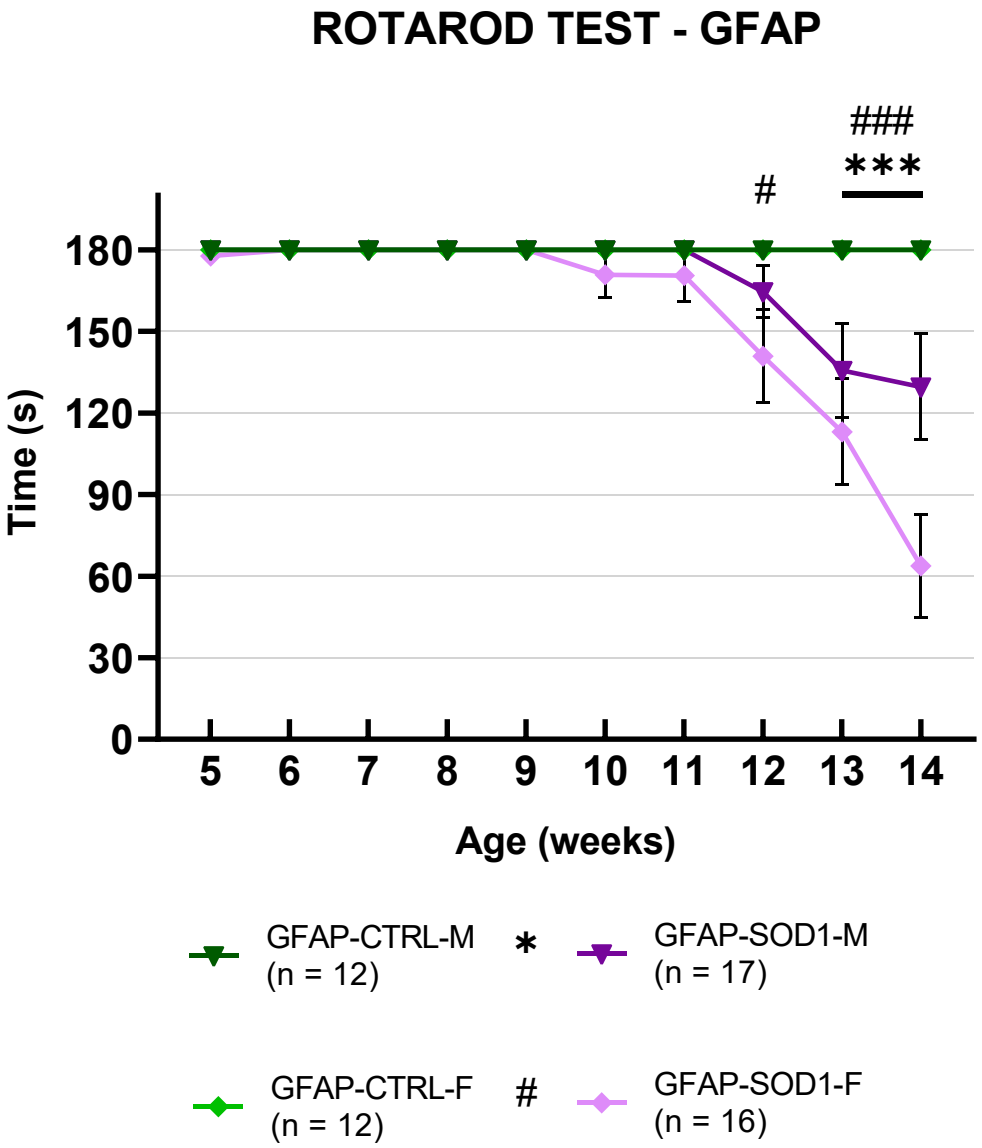

Fig. 13. Time-dependent changes in rotarod test performance of *GFAP* mice. On average, GFAP-CTRL mice (both male and female) were able to maintain a 180-second rotarod duration throughout the study, while *GFAP*-SOD1 mice (both male and female) became unable to maintain the duration from 12th week of age onwards. * indicates significant differences between males, # indicates significant differences between females

We again further focused only on the mutants (**Figure 14**). Similarly to wire hang test, mutants showed different rates of decline. No decline was observed for the Bl6-SOD1 females. Mild decline was observed in males from both strains. Fastest decline was observed in GFAP-SOD1 females, similarly to the wire hang test.

6.1.1.3.1 The effect of gender on rotarod performance

Bl6-SOD1 males and females showed similar performance over majority of the course. Differences between males and females were significant from 13th week of age onwards. At the 14th week of age, the average performance value of males was 140.12 ± 17.99 s, the average performance value of the females was 178.06 ± 1.94 s. The mean difference was 37.94 s.

GFAP-SOD1 males and females showed similar changes in performance over time until the last week of testing, where males experienced alleviation in performance decline. At week 14, the average performance value of males was 129.65 ± 19.53 s, the average performance value of females was 63.81 ± 18.83 s. The mean difference was 65.83 s.

6.1.1.3.2 The effect of strain on rotarod performance

Males from both strains shared similar performance development over time with no significant differences. Similarly to wire hang test, the biggest differences were observed when comparing females from both strains. While Bl6-SOD1 females showed no decline at all, their GFAP-SOD1 counterparts experienced sharp decline in performance from the 12th week onward; these differences were statistically significant.

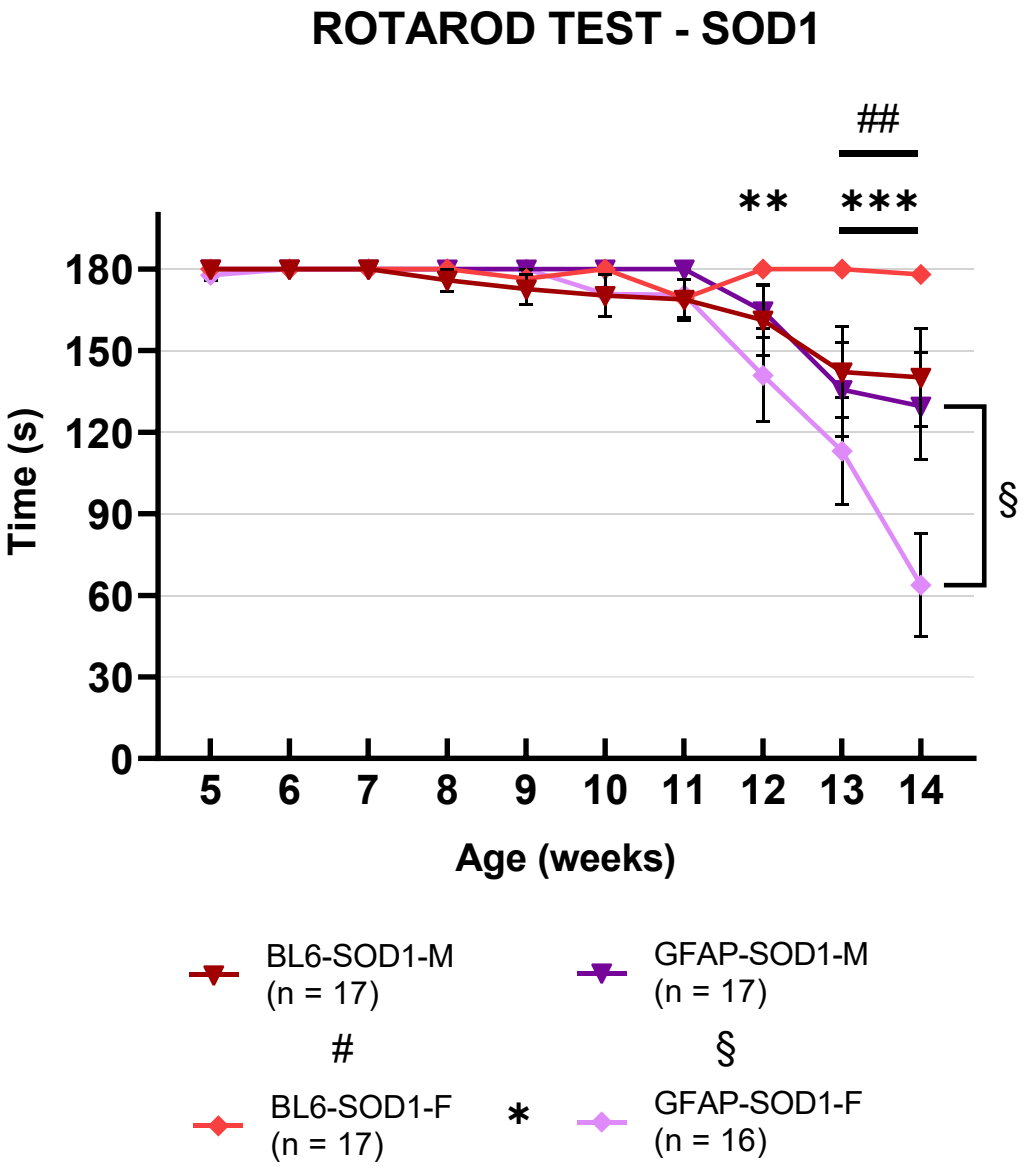

Fig. 14. Time-dependent changes in rotarod test performance of SOD1 mice. On average, SOD1 mice were not able to maintain a 180-second rotarod duration throughout the study with the exception Bl6-SOD1 females. Differences in performance occurred between the Bl6-SOD1 and GFAP-SOD1 females (from 12th week of age onwards), between Bl6-SOD1 males and females (from 13th week of age onwards) and between GFAP-SOD1 males and females (14th week). * indicates significant differences between females, # indicates significant differences between Bl6-SOD1 males and females, § indicates significant differences between GFAP-SOD1 males and females

6.1.1.4 Weight

Weight of the animals was measured on a weekly basis. First, we explored whether expression of mSOD1 affects the weight of the mutants. As expected, there were significant differences observed between the mutants and the controls. Mutants from both strains and both sexes had similar weight up to the 10^{th} week of age when compared to the controls. From 11^{th} week onward, there were significant differences in weight between controls and mutants. While the controls continued to gain weight over time, on average, all mutants stopped gaining weight due to muscle degeneration. The weight differences continued to grow after 14^{th} week of age (data not shown; see discussion), which is consistent with general ALS-like phenotype.

In Bl6 mice, differences between controls and mutants were statistically significant from 13^{th} (males) and 11^{th} week (females) of age onward. Average weight of males at 14^{th} week of age was 28.75 ± 0.62 g (controls) and 25.94 ± 0.47 g (mutants), mean difference was 2.81 g. Average weight of females was 21.17 ± 0.42 g (controls) and 19.24 ± 0.28 g (mutants), mean difference was 1.93 g. Observed differences in weight were bigger in males than in females (**Figure 15**).

In GFAP mice, differences in weight between controls and mutants were present, though these were only significant in females, starting at the 11^{th} week of age. Average weight of males at 14^{th} week of age was 30.25 ± 0.93 g (controls) and 28.12 ± 0.85 g (mutants), mean difference was 2.13 g. Average weight of females was 24.67 ± 0.31 g (controls) and 21.75 ± 0.54 g (mutants), mean difference was 2.92 g. Observed differences in weight were bigger in females than in males (**Figure 16**).

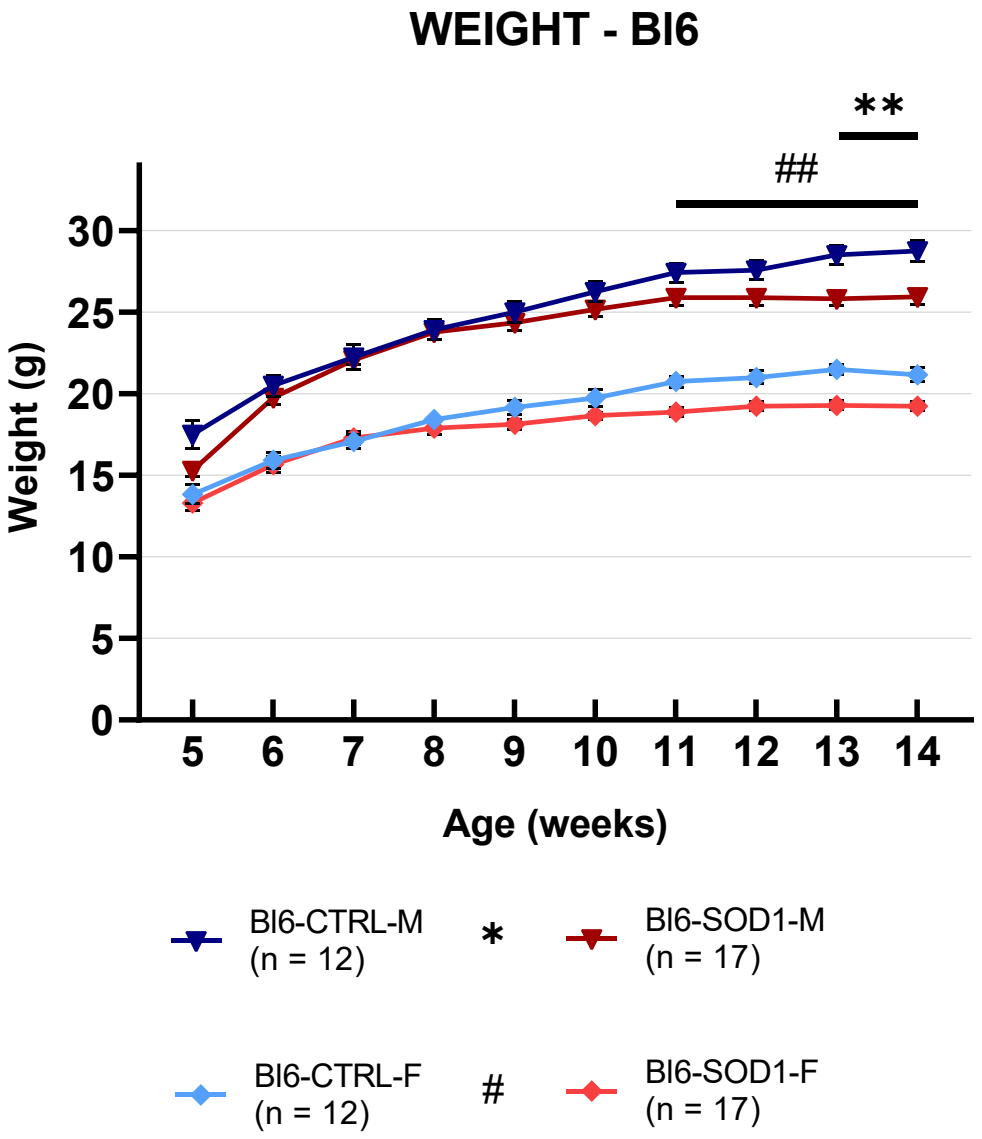

Fig. 15. Time-dependent changes in weight of Bl6 mice. On average, both Bl6-SOD1 males and females had comparable weight to their respective controls up to the 10th and 12th week of age; afterwards, differences among both males and females were statistically significant. * indicates significant differences between males, # indicates significant differences between females

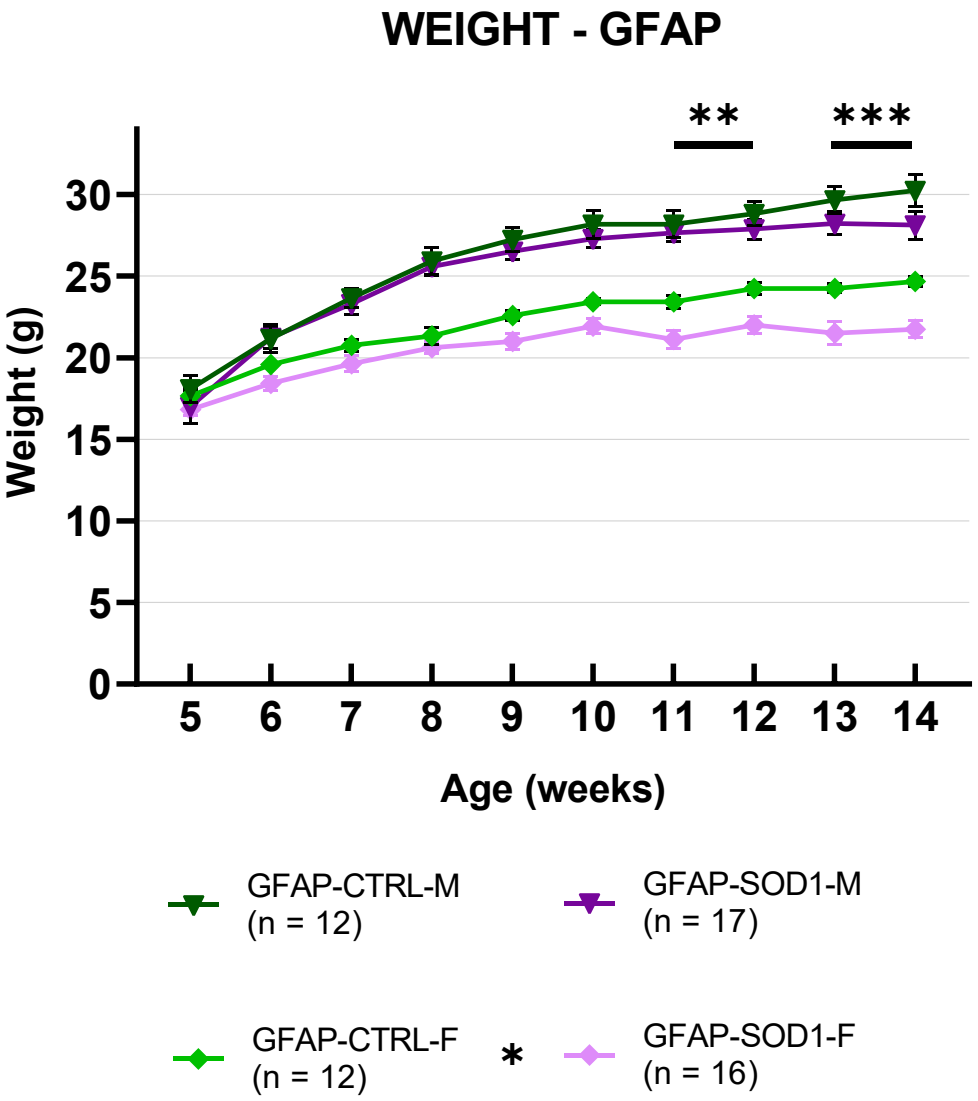

Fig. 16. Time-dependent changes in weight of GFAP mice. On average, GFAP-SOD1 males had comparable weight to the controls. GFAP-SOD1 females had comparable weight to the controls up to 10th week of age; afterwards, differences among females were statistically significant. * indicates significant differences between females

6.1.1.4.1 The effect of gender and strain on weight

Comparison of strains separately among controls and mutants brings additional insight. As mentioned above, all control groups gained weight continuously over time (**Figure 17**), which was not true for the mutants (**Figure 18**). Differences in weight were smaller among males than among females. This was true both for the mutants and the controls.

Bl6 and GFAP control males had comparable weight; the same can be said for Bl6 and GFAP mutant males. In contrast, differences in weight between Bl6 and GFAP control females were extremely significant at any given timepoint, with mean difference of 3.5 g at the 14^{th} week of age. Similarly, differences in weight between Bl6 and GFAP mutant females were also extremely significant at any given timepoint, with mean difference of 2.52 g at the 14^{th} week of age. Both males and females from both mutant and control groups had comparable growth curves.

Last insight into the problematic brings the graphical comparison of weight among males and females. This comparison allows for better look on the facts described above. While there were relatively small differences in the weight and growth curves among males, female mice showed visible substantial differences between the tested groups (**Figure 19**). Purpose of this comparison is to better illustrate the above described differences and as such, no additional statistical analysis was performed.

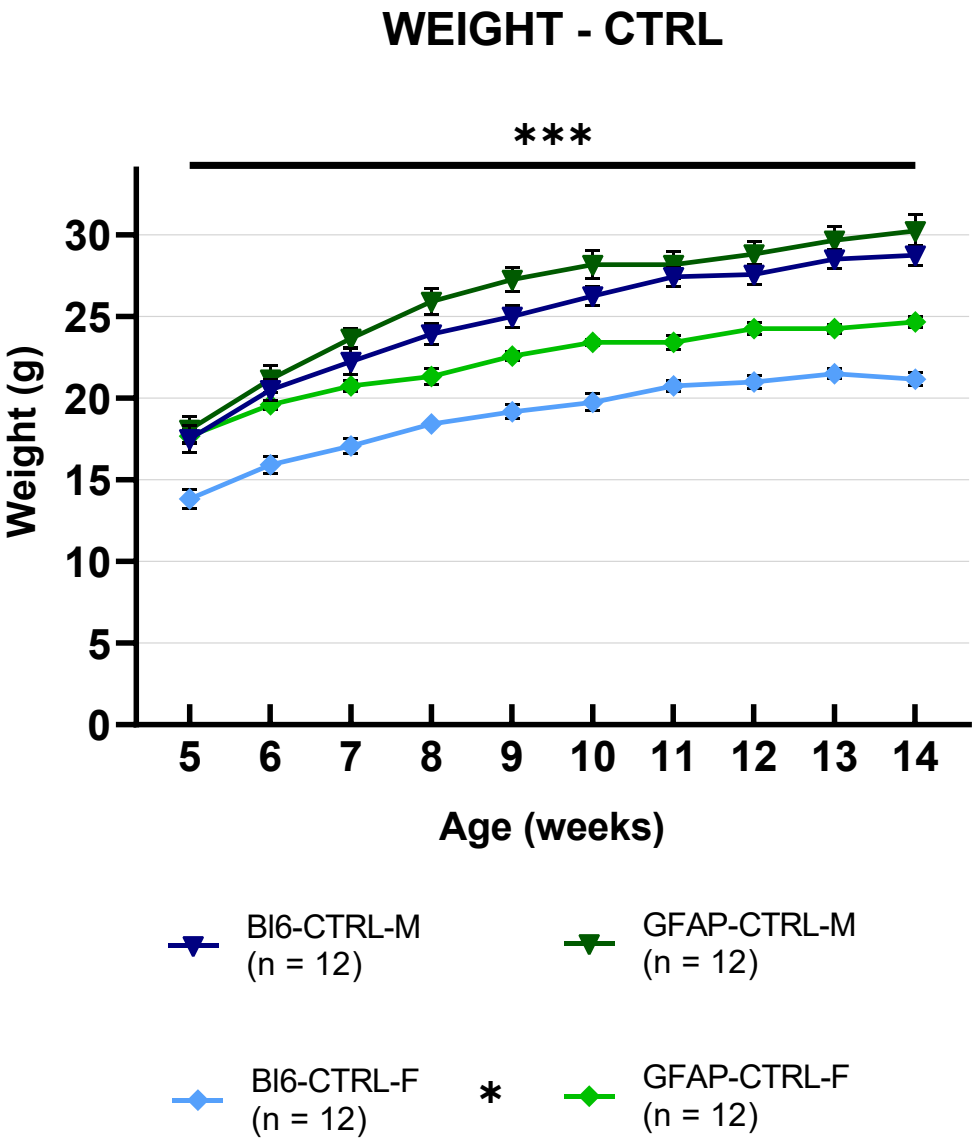

Fig. 17. Comparison of time-dependent changes in weight of CTRL mice. Bl6 males had weight comparable to GFAP males. Bl6 females had extremely significant differences in weight at any given timepoint compared to GFAP females. * indicates significant differences between females

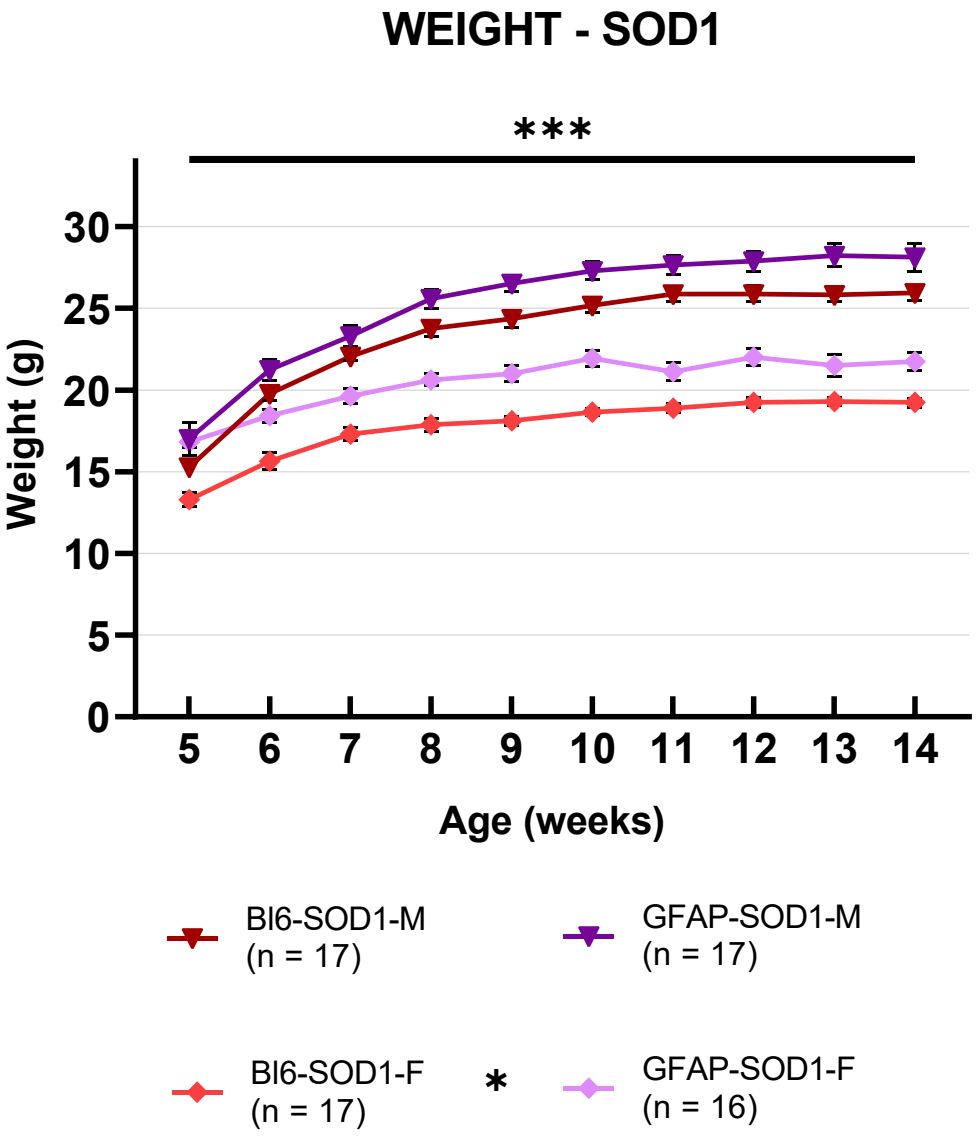

Fig. 18. Comparison of time-dependent changes in weight of SOD1 mice. Bl6 males had weight comparable to GFAP males. Bl6 females had extremely significant differences in weight at any given timepoint compared to GFAP females. * indicates significant differences between females

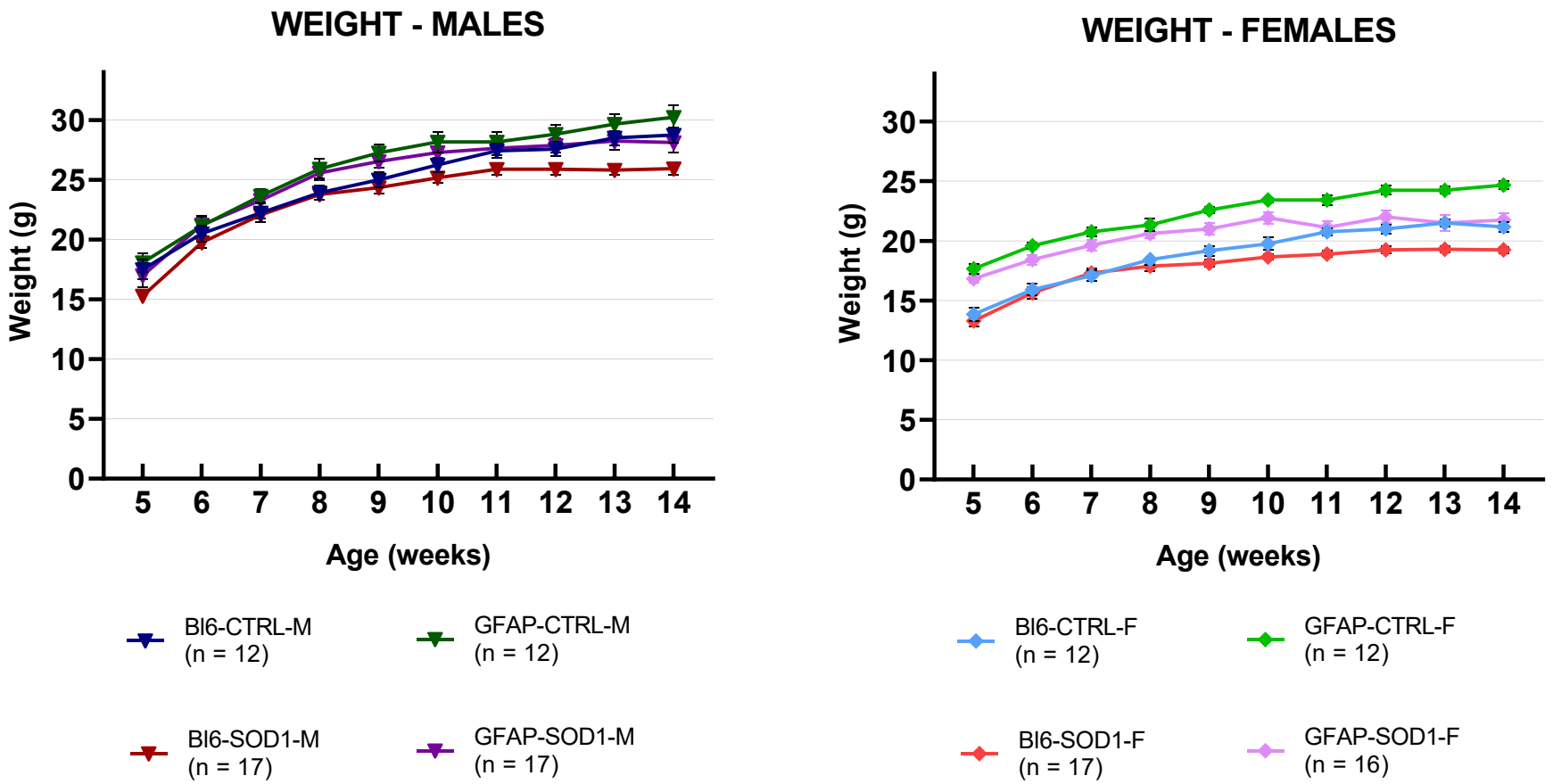

Fig. 19. Graphical comparison of time-dependent changes in weight among males (left) and females (right).

6.1.2 Immunohistochemical analysis the mbGFAP-SOD1 model

We used immunohistochemistry to confirm the phenotype of the mbGFAP-SOD1 model on the cellular level. We looked for the hallmarks of ALS progression (astrogliosis and loss of motor neurons) both in the brain and the spinal cord.

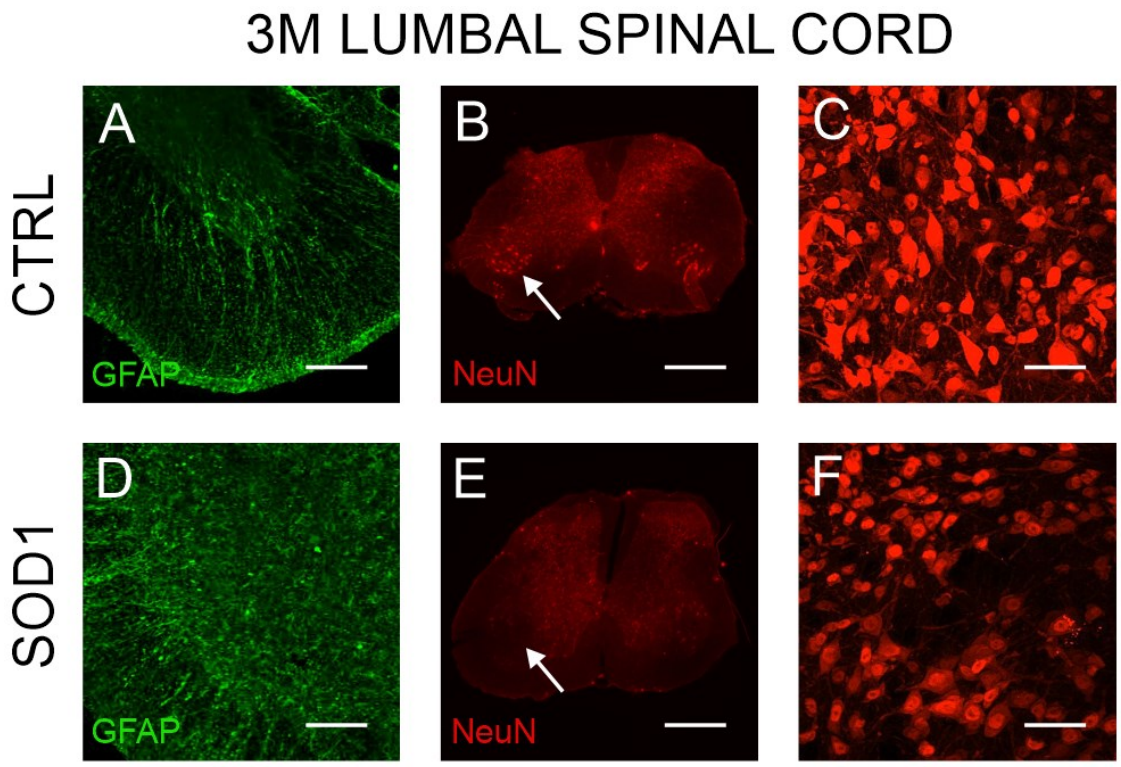

Fig. 20. Immunohistochemical staining of lumbal spinal cord slices isolated from 3M old GFAP-CTRL and GFAP-SOD1 mice. There are visible signs of astrogliosis (A,D) and loss of motor neurons in the ventral horn (B,E) as indicated by the white arrow. Detailed view of the ventral horn is presented (C,F). Bars: 0.2 mm (A,D), 0.5 mm (B, E) and 40 μm (C,F).

We first searched for ALS phenotype in the lumbal spinal cord of 3M GFAP-SOD1 mice (**Figure 20**). Indeed, we observed loss of motor neurons in the ventral horns of the spinal cord. While NeuN (Neuronal Nuclei) non-specifically stains majority of neurons, motor neurons ale distinguishable from other neurons by their large bodies. We also observed signs of astrogliosis.

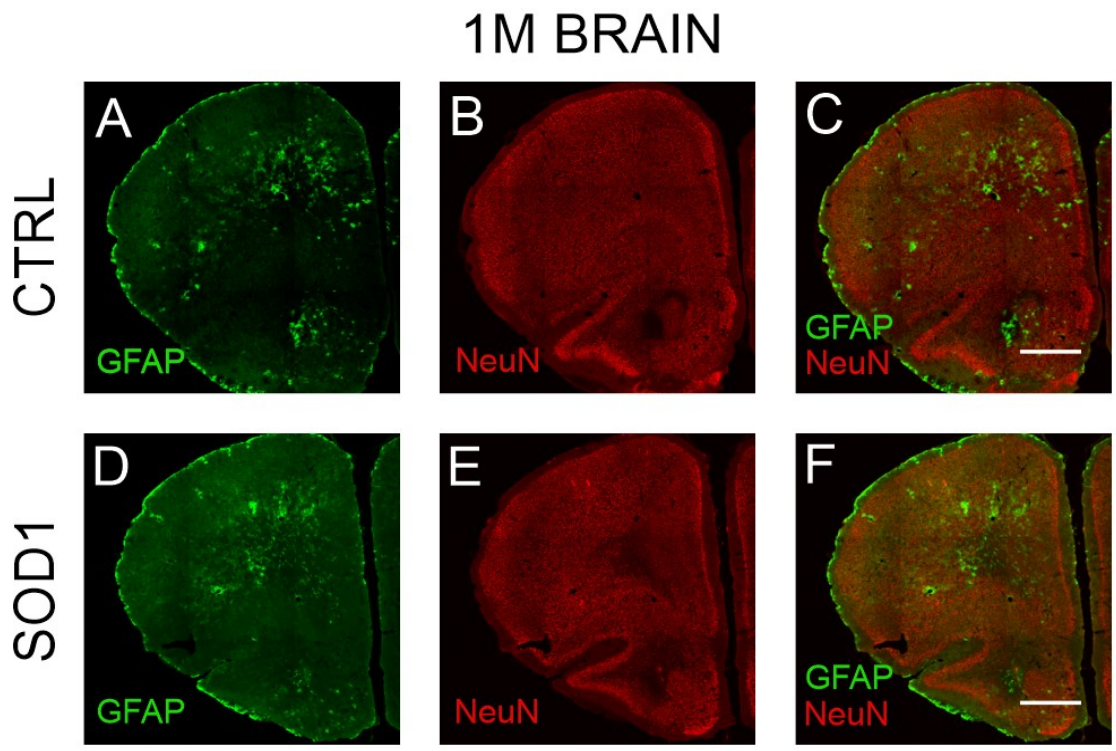

Fig. 21. Immunohistochemical staining of brain slices isolated from 1M old GFAP-CTRL and GFAP-SOD1 mice. There are no visible signs of astrogliosis (A,D) or loss of motor neurons (B,E) Bar: 0.5 mm.

Afterwards, we looked for the ALS hallmarks in the brains of 1M old GFAP-SOD1 mice as this age was used for further electrophysiological analysis (**Figure 21**). We observed no signs of motor neuron degeneration or astrogliosis.

6.2 Patch clamp recordings

To examine differences in astrocytic electrophysiological properties and membrane currents between GFAP-CTRL and GFAP-SOD1 mice, recordings from $eGFP^+$ cells in acutely isolated brain slices were performed. The cells were identified in the slice pre-recording by the presence of fluorescent signal and by the absence of an action potential during seal formation. Both male and female mice were used in the recordings, the mice were 30 days old. $eGFP^+$ cells recorded in mutants and controls are further termed "SOD1" and "CTRL" cells, respectively.

6.2.1 Current patterns

In total, 80 cells were recorded (29 SOD1 and 51 CTRL). Based on the quality of the recordings, 70 cells (26 SOD1 and 44 CTRL) were selected for analysis. These were further distinguished by the appearance of a specific current pattern.

Two distinct current patterns were identified in $eGFP^+$ cells: a complex current profile and a passive current pattern (**Figure 22**). However, the complex pattern was observed only in 2 cells (1 SOD1, 1 CTRL). Both cells had highly negative RMP of -90 mV and membrane resistance (IR) around 65 MΩ. Given their low incidence, these cells were omitted from the analysis. Vast majority of cells (n = 68) were represented by the passive current pattern with variable RMP ranging from -50 to -92 mV and IR ranging between 15 and 170 MΩ.

After detailed analysis of these cells two different passive current patterns were identified: a "classic" passive current pattern represented by time- and voltage-independent K^+ conductance and weak K_{IR} currents, and an "altered" passive current pattern represented by time- and voltage-independent K^+ conductance with a reduction in inwardly rectifying K^+ (K_{IR}) currents and, in some cases, additional delayed outwardly rectifying currents, presumably delayed outwardly rectifying K^+ (K_{DR}) currents (**Figure 22**). Both passive current patterns were present in both SOD1 and CTRL cells, but their incidence differed between the two groups (**Figure 23**). There was an increased incidence of altered passive current pattern in SOD1 cells when compared to controls.

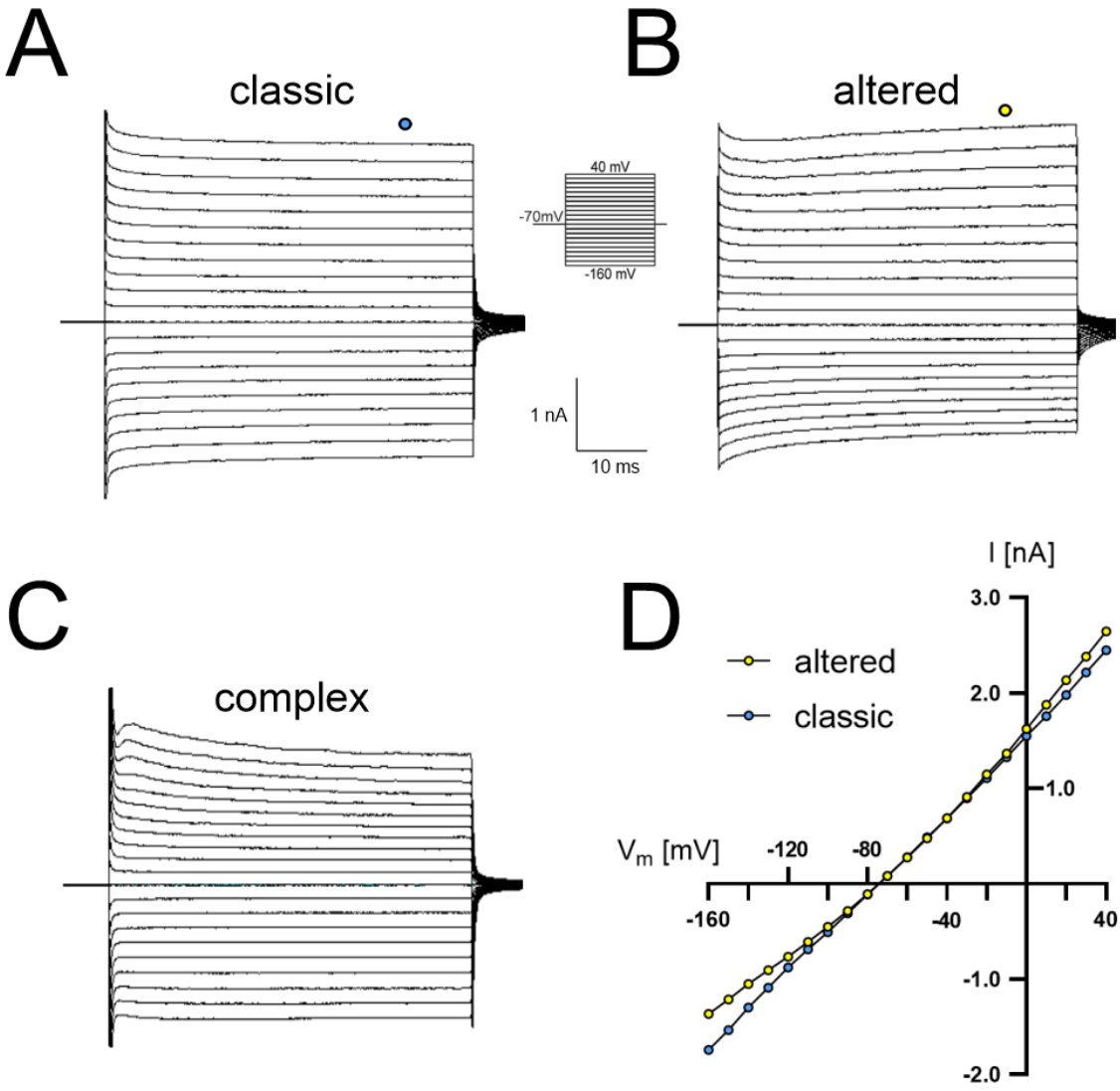

Fig. 22. Typical current profiles of eGFP$^+$ cells obtained by hyper- and depolarizing the cell membrane from a holding potential of -70 mV to potentials ranging from -160 to 40 mV. (A) eGFP$^+$ cells displaying a predominant time- and voltage-independent K^+ (passive) current. **(B)** eGFP$^+$ cells displaying a combined passive current with reduction of K_{IR} and gain of K_{DR} current. **(C)** eGFP$^+$ cells displaying combined expression of K_{IR}, K_{DR} and K_A current. **(D)** Current-voltage (I-V) plot of GFAP$^+$ cells with currents displayed in A and B. Duration of the pulse was 50 ms. The values of membrane current (I) were taken at 40ms as indicated by points).

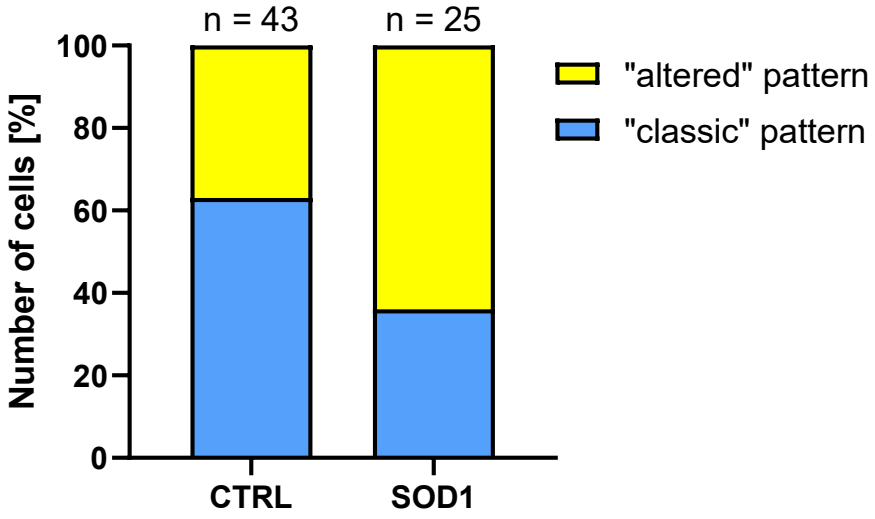

Fig. 23. Incidence of classic and altered passive current patterns recorded from eGFP$^+$ cells. There is an increased incidence of altered passive current pattern in SOD1 cells compared to controls.

6.2.2 Electrophysiological properties

Following parameters were compared: membrane potential (V_m), input resistance (IR), membrane capacitance (Cm) and current densities of K_{IR} and K_{DR} (**Table 5**).

Table 5. Electrophysiological properties of eGFP$^+$ cells recorded *in situ* from the cortex of GFAP-CTRL and GFAP-SOD1 mice.

Passive cells	CTRL	SOD1	n	
			CTRL	SOD1
V_m [mV]	-67.77 ± 1.70	-70.48 ± 2.76	43	25
IR [MΩ]	63.30 ± 5.72	89.16 ± 11.24	43	25
Cm [pF]	39.23 ± 5.40	26.15 ± 6.86	43	25
K_{IR} [pA/pF]	2.24 ± 0.53	1.37 ± 0.61	20	5
K_{DR} [pA/pF]	5.79 ± 0.88	18.96 ± 3.22	29	21

Out of 43 CTRL cells, 20 had detectable K_{IR} current and 29 had detectable K_{DR} current. Only 5 out of 25 SOD1 cells recorded had barely detectable K_{IR} currents, but most of them (21 out of 25) had detectable K_{DR} currents.

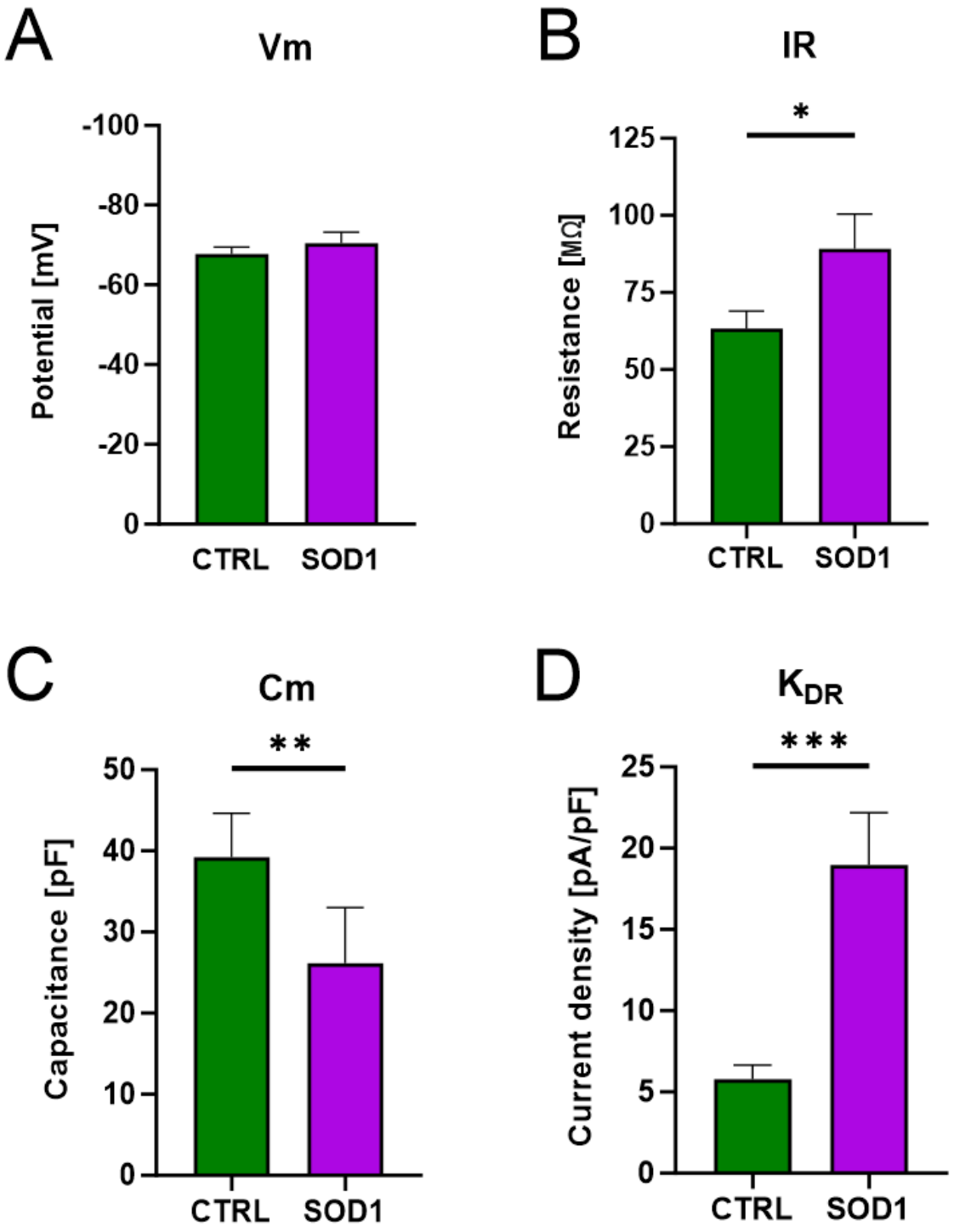

Fig. 24. Analysis of electrophysiological properties of eGFP$^+$ cells recorded *in situ* from the cortex of GFAP-CTRL and GFAP-SOD1 mice. (A) There is not a significant difference in membrane potentials. **(B,C,D)** There are significant differences in input resistance, membrane capacitance and amplitude of K_{DR} currents. Values of *($p < 0.05$) were considered significant, **($p < 0.01$) very significant and ***($p < 0.001$) extremely significant.

There was no significant difference in membrane potential between CTRL and SOD1 cells. However, SOD1 cells had significantly higher input resistance and lower membrane capacitance than CTRL cells. Interestingly, K_{DR} current density in SOD1 cells was increased 3.5-fold when compared to CTRL cells (**Figure 24**). Due to low incidence of K_{IR} currents in SOD1 cells, no statistical comparison was performed. Possible implications of these findings are discussed in chapter 8.

6.2.3 Immunohistochemical analysis of Kir4.1 channel

Based on the low incidence of K_{IR} currents in SOD1 cells, we further explored expression of Kir4.1, which is considered to be a predominant Kir channel in astrocytes, in the motor cortex of GFAP-CTRL and GFAP-SOD1 mice (**Figure 25**). There were no changes in Kir4.1 immunostaining between 1M controls and mutants. However the same comparison in 3M mice revealed decreased Kir4.1 immunostaining in GFAP-SOD1 mice compared to GFAP-CTRL.

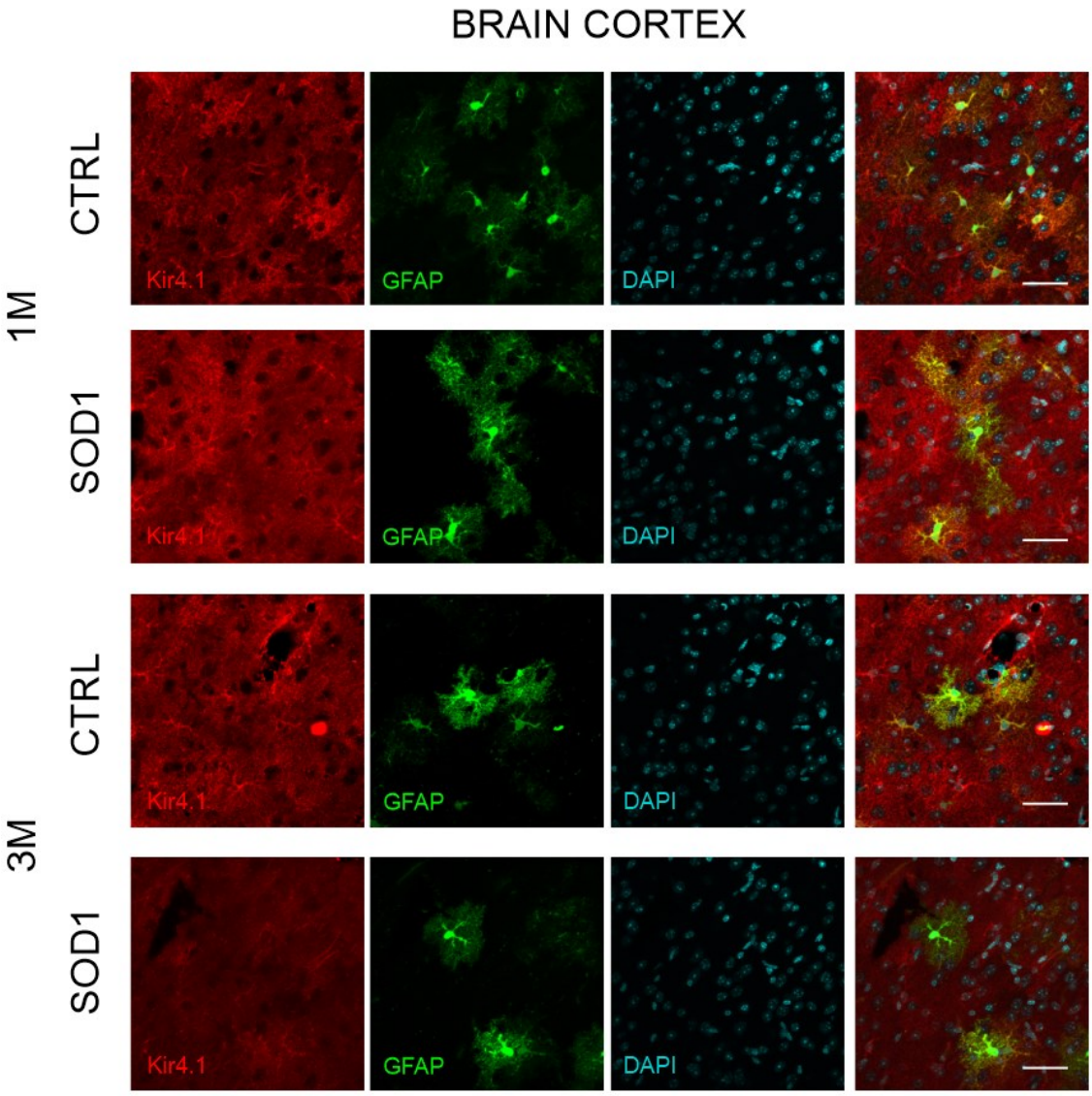

Fig. 25 Immunohistochemical staining of brain cortex slices isolated from GFAP-CTRL and GFAP-SOD1 mice. There are no differences in Kir4.1 channel expression between controls and GFAP-SOD1 mice and the controls in the cortex of 1M old mice. There is an increased expression of Kir4.1 channel in the cortex of 3M old GFAP-SOD1 mice when compared to controls. Bars: 40 μm.

7 Discussion

First part of this thesis focused on the analysis of the mouse models. Two mouse models were used for the experiments: the C57Bl6-SOD1 model purchased from Jackson laboratory and the mbGFAP-SOD1 model that we generated from the FVB-GFAP/eGFP model obtained directly from the authors of the original article describing this model (Nolte et al. 2001). We focused on the differences occurring at 14th week of age (3 months), because mice at this age are used in other experiments (see further text). Our first question was whether the generated model exerts ALS-like symptoms at all.

According to our expectations, mutant mice exhibited a typical ALS-like phenotype represented by decreased gain in weight, gradual paralysis and tremors in the hind limbs when suspended by the tail. This phenotype was described by the authors of the original study (Gurney et al. 1994). On average, the control mice had higher weight than mutants. This difference can be seen in both strains and sexes and is most noticeable in GFAP-SOD1 females. Results from the sensorimotor tests confirmed the presence of ALS-like phenotype.

The results from wire grid hang test show gradual decrease in motor strength. These changes are present in both strains and sexes with some differences between the groups (discussed below). For Bl6-SOD1 mice, our observations are comparable to results from studies conducted on this model (C. Zhou et al. 2007; Oliván et al. 2014), though other studies often describe later onset and sharper rate in performance decline (Miana-Mena et al. 2005; Alves et al. 2011). This variance can be partially explained by the use of different Bl6 substrains or by the differences in methodological approaches. Possible effects of the laboratory environment should be also taken into consideration. Studies have shown that the phenotype observed in behavioral tests can be affected by various environmental factors such as presence of cage enrichment (Chesler et al. 2002) or differences in animal handling (Kulesskaya, Rauvala, and Voikar 2011). Though all animals were treated equally and were housed and tested under the same conditions, we cannot exclude the possibility that the environment differently affects motor function of mice from different strains, as shown by (Võikar et al. 2001).

Similar results were observed in the rotarod test. Rotarod test is designed to assess motor coordination and balance rather than pure physical strength. Changes in rotarod test performance were generally detectable later than changes in strength, which is in line

with the progression of ALS symptoms. This fact likely explains the observation that Bl6-SOD1 females showed no decrease in rotarod performance at 14th week of age. Motor deficits were present in GFAP-SOD1 mice with similar onset but accelerated decline in performance in both tests. Thus, we confirmed the presence of ALS-like phenotype in both strains.

Importantly, it should be noted that the presented data from this study represent average values for different groups of mice. However, there were great differences in the performance values and weight between individuals. For example, one of the Bl6-SOD1 males showed decreased performance in the wire grid hang test since the first week of testing and became almost completely paralyzed by the age of 14 weeks. Another Bl6-SOD1 male on the other hand showed no decrease in performance over time at all. Possible consequences of this observation are discussed below. Additionally, individuals from the same litter showed similar performance in most cases, suggesting a litter effect on the disease progression.

Our second question was whether there are differences between the models. It is important to note that the original FVB-GFAP/eGFP model has a different genetic background (FVB, “Albino”) than the C57Bl6-SOD1 model (C57Bl6, “Black”), therefore our double transgenic model has a mixed background. To limit the possible effect of background on the phenotype, a simple approach would be to backcross the double transgenic SOD1 males with females from the original C57Bl6 strain without the SOD1 mutation. However, this approach from our experience results in decreased litter sizes and more importantly, in reduced number of mice expressing eGFP and to diminished expression of eGFP over time. On the other hand, mice on FVB background carry a mutation in the *PDE6B* gene (phosphodiesterase 6B, cGMP, rod receptor, beta polypeptide), which in homozygotes results in progressive retinal degeneration and loss of sight, making them less suitable for behavioral tests (Chang et al. 2013). To circumvent these problems as much as possible, we therefore established and maintain an inbred strain on a mixed background.

The use of different backgrounds is important because this work is a part of a larger project. Apart from patch clamp recording, the double transgenic strain is also used in other experiments, specifically 3D morphometry and calcium imaging. Part of the project are single-cell RNA sequencing experiments; however, those are performed on

the original C57Bl6-SOD1 strain. The idea was whether both strains can be used for all the experiments at specific time-points (1M, 3M), i.e. whether animals studied at these time-points have comparable characteristics on the gross phenotype level (strength, coordination, weight) and on the cellular level (features characteristic for ALS – loss of motor neurons, astrogliosis). The important question regarding this thesis was whether the data gathered from experiments with mbGFAP-SOD1 mice can be compared with the data obtained from single-cell RNA sequencing. Our third question was whether there were differences between sexes.

The initial hypothesis was that the background does not affect the gross phenotype and animals from both strains can be expected to have similar performance when compared at the same time-points in life. However, the results from behavioral testing proved this statement not to be entirely true. First signs of the differences between the strains came from our observations prior to the testing. Bl6-SOD1 mice were generally smaller and expressed relatively low activity. On the other hand, GFAP-SOD1 mice were generally bigger, active and showed increased resistance to handling, especially in the first weeks of the testing.

In this study and also in the studies mentioned above, Bl6-SOD1 males generally performed worse than Bl6-SOD1 females. This is likely thanks to their increased body weight, as body weight inversely correlates with rotarod performance (Mao et al. 2015) and likely affects wire grid hang test performance as well. GFAP-SOD1 mice performed generally worse in both tests. In wire grid hang test, they showed slightly delayed onset compared to Bl6-SOD1 mice but faced an accelerated decline in motor functions. Perhaps the most striking difference can be seen between the females. While performance of Bl6-SOD1 females is relatively unaffected even in the last week of testing, this cannot be said for the GFAP-SOD1 females, which show substantial decline in motor function in both tests. Given the fact that GFAP mice generally have higher weight than Bl6 mice (both mutants and controls), it was rather unsurprising that they performed worse in both tests. Most surprisingly and unlike in Bl6-SOD1 mice, GFAP-SOD1 females performed worse than GFAP-SOD1 males. This was an interesting and unexpected observation. As seen in **Figure 7** (chapter 4.2.2), specificity of the rotarod is limited amount of space for the mice to remain in. Weight and therefore body size can thus have an effect on the performance when motor functions are impaired. Though this fact could explain the differences in performance between females (both sexes in general), it cannot explain the observed

difference in performance between GFAP-SOD1 males and females and also does not explain the observations from wire grid hang test, where the amount of space is far less limited. It is also possible that the visual impairment characteristic for the FVB strains (discussed above) has an effect on the GFAP-SOD1 mice performance. However, our mbGFAP mice reacted normally to the visual stimuli, we therefore assume that the visual impairment is diminished or has a later onset/slower progression in mice with mixed background. Again, though this fact could explain the differences in performance between females (both sexes in general), it cannot explain the observed difference in performance between GFAP-SOD1 males and females.

An interplay between muscle volume, strength and weight likely plays a role here and it should be considered when trying to explain this phenomenon. Unfortunately, the literature regarding the topic of motor function dysfunction in mice with FVB or mixed FVB background is very limited. One study by Pan et al. (2012) explored the differences between C57Bl6 and FVB strains with SOD1 mutation, while also comparing the effect of different mutations in this protein, specifically G93A and H64R. In agreement with this work are our observations of differences in weight. However, the authors focused solely on the differences in weight and survival probability and thus this cannot explain the differences between the sexes observed in both tests. Another study (Võikar et al. 2001) exploring the effect of strain and gender on motor performance of healthy mice showed differences in the rotarod performance between FVB and Bl6 males and females. In agreement with our data is the finding that Bl6 mice perform better than FVB mice. On the other hand, this study also reported better performance in FVB females than in males. However, this study used different methodological approach and the results from healthy mice cannot be directly translated into SOD1 mutants. No other studies exploring the motor function or its impairment in FVB mice are known to author of this thesis.

While almost none of the studies focused on differences in motor function, studies describing other aspects of differences between C57Bl6 and FVB backgrounds exist and could partially clarify the unexpected phenotype observed in mbGFAP mice. For example, one study described the effect of crossbreeding on cytokine expression (Szade et al. 2015). Interestingly, FVB mice have been found to be more susceptible to induced excitotoxicity than Bl6 mice (Schauwecker and Steward 1997; Schauwecker 2002). Sellers et al. (2012) described immunological differences between various commonly

used mice strains. This could be of possible significance because ALS phenotype also results from impaired communication between microglia and other cell types (reviewed by Geloso et al. 2017). We therefore hypothesize that the phenotype differences observed in males and females between strains could arise from sex-dependent differences in the immune system.

While the original purpose of the behavioral tests was to confirm similar phenotypic progression in our double transgenic model, our findings from this part of the study embraced us to further explore how different genetic backgrounds and gender affect the phenotype in our SOD1 models. Additionally, we extended the duration of both tests by four weeks and employed another method to assess motor dysfunction. We will also characterize the weight differences and the degree of muscle degeneration in the mutants by assessing the weight of main muscle groups and measure the ratio of muscles to body fat. It is likely that our findings will have functional consequences. Given the substantial differences between strains, sexes and most importantly between individuals, we will consider the possibility to adapt different experimental approach. Animals will be employed based on their performance in sensorimotor tests (or by other measures) prior to the experiment rather than their age, where simple split of the animals into two or three groups based on the phenotypical progression would be sufficient.

To further confirm the presence of ALS-like phenotype on the cellular level, we searched for the features in the CNS typical for ALS, specifically astrogliosis and loss of motor neurons. Specifically for the SOD1(G93A) model, astrogliosis occurs at the onset of symptoms after the loss of motor neurons can be detected. Furthermore, changes in the spinal cord are more apparent than the changes in the cortex (Gurney et al. 1994; Hall et al. 1998; Levine et al. 1999). Therefore, we first decided to analyze the spinal cord of 3M old mice. Indeed, we observed clear loss of motor neurons in the spinal cord ventral horns. We also looked for this feature in the cortex of 1M old mice, as this age and CNS region are relevant to this work, and we did not see any apparent changes.

We obtained the same results when we looked for signs of reactive astrogliosis, characterized by increased GFAP expression and hypertrophy. In relation to this thesis, it is important to make a note on GFAP and astrocyte reactivity. GFAP is generally accepted as a marker used for identification of reactive astrocytes. However, results from studies conducted in the last years question the validity of this assumption. This is for

several reasons. Not all reactive astrocytes express GFAP to the same extent (Liddelow and Barres 2017). Furthermore, some cells express GFAP-coding mRNA but not the protein (M. Zhou and Kimelberg 2000; Nolte et al. 2001), and in the FVB-GFAP/eGFP model, eGFP expression does not ultimately overlap with GFAP immunostaining (M. Zhou and Kimelberg 2000; Nolte et al. 2001). Astrocytes differently expressing GFAP are also present in the healthy CNS (Walz and Lang 1998). In addition, expression of GFAP in CNS changes during ontogenesis and differs both between and within specific CNS structures (Kohama et al. 1995; Yoshida et al. 1996). GFAP expression also changes after CNS injury and during pathological CNS states. To add to the complexity of this problem, OPCs have been shown to differentiate into GFAP-expressing astrocytes under specific pathological conditions (Honsa et al. 2012; Hackett et al. 2018). Taken together, the use of GFAP as a marker for astrocyte identification has its limitations, which should be accounted for when designing an experiment. For more information on the complex topic of GFAP and astrocyte reactivity see the works of Hol and Pekny (Middeldorp and Hol 2011; Hol and Pekny 2015; Pekny and Pekna 2016). Though use of GFAP as an astrocytic marker for the detection of astrogliosis is relevant, GFAP-expressing astrocytes do not represent majority of astrocytes found in the CNS and data gathered from this specific subpopulation cannot be directly extrapolated to all astrocytes. Therefore, we will consider the use of other astrocytic markers in the future.

Last part of this thesis focused on the electrophysiological properties of astrocytes. First, it is necessary to clarify the specificities of this study. Our goal was to explore whether any alterations in properties of astrocytes can be seen in the pre-symptomatic stage of the disease (1M), because it is necessary to disclose subtle changes, before they can actually drive the disease progression. We focused specifically on the motor cortex for two reasons. First, ALS is a disease of motor neurons, so the motor cortex is the CNS region where the pathology appears. Second, the ALS research mostly focuses on the changes in the spinal cord, as this is the region where the changes are the most apparent, and the cortex is often overlooked. It is also important to distinguish whether the recordings are performed *in vitro*, *in situ* or *in vivo*. Studies *in vitro* face validity issues, as cell cultures present a system that has lost its connection to the natural environment of the brain. Regarding astrocytes electrophysiology, this could for example affect the syncytial K^+ conduction. There might also be a lost information in relation to subtle differences between heterogenic astrocytic subpopulations, even when isolated from

specific brain structure. Though more relevant to the physiological state of the brain, *in situ* electrophysiological studies are more technically difficult to execute and are usually carried out at room temperatures, which can substantially affect the activity of some channels and ultimately electrophysiological properties of cells in general. This was demonstrated for example for some K_{2P} (D. Kang, Choe, and Kim 2005) and K_v channels (F. Yang and Zheng 2014). Another important aspect that needs to be taken into consideration when comparing results from different studies is the astrocyte heterogeneity. Astrocytic subpopulations with distinct electrophysiological properties can be found throughout the brain and even within specific structures, including the brain cortex (reviewed by Matias, Morgado, and Gomes 2019). This study specifically focused on the $eGFP^+$ astrocytes found in cortical layers V and VI.

On average, $eGFP^+$ cells recorded from slices of GFAP-CTRL mice (CTRL cells) and those from GFAP-SOD1 mice (SOD1 cells) had comparable membrane potentials. SOD1 cells had higher input resistance and lower membrane capacitance compared to CTRL cells. Simplified, input resistance is an indicator of amplitude of currents that flow through the cell membrane. It depends on the shape and size of the cell and depends on density of ion channels in the membrane. Therefore, increased membrane resistance can result from decrease of the cell size and/or from decreased amount of ion channels in the membrane. These however are concomitant states, since the volume (and so the size) of astrocytes dynamically changes in response to alterations in concentration and flow of ions across the membrane, which is in turn determined by the activity of ion channels and transporters. Membrane capacitance is an indicator of cell size and directly proportional to membrane surface area/cell volume. Our data therefore suggest a decrease in the cell surface/volume of SOD1 cells, which is in line with the increase in input resistance. This can partially be explained by decreased influx of water into the SOD1 cells that results from impaired K^+ uptake. It is also consistent with finding that astrogliosis in ALS occurs later in the symptomatic phase and astrocytes in the pre-symptomatic phase do not show hypertrophy (Tu et al. 1996; Hall et al. 1998). Of note, early stages of Alzheimer's disease are accompanied by astrocyte atrophy (Olabarria et al. 2010), so it is possible that shrinkage of astrocytes might represent an early pathophysiological sign in some neurodegenerative diseases including ALS.

Recordings from astrocytes in the present work revealed only the presence of a passive current pattern with alterations in K_{IR} and K_{DR} currents in some cells. This is in

contrast to earlier study from our laboratory that reported presence of $eGFP^+$ astrocytes with different current profiles in the brain cortex (Anděrová et al. 2004). This could be partially explained by the fact that the incidence of electrophysiological phenotypes likely changes throughout the development, with mature astrocyte having passive current profile (Schools, Zhou, and Kimelberg 2006; M. Zhou, Schools, and Kimelberg 2006). Other possible explanation is that astrocytes vary in electrophysiological phenotypes between cortical layers (Lanjakornsiripan et al. 2018; Bayraktar et al. 2020).

The incidence of the altered current pattern varied between CTRL and SOD1 cells. This would suggest an ongoing cell process present in the healthy cells that is either amplified or downregulated in the mutant cells. The alterations in the passive profile are represented by the loss of K_{IR} and gain in K_{DR} current. Loss of K_{IR} current has been previously described in ALS astrocytes as Kir4.1, a predominant Kir channel in astrocytes, was shown to be downregulated in ALS pathology (Kaiser et al. 2006; Bataveljić et al. 2012). We also confirmed downregulation of Kir4.1 in the cortex by immunostaining, however the changes were not apparent in the 1M old mice. Downregulation of Kir4.1 contributes to increased neuronal excitability as it interferes with the astrocyte ability to regulate the amount of K^+ in the synaptic cleft during synaptic activity (Djukic et al. 2007). It should also be noted that while astrocytes express various ion channels, those are often found localized into the perisynaptic processes and astrocytic endfeet and are found in much lesser densities on the cell body. Different sensitivity of the methods could partially explain the fact that we detected changes in the incidence of K_{IR} currents in 1M old mice but did not see any changes after immunostaining. This phenomenon will require further exploration.

Unlike K_{IR} currents, there is very limited information about the presence of K_{DR} currents in passive astrocytes and no information regarding this topic in ALS. MacFarlane and Sontheimer (1997) showed the increase in K_{DR} and decrease in K_{IR} currents in proliferating astrocytes after *in vitro* scarring. Similar phenotype was observed by Bordey et al. (2001) in a model of induced cortical freeze lesion. Anděrová et al. (2004) have also confirmed this phenotype in a model of cortical stab wound, which correlated with proliferating astrocytes. Incidence of astrocytes with increased K_{DR} density gradually increased in time after stab wound induction. It is possible that such increases in K_{DR} current densities and also their increased incidence in SOD1 cells might be caused by proliferation unrelated to the neuronal tissue damage, but rather to proliferation related to

astrocyte reactivity. This study also confirmed that these currents are mainly carried by K^+. Other studies have shown that changes in expression of Kir4.1 correlate with cell cycle progression (Higashimori and Sontheimer 2007; E. Arai et al. 2015).

There are no clear answers to the question of K_{DR} current origin. It is likely that it is caused by increased expression of specific K_v channels, as astrocytes perform mainly K^+ conductance. Physiological function of these currents in astrocytes remains unknown. In neurons, K_v channels activate at positive potentials after membrane depolarization and allow for its quick repolarization. However, as astrocytes have a strong K^+ buffering capacity and rarely (if at all) change their membrane potential to positive values, the purpose of these channels in astrocytes remains elusive. Rather than having a function in regulation of K^+ concentration, we hypothesize that (presumed) increased expression of these channels in astrocytes could have a role in signaling in proliferation and/or cell cycle progression, as it has been previously described for $K_v1.3$ and $K_v1.5$ (Kotecha and Schlichter 1999; Jiménez-Pérez et al. 2016). Given the fact that astrocytes have been shown to express various K_v channels, we decided not to further explore the identity of K_{DR} currents until the results from the single-cell RNA sequencing experiments become available later this year. Still the option of other channels contributing to this current cannot be completely excluded. Some chloride channels such as ClC-4 and ClC-5 are known to carry outward current at positive potentials (Friedrich, Breiderhoff, and Jentsch 1999), however those have not been shown to be expressed in astrocytes under physiological nor pathological conditions. On the same note: though inward currents are mediated mostly by Kir4.1/Kir5.1 subunits, contribution of other Kir channels or other channels such as HCN channels cannot be completely excluded.

To further explore the topic of changes in astrocyte electrophysiology, we will compare the data from this study with data gathered from astrocytes in the symptomatic stage (3 months). We will discuss the option of *in situ* staining of astrocytes to circumvent the limitations of the GFAP/eGFP model described above. We will also compare the patch clamp data with data gathered from 3D morphometry and calcium-imaging experiments and most importantly, with the data from single-cell RNA sequencing.

8 Conclusion

In this study we examined the phenotype of the newly produced double transgenic strain used for visualization of astrocytes in the pathology of ALS. We confirmed that on the whole-organism level there are differences between control mice and mice carrying the SOD1 mutation. We also observed differences between and among both sexes and also between the double transgenic and the original SOD1 model. We confirmed that the double transgenic model exhibits signs of ALS progression (loss of motor neurons, astrogliosis) on the cellular level and thus further confirmed validity of the model. Moreover, we explored the differences in basic electrophysiological properties and changes in the ionic currents and current patterns of astrocytes recorded *in situ* from the motor cortex of 1M old mice carrying the SOD1 mutation and controls. Indeed, we observed changes in the electrophysiological properties and currents that might be of physiological relevance. While the loss of Kir4.1 channel has been previously described in ALS pathology and likely affects the astrocyte function, gain of K_{DR} current has been previously described only in a limited amount of studies and its purpose remains unclear. Our findings will be further examined and compared to data gathered from other experiments. We will also discuss the possibility of alternative methodical approaches and employment of a different model for astrocyte visualization.

9 References

*Abbott, Geoffrey W. 2020. “KCNQs: Ligand- and Voltage-Gated Potassium Channels.” *Frontiers in Physiology*. https://doi.org/10.3389/fphys.2020.00583.

Adermark, Louise, and David M. Lovinger. 2008. “Electrophysiological Properties and Gap Junction Coupling of Striatal Astrocytes.” *Neurochemistry International* 52 (7): 1365–72. https://doi.org/10.1016/j.neuint.2008.02.006.

*Allen, Nicola J., and David A. Lyons. 2018. “Glia as Architects of Central Nervous System Formation and Function.” *Science*. https://doi.org/10.1126/science.aat0473.

Alves, Chrystian Junqueira, Luana Pereira De Santana, Angélica Janaína Dias Dos Santos, Gabriela Pintar De Oliveira, Tatiana Duobles, Juliana Milani Scorisa, Roberto Sérgio Martins, Jessica Ruivo Maximino, and Gerson Chadi. 2011. “Early Motor and Electrophysiological Changes in Transgenic Mouse Model of Amyotrophic Lateral Sclerosis and Gender Differences on Clinical Outcome.” *Brain Research* 1394 (June): 90–104. https://doi.org/10.1016/j.brainres.2011.02.060.

Anděrová, Miroslava, Tatiana Antonova, David Petřík, Helena Neprašová, Alexandr Chvátal, and Eva Syková. 2004. “Voltage-Dependent Potassium Currents in Hypertrophied Rat Astrocytes after a Cortical Stab Wound.” *GLIA* 48 (4): 311–26. https://doi.org/10.1002/glia.20076.

Anderson, Mark A, Joshua E Burda, Yilong Ren, Yan Ao, Timothy M. O’Shea, Riki Kawaguchi, Giovanni Coppola, Baljit S Khakh, Timothy J Deming, and Sofroniw V Michael. 2016. “Astrocyte Scar Formation Aids CNS Axon Regeneration.” *Nature* 532 (7598): 195–200. https://doi.org/10.1038/nature17623.

Anlauf, Enrico, and Amin Derouiche. 2013. “Glutamine Synthetase as an Astrocytic Marker: Its Cell Type and Vesicle Localization.” *Frontiers in Endocrinology* 4 (October): 144. https://doi.org/10.3389/fendo.2013.00144.

Arai, Eisuke, Yukihiro Baba, Toshiro Iwagawa, Hiroshi Kuribayashi, Yujin Mochizuki, Akira Murakami, and Sumiko Watanabe. 2015. “Ablation of Kcnj10 Expression in Retinal Explants Revealed Pivotal Roles for Kcnj10 in the Proliferation and Development of Müller Glia.” *Molecular Vision* 21 (February): 148–59. https://pubmed.ncbi.nlm.nih.gov/25684980/.

Arai, Tetsuaki, Masato Hasegawa, Haruhiko Akiyama, Kenji Ikeda, Takashi Nonaka, Hiroshi Mori, David Mann, et al. 2006. “TDP-43 Is a Component of Ubiquitin-Positive Tau-Negative Inclusions in Frontotemporal Lobar Degeneration and Amyotrophic Lateral Sclerosis.” *Biochemical and Biophysical Research Communications* 351 (3): 602–11. https://doi.org/10.1016/j.bbrc.2006.10.093.

*Araque, Alfonso, Vladimir Parpura, Rita P. Sanzgiri, and Philip G. Haydon. 1999. “Tripartite Synapses: Glia, the Unacknowledged Partner.” *Trends in Neurosciences*. https://doi.org/10.1016/S0166-2236(98)01349-6.

Ayala, Youhna M., Paola Zago, Andrea D’Ambrogio, Ya Fei Xu, Leonard Petrucelli, Emanuele Buratti, and Francisco E. Baralle. 2008. “Structural Determinants of the Cellular Localization and Shuttling of TDP-43.” *Journal of Cell Science* 121 (22): 3778–85. https://doi.org/10.1242/jcs.038950.

*Bak, Lasse K., Arne Schousboe, and Helle S. Waagepetersen. 2006. “The Glutamate/GABA-Glutamine Cycle: Aspects of Transport, Neurotransmitter Homeostasis and Ammonia Transfer.” *Journal of Neurochemistry*. https://doi.org/10.1111/j.1471-4159.2006.03913.x.

Barbour, Boris, Helen Brew, and David Attwell. 1988. “Electrogenic Glutamate Uptake in Glial Cells Is

Activated by Intracellular Potassium." *Nature*. https://doi.org/10.1038/335433a0.

Bataveljić, Danijela, Ljiljana Nikolić, Milena Milosević, Nataša Todorović, and Pavle R. Andjus. 2012. "Changes in the Astrocytic Aquaporin-4 and Inwardly Rectifying Potassium Channel Expression in the Brain of the Amyotrophic Lateral Sclerosis SOD1G93A Rat Model." *GLIA* 60 (12): 1991–2003. https://doi.org/10.1002/glia.22414.

Bayraktar, Omer Ali, Theresa Bartels, Staffan Holmqvist, Vitalii Kleshchevnikov, Araks Martirosyan, Damon Polioudakis, Lucile Ben Haim, et al. 2020. "Astrocyte Layers in the Mammalian Cerebral Cortex Revealed by a Single-Cell in Situ Transcriptomic Map." *Nature Neuroscience* 23 (4): 500–509. https://doi.org/10.1038/s41593-020-0602-1.

Begum, Rahima, Yamina Bakiri, Kirill E. Volynski, and DImitri M. Kullmann. 2016. "Action Potential Broadening in a Presynaptic Channelopathy." *Nature Communications* 7 (1): 12102. https://doi.org/10.1038/ncomms12102.

Benfenati, Valentina, Marco Caprini, Melania Dovizio, Maria N. Mylonakou, Stefano Ferroni, Ole P. Ottersen, and Mahmood Amiry-Moghaddam. 2011. "An Aquaporin-4/Transient Receptor Potential Vanilloid 4 (AQP4/TRPV4) Complex Is Essential for Cell-Volume Control in Astrocytes." *Proceedings of the National Academy of Sciences of the United States of America* 108 (6): 2563–68. https://doi.org/10.1073/pnas.1012867108.

Biel, Martin, Christian Wahl-Schott, Stylianos Michalakis, and Xiangang Zong. 2009. "Hyperpolarization-Activated Cation Channels: From Genes to Function." *Physiological Reviews*. https://doi.org/10.1152/physrev.00029.2008.

Bissaro, Maicol, Stephanie Federico, Veronica Salmaso, Mattia Sturlese, Giampiero Spalluto, and Stefano Moro. 2018. "Targeting Protein Kinase CK1δ with Riluzole: Could It Be One of the Possible Missing Bricks to Interpret Its Effect in the Treatment of ALS from a Molecular Point of View?" *ChemMedChem* 13 (24): 2601–5. https://doi.org/10.1002/cmdc.201800632.

*Blanco-Suárez, Elena, Alison L.M. Caldwell, and Nicola J. Allen. 2017. "Role of Astrocyte–Synapse Interactions in CNS Disorders." *Journal of Physiology* 595 (6): 1903–16. https://doi.org/10.1113/JP270988.

Boillée, Séverine, Koji Yamanaka, Christian S. Lobsiger, Neal G. Copeland, Nancy A. Jenkins, George Kassiotis, George Kollias, and Don W. Cleveland. 2006. "Onset and Progression in Inherited ALS Determined by Motor Neurons and Microglia." *Science* 312 (5778): 1389–92. https://doi.org/10.1126/science.1123511.

Bordey, A., S. A. Lyons, J. J. Hablitz, and H. Sontheimer. 2001. "Electrophysiological Characteristics of Reactive Astrocytes in Experimental Cortical Dysplasia." *Journal of Neurophysiology* 85 (4): 1719–31. https://doi.org/10.1152/jn.2001.85.4.1719.

*Bradbury, Elizabeth J., and Emily R. Burnside. 2019. "Moving beyond the Glial Scar for Spinal Cord Repair." *Nature Communications*. https://doi.org/10.1038/s41467-019-11707-7.

Brohawn, Stephen G., Josefina Del Mármol, and Roderick MacKinnon. 2012. "Crystal Structure of the Human K2P TRAAK, a Lipid- and Mechano-Sensitive K+ Ion Channel." *Science* 335 (6067): 436–41. https://doi.org/10.1126/science.1213808.

Bruijn, Lucie I., Megan K. Houseweart, Shinsuke Kato, Karen L. Anderson, Scott D. Anderson, Eisaku Ohama, Andrew G. Reaume, Rick W. Scott, and Don W. Cleveland. 1998. "Aggregation and Motor Neuron Toxicity of an ALS-Linked SOD1 Mutant Independent from Wild-Type SOD1." *Science* 281 (5384): 1851–54. https://doi.org/10.1126/science.281.5384.1851.

Burberry, Aaron, Naoki Suzuki, Jin Yuan Wang, Rob Moccia, Daniel A. Mordes, Morag H. Stewart, Satomi Suzuki-Uematsu, et al. 2016. "Loss-of-Function Mutations in the C9ORF72 Mouse Ortholog Cause Fatal Autoimmune Disease." *Science Translational Medicine* 8 (347): 347ra93-347ra93. https://doi.org/10.1126/scitranslmed.aaf6038.

Bushong, Eric A., Maryann E. Martone, Ying Z. Jones, and Mark H. Ellisman. 2002. "Protoplasmic Astrocytes in CA1 Stratum Radiatum Occupy Separate Anatomical Domains." *Journal of Neuroscience* 22 (1): 183–92. https://doi.org/10.1523/jneurosci.22-01-00183.2002.

Cahoy, John D., Ben Emery, Amit Kaushal, Lynette C. Foo, Jennifer L. Zamanian, Karen S. Christopherson, Yi Xing, et al. 2008. "A Transcriptome Database for Astrocytes, Neurons, and Oligodendrocytes: A New Resource for Understanding Brain Development and Function." *Journal of Neuroscience* 28 (1): 264–78. https://doi.org/10.1523/JNEUROSCI.4178-07.2008.

Cataldo, Anne M., and Richard D. Broadwell. 1986. "Cytochemical Identification of Cerebral Glycogen and Glucose-6-Phosphatase Activity under Normal and Experimental Conditions. II. Choroid Plexus and Ependymal Epithelia, Endothelia and Pericytes." *Journal of Neurocytology* 15 (4): 511–24. https://doi.org/10.1007/BF01611733.

Chang, Bo, Ron Hurd, Jieping Wang, and Patsy Nishina. 2013. "Survey of Common Eye Diseases in Laboratory Mouse Strains." *Investigative Ophthalmology and Visual Science* 54 (7): 4974–81. https://doi.org/10.1167/iovs.13-12289.

Chaudhry, Farrukh A., Knut P. Lehre, Menno van Lookeren Campagne, Ole P. Ottersen, Niels C. Danbolt, and Jon Storm-Mathisen. 1995. "Glutamate Transporters in Glial Plasma Membranes: Highly Differentiated Localizations Revealed by Quantitative Ultrastructural Immunocytochemistry." *Neuron* 15 (3): 711–20. https://doi.org/10.1016/0896-6273(95)90158-2.

*Chen, Sheng, Pavani Sayana, Xiaojie Zhang, and Weidong Le. 2013. "Genetics of Amyotrophic Lateral Sclerosis: An Update." *Molecular Neurodegeneration*. BioMed Central. https://doi.org/10.1186/1750-1326-8-28.

Chesler, Elissa J., Sonya G. Wilson, William R. Lariviere, Sandra L. Rodriguez-Zas, and Jeffrey S. Mogil. 2002. "Influences of Laboratory Environment on Behavior." *Nature Neuroscience*. https://doi.org/10.1038/nn1102-1101.

Chiang, Po Min, Jonathan Ling, Yun Ha Jeong, Donald L. Price, Susan M. Aja, and Philip C. Wong. 2010. "Deletion of TDP-43 down-Regulates Tbc1d1, a Gene Linked to Obesity, and Alters Body Fat Metabolism." *Proceedings of the National Academy of Sciences of the United States of America* 107 (37): 16320–24. https://doi.org/10.1073/pnas.1002176107.

Chiu, Arlene Y., Ping Zhai, Mauro C. Dal Canto, Theresa M. Peters, Young W. Kwon, Susan M. Prattis, and Mark E. Gurney. 1995. "Age-Dependent Penetrance of Disease in a Transgenic Mouse Model of Familial Amyotrophic Lateral Sclerosis." *Molecular and Cellular Neurosciences* 6 (4): 349–62. https://doi.org/10.1006/mcne.1995.1027.

Chu, Kuo Chang, Cheng Di Chiu, Tsan Ting Hsu, Yu Ming Hsieh, Yu Yin Huang, and Cheng Chang Lien. 2010. "Functional Identification of an Outwardly Rectifying PH- and Anesthetic-Sensitive Leak K+ Conductance in Hippocampal Astrocytes." *European Journal of Neuroscience* 32 (5): 725–35. https://doi.org/10.1111/j.1460-9568.2010.07323.x.

Chvátal, Alexandr, Thomas Berger, Ivan Voříšek, Richard K. Orkand, Helmut Kettenmann, and Eva Syková. 1997. "Changes in Glial K+ Currents with Decreased Extracellular Volume in Developing Rat White Matter." *Journal of Neuroscience Research* 49 (1): 98–106. https://doi.org/10.1002/(SICI)1097-4547(19970701)49:1<98::AID-JNR11>3.0.CO;2-0.

Chvátal, Alexandr, Andrea Pastor, Marianne Mauch, Eva Syková, and Helmut Kettenmann. 1995. "Distinct Populations of Identified Glial Cells in the Developing Rat Spinal Cord Slice: Ion Channel Properties and Cell Morphology." *European Journal of Neuroscience* 7 (1): 129–42. https://doi.org/10.1111/j.1460-9568.1995.tb01027.x.

Cui, N., L. R. Giwa, H. Xu, A. Rojas, L. Abdulkadir, and C. Jiang. 2001. "Modulation of the Heteromeric Kir4.1-Kir5.1 Channels by PCO2 at Physiological Levels." *Journal of Cellular Physiology* 189 (2): 229–36. https://doi.org/10.1002/jcp.10021.

Damme, Philip Van, Elke Bogaert, Maarten Dewil, Nicole Hersmus, Dora Kiraly, Wendy Scheveneels, Ilse Bockx, et al. 2007. "Astrocytes Regulate GluR2 Expression in Motor Neurons and Their Vulnerability to Excitotoxicity." *Proceedings of the National Academy of Sciences of the United States of America* 104 (37): 14825–30. https://doi.org/10.1073/pnas.0705046104.

Dezonne, Rômulo S., Joice Stipursky, Ana P. B. Araujo, Jader Nones, Mauro S. G. Pavão, Marimélia Porcionatto, and Flávia C. A. Gomes. 2013. "Thyroid Hormone Treated Astrocytes Induce Maturation of Cerebral Cortical Neurons through Modulation of Proteoglycan Levels." *Frontiers in Cellular Neuroscience* 7 (JUL): 125. https://doi.org/10.3389/fncel.2013.00125.

Diniz, Luan Pereira, Juliana Carvalho Almeida, Vanessa Tortelli, Charles Vargas Lopes, Pedro Setti-Perdigão, Joice Stipursky, Suzana Assad Kahn, et al. 2012. "Astrocyte-Induced Synaptogenesis Is Mediated by Transforming Growth Factor β Signaling through Modulation of d-Serine Levels in Cerebral Cortex Neurons." *Journal of Biological Chemistry* 287 (49): 41432–45. https://doi.org/10.1074/jbc.M112.380824.

Diniz, Luan Pereira, Isadora C.Pereira Matias, Matheus Nunes Garcia, and Flávia Carvalho Alcantara Gomes. 2014. "Astrocytic Control of Neural Circuit Formation: Highlights on TGF-Beta Signaling." *Neurochemistry International*. https://doi.org/10.1016/j.neuint.2014.07.008.

Djukic, Biljana, Kristen B. Casper, Benjamin D. Philpot, Lih Shen Chin, and Ken D. McCarthy. 2007. "Conditional Knock-out of Kir4.1 Leads to Glial Membrane Depolarization, Inhibition of Potassium and Glutamate Uptake, and Enhanced Short-Term Synaptic Potentiation." *Journal of Neuroscience* 27 (42): 11354–65. https://doi.org/10.1523/JNEUROSCI.0723-07.2007.

Doble, A. 1996. "The Pharmacology and Mechanism of Action of Riluzole." *Neurology*. Lippincott Williams and Wilkins. https://doi.org/10.1212/wnl.47.6_suppl_4.233s.

Dossi, Elena, Flora Vasile, and Nathalie Rouach. 2018. "Human Astrocytes in the Diseased Brain." *Brain Research Bulletin*. https://doi.org/10.1016/j.brainresbull.2017.02.001.

Eng, L. F., J. J. Vanderhaeghen, A. Bignami, and B. Gerstl. 1971. "An Acidic Protein Isolated from Fibrous Astrocytes." *Brain Research* 28 (2): 351–54. https://doi.org/10.1016/0006-8993(71)90668-8.

Erecińska, M, D Nelson, Y Daikhin, and M Yudkoff. 1996. "Regulation of GABA Level in Rat Brain Synaptosomes: Fluxes through Enzymes of the GABA Shunt and Effects of Glutamate, Calcium, and Ketone Bodies." *Journal of Neurochemistry* 67 (6): 2325–34. https://doi.org/10.1046/j.1471-4159.1996.67062325.x.

Farg, Manal A., Vinod Sundaramoorthy, Jessica M. Sultana, Shu Yang, Rachel A.K. Atkinson, Vita Levina, Mark A. Halloran, et al. 2014. "C9ORF72, Implicated in Amytrophic Lateral Sclerosis and Frontotemporal Dementia, Regulates Endosomal Trafficking." *Human Molecular Genetics* 23 (13): 3579–95. https://doi.org/10.1093/hmg/ddu068.

Feinshreiber, Lori, Dafna Singer-Lahat, Reut Friedrich, Ulf Matti, Anton Sheinin, Ofer Yizhar, Rachel

Nachman, et al. 2010. “Non-Conducting Function of the Kv2.1 Channel Enables It to Recruit Vesicles for Release in Neuroendocrine and Nerve Cells.” *Journal of Cell Science* 123 (11): 1940–47. https://doi.org/10.1242/jcs.063719.

*Feliciangeli, Sylvain, Frank C. Chatelain, Delphine Bichet, and Florian Lesage. 2015. “The Family of K2P Channels: Salient Structural and Functional Properties.” *Journal of Physiology*. https://doi.org/10.1113/jphysiol.2014.287268.

Ferraiuolo, Laura, Adrian Higginbottom, Paul R Heath, Sian Barber, David Greenald, Janine Kirby, and Pamela J Shaw. 2011. “Dysregulation of Astrocyte-Motoneuron Cross-Talk in Mutant Superoxide Dismutase 1-Related Amyotrophic Lateral Sclerosis.” *Brain* 134 (9): 2627–41. https://doi.org/10.1093/brain/awr193.

*Filipi, Tereza, Zuzana Hermanova, Jana Tureckova, Ondrej Vanatko, and Miroslava Anderova. 2020. “Glial Cells—The Strategic Targets in Amyotrophic Lateral Sclerosis Treatment.” *Journal of Clinical Medicine* 9 (1): 261. https://doi.org/10.3390/jcm9010261.

Filosa, Jessica A., Adrian D. Bonev, Stephen V. Straub, Andrea L. Meredith, M. Keith Wilkerson, Richard W. Aldrich, and Mark T. Nelson. 2006. “Local Potassium Signaling Couples Neuronal Activity to Vasodilation in the Brain.” *Nature Neuroscience* 9 (11): 1397–1403. https://doi.org/10.1038/nn1779.

Flügge, Gabriele, Carolina Araya-Callis, Enrique Garea-Rodriguez, Christine Stadelmann-Nessler, and Eberhard Fuchs. 2014. “NDRG2 as a Marker Protein for Brain Astrocytes.” *Cell and Tissue Research* 357 (1): 31–41. https://doi.org/10.1007/s00441-014-1837-5.

Friedrich, Thomas, Tilman Breiderhoff, and Thomas J. Jentsch. 1999. “Mutational Analysis Demonstrates That ClC-4 and ClC-5 Directly Mediate Plasma Membrane Currents.” *Journal of Biological Chemistry* 274 (2): 896–902. https://doi.org/10.1074/jbc.274.2.896.

Furnari, Frank B., Tim Fenton, Robert M. Bachoo, Akitake Mukasa, Jayne M. Stommel, Alexander Stegh, William C. Hahn, et al. 2007. “Malignant Astrocytic Glioma: Genetics, Biology, and Paths to Treatment.” *Genes and Development*. https://doi.org/10.1101/gad.1596707.

Gabel, Lisa A., and Eric S. Nisenbaum. 1998. “Biophysical Characterization and Functional Consequences of a Slowly Inactivating Potassium Current in Neostriatal Neurons.” *Journal of Neurophysiology* 79 (4): 1989–2002. https://doi.org/10.1152/jn.1998.79.4.1989.

*Geloso, Maria Concetta, Valentina Corvino, Elisa Marchese, Alessia Serrano, Fabrizio Michetti, and Nadia D’Ambrosi. 2017. “The Dual Role of Microglia in ALS: Mechanisms and Therapeutic Approaches.” *Frontiers in Aging Neuroscience*. https://doi.org/10.3389/fnagi.2017.00242.

Gibb, Stuart L., William Boston-Howes, Zeno S. Lavina, Stefano Gustincich, Robert H. Brown, Piera Pasinelli, and Davide Trotti. 2007. “A Caspase-3-Cleaved Fragment of the Glial Glutamate Transporter EAAT2 Is Sumoylated and Targeted to Promyelocytic Leukemia Nuclear Bodies in Mutant SOD1-Linked Amyotrophic Lateral Sclerosis.” *Journal of Biological Chemistry* 282 (44): 32480–90. https://doi.org/10.1074/jbc.M704314200.

Girouard, Hélène, Adrian D. Bonev, Rachael M. Hannah, Andrea Meredith, Richard W. Aldrich, and Mark T. Nelson. 2010. “Astrocytic Endfoot Ca2+ and BK Channels Determine Both Arteriolar Dilation and Constriction.” *Proceedings of the National Academy of Sciences of the United States of America* 107 (8): 3811–16. https://doi.org/10.1073/pnas.0914722107.

Glazebrook, Patricia A., Angelina N. Ramirez, John H. Schild, Char Chang Shieh, Thanh Doan, Barbara A. Wible, and Diana L. Kunze. 2002. “Potassium Channels Kv1.1, Kv1.2 and Kv1.6 Influence

Excitability of Rat Visceral Sensory Neurons." *Journal of Physiology* 541 (2): 467–82. https://doi.org/10.1113/jphysiol.2001.018333.

Gnatenco, Carmen, Jaehee Han, Ann K. Snyder, and Donghee Kim. 2002. "Functional Expression of TREK-2 K+ Channel in Cultured Rat Brain Astrocytes." *Brain Research* 931 (1): 56–67. https://doi.org/10.1016/S0006-8993(02)02261-8.

*Gois, Auderlan M., Deise M.F. Mendonça, Marco Aurelio M. Freire, and Jose R. Santos. 2020. "IN VITRO AND IN VIVO MODELS OF AMYOTROPHIC LATERAL SCLEROSIS: AN UPDATED OVERVIEW." *Brain Research Bulletin*. Elsevier Inc. https://doi.org/10.1016/j.brainresbull.2020.03.012.

Gomes, Flávia Carvalho Alcantara, Cecilia Garcia Maia, João Ricardo Lacerda De Menezes, and Vivaldo Moura Neto. 1999. "Cerebellar Astrocytes Treated by Thyroid Hormone Modulate Neuronal Proliferation." *Glia* 25 (3): 247–55. https://doi.org/10.1002/(SICI)1098-1136(19990201)25:3<247::AID-GLIA5>3.0.CO;2-2.

Gothelf, Y., M. Cudkowicz, J. Berry, A. Windebank, N. Staff, M. Owegi, Y.S. Levy, et al. 2017. "Safety and Efficacy of Transplantation of Nurown (Autologous Mesenchymal Stromal Cells Secreting Neurotrophic Factors) in Patients with ALS: A Phase 2 Randomized Double Blind Placebo Controlled Trial." *Cytotherapy* 19 (5): S23. https://doi.org/10.1016/j.jcyt.2017.02.040.

*Goutman, Stephen A., Masha G. Savelieff, Stacey A. Sakowski, and Eva L. Feldman. 2019. "Stem Cell Treatments for Amyotrophic Lateral Sclerosis: A Critical Overview of Early Phase Trials." *Expert Opinion on Investigational Drugs* 28 (6): 525–43. https://doi.org/10.1080/13543784.2019.1627324.

Gurney, Mark E, Haifeng Pu, Arlene Y Chiu, Mauro C Dal Canto, Cynthia Y Polchow, Denise D Alexander, Jan Caliendo, et al. 1994. "Motor Neuron Degeneration in Mice That Express a Human Cu,Zn Superoxide Dismutase Mutation." *Science* 264 (5166): 1772–75. https://doi.org/10.1126/science.8209258.

Hackett, Amber R., Stephanie L. Yahn, Kirill Lyapichev, Angela Dajnoki, Do Hun Lee, Mario Rodriguez, Natasha Cammer, et al. 2018. "Injury Type-Dependent Differentiation of NG2 Glia into Heterogeneous Astrocytes." *Experimental Neurology* 308 (October): 72–79. https://doi.org/10.1016/j.expneurol.2018.07.001.

Haidet-Phillips, Amanda M., Mark E. Hester, Carlos J. Miranda, Kathrin Meyer, Lyndsey Braun, Ashley Frakes, Sungwon Song, et al. 2011. "Astrocytes from Familial and Sporadic ALS Patients Are Toxic to Motor Neurons." *Nature Biotechnology* 29 (9): 824–28. https://doi.org/10.1038/nbt.1957.

Hall, Edward D., Paula K. Andrus, Jo A. Oostveen, Timothy J. Fleck, and Mark E. Gurney. 1998. "Relationship of Microglial and Astrocytic Activation to Disease Onset and Progression in a Transgenic Model of Familial ALS." *Journal of Neuroscience Research* 53 (1): 66–77. https://doi.org/10.1002/(SICI)1097-4547(19980701)53:1<66::AID-JNR7>3.0.CO;2-H.

Han, Jaehee, Dawon Kang, and Donghee Kim. 2003. "Functional Properties of Four Splice Variants of a Human Pancreatic Tandem-Pore K+ Channel, TALK-1." *American Journal of Physiology - Cell Physiology* 285 (3 54-3). https://doi.org/10.1152/ajpcell.00601.2002.

*Hayashi, Yuki, Kengo Homma, and Hidenori Ichijo. 2016. "SOD1 in Neurotoxicity and Its Controversial Roles in SOD1 Mutation-Negative ALS." *Advances in Biological Regulation*. https://doi.org/10.1016/j.jbior.2015.10.006.

Heginbotham, L., Z. Lu, T. Abramson, and R. MacKinnon. 1994. "Mutations in the K+ Channel Signature Sequence." *Biophysical Journal* 66 (4): 1061–67. https://doi.org/10.1016/S0006-

3495(94)80887-2.

Hennig, Sven, Geraldine Kong, Taro Mannen, Agata Sadowska, Simon Kobelke, Amanda Blythe, Gavin J. Knott, et al. 2015. "Prion-like Domains in RNA Binding Proteins Are Essential for Building Subnuclear Paraspeckles." *Journal of Cell Biology* 210 (4): 529–39. https://doi.org/10.1083/jcb.201504117.

Hensley, Kenneth, Haitham Abdel-Moaty, Jerrod Hunter, Molina Mhatre, Shenyun Mhou, Kim Nguyen, Tamara Potapova, et al. 2006. "Primary Glia Expressing the G93A-SOD1 Mutation Present a Neuroinflammatory Phenotype and Provide a Cellular System for Studies of Glial Inflammation." *Journal of Neuroinflammation* 3 (January). https://doi.org/10.1186/1742-2094-3-2.

Hibino, Hiroshi, Akikazu Fujita, Kaori Iwai, Mitsuhiko Yamada, and Yoshihisa Kurachi. 2004. "Differential Assembly of Inwardly Rectifying K+ Channel Subunits, Kir4.1 and Kir5.1, in Brain Astrocytes." *Journal of Biological Chemistry* 279 (42): 44065–73. https://doi.org/10.1074/jbc.M405985200.

*Hibino, Hiroshi, Atsushi Inanobe, Kazuharu Furutani, Shingo Murakami, Ian Findlay, and Yoshihisa Kurachi. 2010. "Inwardly Rectifying Potassium Channels: Their Structure, Function, and Physiological Roles." *Physiological Reviews*. Physiol Rev. https://doi.org/10.1152/physrev.00021.2009.

Hibino, Hiroshi, and Yoshihisa Kurachi. 2007. "Distinct Detergent-Resistant Membrane Microdomains (Lipid Rafts) Respectively Harvest K+ and Water Transport Systems in Brain Astroglia." *European Journal of Neuroscience* 26 (9): 2539–55. https://doi.org/10.1111/j.1460-9568.2007.05876.x.

Higashi, Kayoko, Akikazu Fujita, Atsushi Inanobe, Masayuki Tanemoto, Katsumi Doi, Takeshi Kubo, and Yoshihisa Kurachi. 2001. "An Inwardly Rectifying K+ Channel, Kir4.1, Expressed in Astrocytes Surrounds Synapses and Blood Vessels in Brain." *American Journal of Physiology - Cell Physiology* 281 (3 50-3). https://doi.org/10.1152/ajpcell.2001.281.3.c922.

Higashimori, Haruki, and Harald Sontheimer. 2007. "Role of Kir4.1 Channels in Growth Control of Glia." *GLIA* 55 (16): 1668–79. https://doi.org/10.1002/glia.20574.

*Hol, Elly M., and Milos Pekny. 2015. "Glial Fibrillary Acidic Protein (GFAP) and the Astrocyte Intermediate Filament System in Diseases of the Central Nervous System." *Current Opinion in Cell Biology*. https://doi.org/10.1016/j.ceb.2015.02.004.

Honsa, Pavel, Helena Pivonkova, David Dzamba, Marcela Filipova, and Miroslava Anderova. 2012. "Polydendrocytes Display Large Lineage Plasticity Following Focal Cerebral Ischemia." *PLoS ONE* 7 (5): e36816. https://doi.org/10.1371/journal.pone.0036816.

Honsa, Pavel, Helena Pivonkova, Lenka Harantova, Olena Butenko, Jan Kriska, David Dzamba, Vendula Rusnakova, Lukas Valihrach, Mikael Kubista, and Miroslava Anderova. 2014. "Increased Expression of Hyperpolarization-Activated Cyclic Nucleotide-Gated (HCN) Channels in Reactive Astrocytes Following Ischemia." *Glia* 62 (12): 2004–21. https://doi.org/10.1002/glia.22721.

Howland, David S., Jian Liu, Yijin She, Beth Goad, Nicholas J. Maragakis, Benjamin Kim, Jamie Erickson, et al. 2002. "Focal Loss of the Glutamate Transporter EAAT2 in a Transgenic Rat Model of SOD1 Mutant-Mediated Amyotrophic Lateral Sclerosis (ALS)." *Proceedings of the National Academy of Sciences of the United States of America* 99 (3): 1604–9. https://doi.org/10.1073/pnas.032539299.

Hu, Chang Long, Xi Min Zeng, Meng Hua Zhou, Ying Tang Shi, Hong Cao, and Yan Ai Mei. 2008. "Kv 1.1 Is Associated with Neuronal Apoptosis and Modulated by Protein Kinase C in the Rat

Cerebellar Granule Cell." *Journal of Neurochemistry* 106 (3): 1125–37. https://doi.org/10.1111/j.1471-4159.2008.05449.x.

Jami, Mohammad Saeid, Zahra Salehi-Najafabadi, Fereshteh Ahmadinejad, Esthelle Hoedt, Morteza Hashemzadeh Chaleshtori, Mahdi Ghatrehsamani, Thomas A. Neubert, Jan Petter Larsen, and Simon Geir Møller. 2015. "Edaravone Leads to Proteome Changes Indicative of Neuronal Cell Protection in Response to Oxidative Stress." *Neurochemistry International* 90 (November): 134–41. https://doi.org/10.1016/j.neuint.2015.07.024.

Jiménez-Pérez, Laura, Pilar Cidad, Inés Álvarez-Miguel, Alba Santos-Hipólito, Rebeca Torres-Merino, Esperanza Alonso, Miguel Ángel De La Fuente, José Ramón López-López, and Teresa Pérez-García. 2016. "Molecular Determinants of Kv1.3 Potassium Channels-Induced Proliferation." *Journal of Biological Chemistry* 291 (7): 3569–80. https://doi.org/10.1074/jbc.M115.678995.

Kaiser, Melanie, Iris Maletzki, Swen Hülsmann, Bettina Holtmann, Walter Schulz-Schaeffer, Frank Kirchhoff, Mathias Bähr, and Clemens Neusch. 2006. "Progressive Loss of a Glial Potassium Channel (KCNJ10) in the Spinal Cord of the SOD1 (G93A) Transgenic Mouse Model of Amyotrophic Lateral Sclerosis." *Journal of Neurochemistry* 99 (3): 900–912. https://doi.org/10.1111/j.1471-4159.2006.04131.x.

Kala, Geeta, Raj Kumarathasan, Liang Peng, Frans H. Leenen, and Leif Hertz. 2000. "Stimulation of Na+,K+-ATPase Activity, Increase in Potassium Uptake, and Enhanced Production of Ouabain-like Compounds in Ammonia-Treated Mouse Astrocytes." *Neurochemistry International* 36 (3): 203–11. https://doi.org/10.1016/S0197-0186(99)00117-5.

Kamasawa, N., A. Sik, M. Morita, T. Yasumura, K. G.V. Davidson, J. I. Nagy, and J. E. Rash. 2005. "Connexin-47 and Connexin-32 in Gap Junctions of Oligodendrocyte Somata, Myelin Sheaths, Paranodal Loops and Schmidt-Lanterman Incisures: Implications for Ionic Homeostasis and Potassium Siphoning." *Neuroscience* 136 (1): 65–86. https://doi.org/10.1016/j.neuroscience.2005.08.027.

Kang, Dawon, Changyong Choe, and Donghee Kim. 2005. "Thermosensitivity of the Two-Pore Domain K+ Channels TREK-2 and TRAAK." *Journal of Physiology* 564 (1): 103–16. https://doi.org/10.1113/jphysiol.2004.081059.

Kang, Shin H., Ying Li, Masahiro Fukaya, Ileana Lorenzini, Don W. Cleveland, Lyle W. Ostrow, Jeffrey D. Rothstein, and Dwight E. Bergles. 2013. "Degeneration and Impaired Regeneration of Gray Matter Oligodendrocytes in Amyotrophic Lateral Sclerosis." *Nature Neuroscience* 16 (5): 571–79. https://doi.org/10.1038/nn.3357.

Ketchum, Karen A., William J. Joiner, Andrew J. Sellers, Leonard K. Kaczmarek, and Steve A.N. Goldstein. 1995. "A New Family of Outwardly Rectifying Potassium Channel Proteins with Two Pore Domains in Tandem." *Nature*. https://doi.org/10.1038/376690a0.

Kimelberg, H. K., S. K. Goderie, S. Higman, S. Pang, and R. A. Waniewski. 1990. "Swelling-Induced Release of Glutamate, Aspartate, and Taurine from Astrocyte Cultures." *Journal of Neuroscience* 10 (5): 1583–91. https://doi.org/10.1523/jneurosci.10-05-01583.1990.

Kindler, Christoph H., Christian Pietruck, C. Spencer Yost, Elizabeth R. Sampson, and Andrew T. Gray. 2000. "Localization of the Tandem Pore Domain K+ Channel TASK-1 in the Rat Central Nervous System." *Molecular Brain Research* 80 (1): 99–108. https://doi.org/10.1016/S0169-328X(00)00136-4.

*Kofuji, P., and E. A. Newman. 2004. "Potassium Buffering in the Central Nervous System." *Neuroscience* 129 (4): 1043–54. https://doi.org/10.1016/j.neuroscience.2004.06.008.

Kohama, Steven G., James R. Goss, Caleb E. Finch, and Thomas H. McNeill. 1995. “Increases of Glial Fibrillary Acidic Protein in the Aging Female Mouse Brain.” *Neurobiology of Aging* 16 (1): 59–67. https://doi.org/10.1016/0197-4580(95)80008-F.

Kotecha, Suhas A., and Lyanne C. Schlichter. 1999. “A Kv1.5 to Kv1.3 Switch in Endogenous Hippocampal Microglia and a Role in Proliferation.” *Journal of Neuroscience* 19 (24): 10680–93. https://doi.org/10.1523/jneurosci.19-24-10680.1999.

Kucheryavykh, Y. V., L. Y. Kucheryavykh, C. G. Nichols, H. M. Maldonado, K. Baksi, A. Reichenbach, S. N. Skatchkov, and Misty J. Eaton. 2007. “Downregulation of Kir4.1 Inward Rectifying Potassium Channel Subunits by RNAi Impairs Potassium Transfer and Glutamate Uptake by Cultured Cortical Astrocytes.” *GLIA* 55 (3): 274–81. https://doi.org/10.1002/glia.20455.

Kucukdereli, Hakan, Nicola J. Allen, Anthony T. Lee, Ava Feng, M. Ilcim Ozlu, Laura M. Conatser, Chandrani Chakraborty, et al. 2011. “Control of Excitatory CNS Synaptogenesis by Astrocyte-Secreted Proteins Hevin and SPARC.” *Proceedings of the National Academy of Sciences of the United States of America* 108 (32): E440–49. https://doi.org/10.1073/pnas.1104977108.

Kuffler, S. W., J. G. Nicholls, and R. K. Orkand. 1966. “Physiological Properties of Glial Cells in the Central Nervous System of Amphibia.” *Journal of Neurophysiology* 29 (4): 768–87. https://doi.org/10.1152/jn.1966.29.4.768.

Kulesskaya, Natalia, Heikki Rauvala, and Vootele Voikar. 2011. “Evaluation of Social and Physical Enrichment in Modulation of Behavioural Phenotype in C57BL/6J Female Mice.” *PLoS ONE* 6 (9). https://doi.org/10.1371/journal.pone.0024755.

Kuo, Anling, Jacqueline M. Gulbis, Jennifer F. Antcliff, Tahmina Rahman, Edward D. Lowe, Jochen Zimmer, Jonathan Cuthbertson, Frances M. Ashcroft, Takayuki Ezaki, and Declan A. Doyle. 2003. “Crystal Structure of the Potassium Channel KirBac1.1 in the Closed State.” *Science* 300 (5627): 1922–26. https://doi.org/10.1126/science.1085028.

Lanjakornsiripan, Darin, Baek Jun Pior, Daichi Kawaguchi, Shohei Furutachi, Tomoaki Tahara, Yu Katsuyama, Yutaka Suzuki, Yugo Fukazawa, and Yukiko Gotoh. 2018. “Layer-Specific Morphological and Molecular Differences in Neocortical Astrocytes and Their Dependence on Neuronal Layers.” *Nature Communications* 9 (1): 1–15. https://doi.org/10.1038/s41467-018-03940-3.

Lee, Soojung, Bo Eun Yoon, Ken Berglund, Soo Jin Oh, Hyungju Park, Hee Sup Shin, George J. Augustine, and C. Justin Lee. 2010. “Channel-Mediated Tonic GABA Release from Glia.” *Science* 330 (6005): 790–96. https://doi.org/10.1126/science.1184334.

Lee, Youngjin, Brett M Morrison, Yun Li, Sylvain Lengacher, Mohamed H Farah, Paul N Hoffman, Yiting Liu, et al. 2012. “Oligodendroglia Metabolically Support Axons and Contribute to Neurodegeneration.” *Nature* 487 (7408): 443–48. https://doi.org/10.1038/nature11314.

Lehre, Knut P., Line M. Levy, Ole P. Ottersen, Jon Storm-Mathisen, and Niels C. Danbolt. 1995. “Differential Expression of Two Glial Glutamate Transporters in the Rat Brain: Quantitative and Immunocytochemical Observations.” *Journal of Neuroscience* 15 (3 I): 1835–53. https://doi.org/10.1523/jneurosci.15-03-01835.1995.

Lemasurier, Meredith, Lise Heginbotham, and Christopher Miller. 2001. “KcsA: It’s a Potassium Channel.” *Journal of General Physiology* 118 (3): 303–13. https://doi.org/10.1085/jgp.118.3.303.

Lengyel, Miklós, Gábor Czirják, David A Jacobson, and Péter Enyedi. 2020. “TRESK and TREK-2 Two Pore-Domain Potassium Channel Subunits Form Functional Heterodimers in Primary

Somatosensory Neurons." *Journal of Biological Chemistry*, July, jbc.RA120.014125. https://doi.org/10.1074/jbc.RA120.014125.

Levine, John B., Jiming Kong, Mark Nadler, and Zuoshang Xu. 1999. "Astrocytes Interact Intimately with Degenerating Motor Neurons in Mouse Amyotrophic Lateral Sclerosis (ALS)." *Glia* 28 (3): 215–24. https://doi.org/10.1002/(SICI)1098-1136(199912)28:3<215::AID-GLIA5>3.0.CO;2-C.

Levitz, Joshua, Perrine Royal, Yannick Comoglio, Brigitte Wdziekonski, Sébastien Schaub, Daniel M. Clemens, Ehud Y. Isacoff, and Guillaume Sandoz. 2016. "Heterodimerization within the TREK Channel Subfamily Produces a Diverse Family of Highly Regulated Potassium Channels." *Proceedings of the National Academy of Sciences of the United States of America* 113 (15): 4194–99. https://doi.org/10.1073/pnas.1522459113.

Li, Luyi, Valerie Head, and Leslie C. Timpe. 2001. "Identification of an Inward Rectifier Potassium Channel Gene Expressed in Mouse Cortical Astrocytes." *GLIA* 33 (1): 57–71. https://doi.org/10.1002/1098-1136(20010101)33:1<57::AID-GLIA1006>3.0.CO;2-0.

Lichter-Konecki, Uta, Jean Marie Mangin, Heather Gordish-Dressman, Eric P. Hoffman, and Vittorio Gallo. 2008. "Gene Expression Profiling of Astrocytes from Hyperammonemic Mice Reveals Altered Pathways for Water and Potassium Homeostasis in Vivo." *GLIA* 56 (4): 365–77. https://doi.org/10.1002/glia.20624.

Liddelow, Shane A., and Ben A. Barres. 2017. "Reactive Astrocytes: Production, Function, and Therapeutic Potential." *Immunity*. Cell Press. https://doi.org/10.1016/j.immuni.2017.06.006.

Liddelow, Shane A., Kevin A. Guttenplan, Laura E. Clarke, Frederick C. Bennett, Christopher J. Bohlen, Lucas Schirmer, Mariko L. Bennett, et al. 2017. "Neurotoxic Reactive Astrocytes Are Induced by Activated Microglia." *Nature* 541 (7638): 481–87. https://doi.org/10.1038/nature21029.

Lino, Maria Maddalena, Corinna Schneider, and Pico Caroni. 2002. "Accumulation of SOD1 Mutants in Postnatal Motoneurons Does Not Cause Motoneuron Pathology or Motoneuron Disease." *Journal of Neuroscience* 22 (12): 4825–32. https://doi.org/10.1523/jneurosci.22-12-04825.2002.

Longden, TA, KM Dunn, HJ Draheim, MT Nelson, AH Weston, and G Edwards. 2011. "Intermediate-Conductance Calcium-Activated Potassium Channels Participate in Neurovascular Coupling." *British Journal of Pharmacology* 164 (3): 922–33. https://doi.org/10.1111/j.1476-5381.2011.01447.x.

*Longinetti, Elisa, and Fang Fang. 2019. "Epidemiology of Amyotrophic Lateral Sclerosis: An Update of Recent Literature." *Current Opinion in Neurology*. https://doi.org/10.1097/WCO.0000000000000730.

Ma, E., and G. G. Haddad. 1997. "Expression and Localization of Na+/H+ Exchangers in Rat Central Nervous System." *Neuroscience* 79 (2): 591–603. https://doi.org/10.1016/S0306-4522(96)00674-4.

MacFarlane, Stacey Nee, and Harald Sontheimer. 1997. "Electrophysiological Changes That Accompany Reactive Gliosis in Vitro." *Journal of Neuroscience* 17 (19): 7316–29. https://doi.org/10.1523/jneurosci.17-19-07316.1997.

Mao, Jian Hua, Sasha A. Langley, Yurong Huang, Michael Hang, Kristofer E. Bouchard, Susan E. Celniker, James B. Brown, Janet K. Jansson, Gary H. Karpen, and Antoine M. Snijders. 2015. "Identification of Genetic Factors That Modify Motor Performance and Body Weight Using Collaborative Cross Mice." *Scientific Reports* 5 (1): 16247. https://doi.org/10.1038/srep16247.

Marina, Nephtali, Isabel N. Christie, Alla Korsak, Maxim Doronin, Alexey Brazhe, Patrick S. Hosford, Jack A. Wells, et al. 2020. "Astrocytes Monitor Cerebral Perfusion and Control Systemic

Circulation to Maintain Brain Blood Flow." *Nature Communications* 11 (1): 1–9. https://doi.org/10.1038/s41467-019-13956-y.

Martier, Raygene, Jolanda M. Liefhebber, Jana Miniarikova, Tom van der Zon, Jolanda Snapper, Iris Kolder, Harald Petry, Sander J. van Deventer, Melvin M. Evers, and Pavlina Konstantinova. 2019. "Artificial MicroRNAs Targeting C9orf72 Can Reduce Accumulation of Intra-Nuclear Transcripts in ALS and FTD Patients." *Molecular Therapy - Nucleic Acids* 14 (March): 593–608. https://doi.org/10.1016/j.omtn.2019.01.010.

Mastrocola, Adam S., Sang Hwa Kim, Anthony T. Trinh, Lance A. Rodenkirch, and Randal S. Tibbetts. 2013. "The RNA-Binding Protein Fused in Sarcoma (FUS) Functions Downstream of Poly(ADP-Ribose) Polymerase (PARP) in Response to DNA Damage." *Journal of Biological Chemistry* 288 (34): 24731–41. https://doi.org/10.1074/jbc.M113.497974.

*Matias, Isadora, Juliana Morgado, and Flávia Carvalho Alcantara Gomes. 2019. "Astrocyte Heterogeneity: Impact to Brain Aging and Disease." *Frontiers in Aging Neuroscience* 11 (March): 59. https://doi.org/10.3389/fnagi.2019.00059.

McKhann, Guy M., Raimondo D'Ambrosio, and Damir Janigro. 1997. "Heterogeneity of Astrocyte Resting Membrane Potentials and Intercellular Coupling Revealed by Whole-Cell and Gramicidin-Perforated Patch Recordings from Cultured Neocortical and Hippocampal Slice Astrocytes." *Journal of Neuroscience* 17 (18): 6850–63. https://doi.org/10.1523/jneurosci.17-18-06850.1997.

McLoon, Linda K., Vahid M. Harandi, Thomas Brännström, Peter M. Andersen, and Jing Xia Liu. 2014. "Wnt and Extraocular Muscle Sparing in Amyotrophic Lateral Sclerosis." *Investigative Ophthalmology and Visual Science* 55 (9): 5482–96. https://doi.org/10.1167/iovs.14-14886.

*Mejzini, Rita, Loren L. Flynn, Ianthe L. Pitout, Sue Fletcher, Steve D. Wilton, and P. Anthony Akkari. 2019. "ALS Genetics, Mechanisms, and Therapeutics: Where Are We Now?" *Frontiers in Neuroscience*. https://doi.org/10.3389/fnins.2019.01310.

Mi Hwang, Eun, Eunju Kim, Oleg Yarishkin, Dong Ho Woo, Kyung Seok Han, Nammi Park, Yeonju Bae, et al. 2014. "A Disulphide-Linked Heterodimer of TWIK-1 and TREK-1 Mediates Passive Conductance in Astrocytes." *Nature Communications* 5 (February). https://doi.org/10.1038/ncomms4227.

Miana-Mena, Francisco J., Maria J. Muñoz, Gema Yagüe, Mario Mendez, Maria Moreno, Jesús Ciriza, Pilar Zaragoza, and Rosario Osta. 2005. "Optimal Methods to Characterize the G93A Mouse Model of ALS." *Amyotrophic Lateral Sclerosis and Other Motor Neuron Disorders* 6 (1): 55–62. https://doi.org/10.1080/14660820510026162.

*Middeldorp, J., and E. M. Hol. 2011. "GFAP in Health and Disease." *Progress in Neurobiology*. https://doi.org/10.1016/j.pneurobio.2011.01.005.

Miller, Alexandria N., and Stephen B. Long. 2012. "Crystal Structure of the Human Two-Pore Domain Potassium Channel K2P1." *Science* 335 (6067): 432–36. https://doi.org/10.1126/science.1213274.

Miller, R. H., and M. C. Raff. 1984. "Fibrous and Protoplasmic Astrocytes Are Biochemically and Developmentally Distinct." *Journal of Neuroscience* 4 (2): 585–92. https://doi.org/10.1523/jneurosci.04-02-00585.1984.

Miller, Timothy M., Alan Pestronk, William David, Jeffrey Rothstein, Ericka Simpson, Stanley H. Appel, Patricia L. Andres, et al. 2013. "An Antisense Oligonucleotide against SOD1 Delivered Intrathecally for Patients with SOD1 Familial Amyotrophic Lateral Sclerosis: A Phase 1, Randomised, First-in-Man Study." *The Lancet Neurology* 12 (5): 435–42.

https://doi.org/10.1016/S1474-4422(13)70061-9.

Mishima, Tsuneko, and Hajime Hirase. 2010. “In Vivo Intracellular Recording Suggests That Gray Matter Astrocytes in Mature Cerebral Cortex and Hippocampus Are Electrophysiologically Homogeneous.” *Journal of Neuroscience* 30 (8): 3093–3100. https://doi.org/10.1523/JNEUROSCI.5065-09.2010.

Mitra, Joy, Erika N. Guerrero, Pavana M. Hegde, Nicole F. Liachko, Haibo Wang, Velmarini Vasquez, Junling Gao, et al. 2019. “Motor Neuron Disease-Associated Loss of Nuclear TDP-43 Is Linked to DNA Double-Strand Break Repair Defects.” *Proceedings of the National Academy of Sciences of the United States of America* 116 (10): 4696–4705. https://doi.org/10.1073/pnas.1818415116.

*Mongin, Alexander A. 2016. “Volume-Regulated Anion Channel—a Frenemy within the Brain.” *Pflugers Archiv European Journal of Physiology*. https://doi.org/10.1007/s00424-015-1765-6.

Murata, Yuzo, Toshiharu Yasaka, Makoto Takano, and Keiko Ishihara. 2016. “Neuronal and Glial Expression of Inward Rectifier Potassium Channel Subunits Kir2.x in Rat Dorsal Root Ganglion and Spinal Cord.” *Neuroscience Letters* 617 (March): 59–65. https://doi.org/10.1016/j.neulet.2016.02.007.

Nagai, Makiko, Diane B. Re, Tetsuya Nagata, Alcmène Chalazonitis, Thomas M. Jessell, Hynek Wichterle, and Serge Przedborski. 2007. “Astrocytes Expressing ALS-Linked Mutated SOD1 Release Factors Selectively Toxic to Motor Neurons.” *Nature Neuroscience* 10 (5): 615–22. https://doi.org/10.1038/nn1876.

Nagelhus, E. A., T. M. Mathiisen, and O. P. Ottersen. 2004. “Aquaporin-4 in the Central Nervous System: Cellular and Subcellular Distribution and Coexpression with KIR4.1.” *Neuroscience* 129 (4): 905–13. https://doi.org/10.1016/j.neuroscience.2004.08.053.

Nagelhus, Erlend A., and Ole P. Ottersen. 2013. “Physiological Roles of Aquaporin-4 in Brain.” *Physiological Reviews* 93 (4): 1543–62. https://doi.org/10.1152/physrev.00011.2013.

Nagy, J. I., D. Patel, P. A.Y. Ochalski, and G. L. Stelmack. 1999. “Connexin30 in Rodent, Cat and Human Brain: Selective Expression in Gray Matter Astrocytes, Co-Localization with Connexin43 at Gap Junction and Late Developmental Appearance.” *Neuroscience* 88 (2): 447–68. https://doi.org/10.1016/S0306-4522(98)00191-2.

Neumann, Manuela, Deepak M. Sampathu, Linda K. Kwong, Adam C. Truax, Matthew C. Micsenyi, Thomas T. Chou, Jennifer Bruce, et al. 2006. “Ubiquitinated TDP-43 in Frontotemporal Lobar Degeneration and Amyotrophic Lateral Sclerosis.” *Science* 314 (5796): 130–33. https://doi.org/10.1126/science.1134108.

*Ng, Louisa, Fary Khan, Carolyn A. Young, and Mary Galea. 2017. “Symptomatic Treatments for Amyotrophic Lateral Sclerosis/Motor Neuron Disease.” *Cochrane Database of Systematic Reviews*. https://doi.org/10.1002/14651858.CD011776.pub2.

Nielsen, So, Erlend Arnulf Nagelhus, Mahmood Amiry-Moghaddam, Charles Bourque, Peter Agre, and Ole Retter Ottersen. 1997. “Specialized Membrane Domains for Water Transport in Glial Cells: High- Resolution Immunogold Cytochemistry of Aquaporin-4 in Rat Brain.” *Journal of Neuroscience* 17 (1): 171–80. https://doi.org/10.1523/jneurosci.17-01-00171.1997.

Nishida, H., and S. Okabe. 2007. “Direct Astrocytic Contacts Regulate Local Maturation of Dendritic Spines.” *Journal of Neuroscience* 27 (2): 331–40. https://doi.org/10.1523/JNEUROSCI.4466-06.2007.

Nishida, Motohiko, and Roderick MacKinnon. 2002. “Structural Basis of Inward Rectification:

Cytoplasmic Pore of the G Protein-Gated Inward Rectifier GIRK1 at 1.8 Å Resolution." *Cell* 111 (7): 957–65. https://doi.org/10.1016/S0092-8674(02)01227-8.

Nixdorf-Bergweiler, Barbara E., Dorothea Albrecht, and Uwe Heinemann. 1994. "Developmental Changes in the Number, Size, and Orientation of GFAP-positive Cells in the CA1 Region of Rat Hippocampus." *Glia* 12 (3): 180–95. https://doi.org/10.1002/glia.440120304.

Nolte, Christiane, Marina Matyash, Tatjyana Pivneva, Carola G. Schipke, Carsten Ohlemeyer, Uwe Karsten Hanisch, Frank Kirchhoff, and Helmut Kettenmann. 2001. "GFAP Promoter-Controlled EGFP-Expressing Transgenic Mice: A Tool to Visualize Astrocytes and Astrogliosis in Living Brain Tissue." *GLIA* 33 (1): 72–86. https://doi.org/10.1002/1098-1136(20010101)33:1<72::AID-GLIA1007>3.0.CO;2-A.

*Nowicka, Natalia, Jakub Juranek, Judyta K. Juranek, and Joanna Wojtkiewicz. 2019. "Risk Factors and Emerging Therapies in Amyotrophic Lateral Sclerosis." *International Journal of Molecular Sciences*. MDPI AG. https://doi.org/10.3390/ijms20112616.

Nübling, Georg S., Eva Mie, Ricarda M. Bauer, Mira Hensler, Stefan Lorenzl, Alexander Hapfelmeier, Debra E. Irwin, Gian Domenico Borasio, and Andrea S. Winkler. 2014. "Increased Prevalence of Bladder and Intestinal Dysfunction in Amyotrophic Lateral Sclerosis." *Amyotrophic Lateral Sclerosis and Frontotemporal Degeneration* 15 (3–4): 174–79. https://doi.org/10.3109/21678421.2013.868001.

Oberheim, Nancy Ann, Takahiro Takano, Xiaoning Han, Wei He, Jane H.C. Lin, Fushun Wang, Qiwu Xu, et al. 2009. "Uniquely Hominid Features of Adult Human Astrocytes." *Journal of Neuroscience* 29 (10): 3276–87. https://doi.org/10.1523/JNEUROSCI.4707-08.2009.

Oberheim, Nancy Ann, Xiaohai Wang, Steven Goldman, and Maiken Nedergaard. 2006. "Astrocytic Complexity Distinguishes the Human Brain." *Trends in Neurosciences* 29 (10): 547–53. https://doi.org/10.1016/j.tins.2006.08.004.

*Obermeier, Birgit, Richard Daneman, and Richard M. Ransohoff. 2013. "Development, Maintenance and Disruption of the Blood-Brain Barrier." *Nature Medicine*. https://doi.org/10.1038/nm.3407.

Ogata, Katuya, and T. Kosaka. 2002. "Structural and Quantitative Analysis of Astrocytes in the Mouse Hippocampus." *Neuroscience* 113 (1): 221–33. https://doi.org/10.1016/S0306-4522(02)00041-6.

Olabarria, Markel, Harun N. Noristani, Alexei Verkhratsky, and José J. Rodríguez. 2010. "Concomitant Astroglial Atrophy and Astrogliosis in a Triple Transgenic Animal Model of Alzheimer's Disease." *Glia* 58 (7): 831–38. https://doi.org/10.1002/glia.20967.

Oliván, Sara, Ana Cristina Calvo, Amaya Rando, María Jesús Muñoz, Pilar Zaragoza, and Rosario Osta. 2014. "Comparative Study of Behavioural Tests in the SOD1G93A Mouse Model of Amyotrophic Lateral Sclerosis." *Experimental Animals* 64 (2): 147–53. https://doi.org/10.1538/expanim.14-0077.

Olsen, M. L., H. Higashimori, S. L. Campbell, J. J. Hablitz, and Harald Sontheimer. 2006. "Functional Expression of Kir4.1 Channels in Spinal Cord Astrocytes." *GLIA* 53 (5): 516–28. https://doi.org/10.1002/glia.20312.

Pan, L, Y Yoshii, A Otomo, H Ogawa, and Y Iwasaki. 2012. "Different Human Copper-Zinc Superoxide Dismutase Mutants, SOD1 G93A and SOD1 H46R , Exert Distinct Harmful Effects on Gross Phenotype in Mice." *PLoS ONE* 7 (3): 33409. https://doi.org/10.1371/journal.pone.0033409.

Papanikolaou, Maria, Anthony Lewis, and Arthur M. Butt. 2019. "Glial and Neuronal Expression of the Inward Rectifying Potassium Channel Kir7.1 in the Adult Mouse Brain." *Journal of Anatomy* 235 (5): 984–96. https://doi.org/10.1111/joa.13048.

Pardo, Andrea C., Victor Wong, Leah M. Benson, Margaret Dykes, Kohichi Tanaka, Jeffrey D. Rothstein, and Nicholas J. Maragakis. 2006. “Loss of the Astrocyte Glutamate Transporter GLT1 Modifies Disease in SOD1G93A Mice.” *Experimental Neurology* 201 (1): 120–30. https://doi.org/10.1016/j.expneurol.2006.03.028.

Park, Hyungju, Kyung Seok Han, Soo Jin Oh, Seonmi Jo, Junsung Woo, Bo Eun Yoon, and C. Justin Lee. 2013. “High Glutamate Permeability and Distal Localization of Best1 Channel in CA1 Hippocampal Astrocyte.” *Molecular Brain* 6 (1): 54. https://doi.org/10.1186/1756-6606-6-54.

Park, Joon Ha, Dae Won Kim, Tae Kyeong Lee, Cheol Woo Park, Young Eun Park, Ji Hyeon Ahn, Hyang Ah Lee, Moo Ho Won, and Choong Hyun Lee. 2019. “Improved HCN Channels in Pyramidal Neurons and Their New Expression Levels in Pericytes and Astrocytes in the Gerbil Hippocampal CA1 Subfield Following Transient Ischemia.” *International Journal of Molecular Medicine* 44 (5): 1801–10. https://doi.org/10.3892/ijmm.2019.4353.

Pasantes-Morales, H., R. A. Murray, R. Sanchez-Olea, and J. Moran. 1994. “Regulatory Volume Decrease in Cultured Astrocytes. II. Permeability Pathway to Amino Acids and Polyols.” *American Journal of Physiology - Cell Physiology* 266 (1 35-1). https://doi.org/10.1152/ajpcell.1994.266.1.c172.

*Pekny, Milos, and Marcela Pekna. 2016. “Reactive Gliosis in the Pathogenesis of CNS Diseases.” *Biochimica et Biophysica Acta - Molecular Basis of Disease* 1862 (3): 483–91. https://doi.org/10.1016/j.bbadis.2015.11.014.

*Pekny, Milos, Marcela Pekna, Albee Messing, Christian Steinhäuser, Jin Moo Lee, Vladimir Parpura, Elly M. Hol, Michael V. Sofroniew, and Alexei Verkhratsky. 2016. “Astrocytes: A Central Element in Neurological Diseases.” *Acta Neuropathologica*. Springer Verlag. https://doi.org/10.1007/s00401-015-1513-1.

Pellerin, Luc, and Pierre J. Magistretti. 1994. “Glutamate Uptake into Astrocytes Stimulates Aerobic Glycolysis: A Mechanism Coupling Neuronal Activity to Glucose Utilization.” *Proceedings of the National Academy of Sciences of the United States of America* 91 (22): 10625–29. https://doi.org/10.1073/pnas.91.22.10625.

Pérez-González, Adriana, and Annia Galano. 2011. “OH Radical Scavenging Activity of Edaravone: Mechanism and Kinetics.” *Journal of Physical Chemistry B* 115 (5): 1306–14. https://doi.org/10.1021/jp110400t.

Pessia, Mauro, Paola Imbrici, Maria Cristina D’Adamo, Lorena Salvatore, and Stephen J. Tucker. 2001. “Differential PH Sensitivity of Kir4.1 and Kir4.2 Potassium Channels and Their Modulation by Heteropolymerisation with Kir5.1.” *Journal of Physiology* 532 (2): 359–67. https://doi.org/10.1111/j.1469-7793.2001.0359f.x.

Petrou, Panayiota, Yael Gothelf, Zohar Argov, Marc Gotkine, Yossef S Levy, Ibrahim Kassis, Adi Vaknin-Dembinsky, et al. 2016. “Safety and Clinical Effects of Mesenchymal Stem Cells Secreting Neurotrophic Factor Transplantation in Patients With Amyotrophic Lateral Sclerosis: Results of Phase 1/2 and 2a Clinical Trials.” *JAMA Neurology* 73 (3): 337–44. https://doi.org/10.1001/jamaneurol.2015.4321.

Philips, Thomas, Andre Bento-Abreu, Annelies Nonneman, Wanda Haeck, Kim Staats, Veerle Geelen, Nicole Hersmus, et al. 2013. “Oligodendrocyte Dysfunction in the Pathogenesis of Amyotrophic Lateral Sclerosis.” *Brain* 136 (2): 471–82. https://doi.org/10.1093/brain/aws339.

Plant, Leigh D., Leandro Zuniga, Dan Araki, Jeremy D. Marks, and Steve A.N. Goldstein. 2012. “SUMOylation Silences Heterodimeric TASK Potassium Channels Containing K2P1 Subunits in

Cerebellar Granule Neurons." *Science Signaling* 5 (251). https://doi.org/10.1126/scisignal.2003431.

Pramatarova, Albéna, Janet Laganière, Julie Roussel, Katéri Brisebois, and Guy A. Rouleau. 2001. "Neuron-Specific Expression of Mutant Superoxide Dismutase 1 in Transgenic Mice Does Not Lead to Motor Impairment." *Journal of Neuroscience* 21 (10): 3369–74. https://doi.org/10.1523/JNEUROSCI.21-10-03369.2001.

Qu, Hong, Asta Håberg, Olav Haraldseth, Geirmund Unsgård, and Ursula Sonnewald. 2000. "13C MR Spectroscopy Study of Lactate as Substrate for Rat Brain." *Developmental Neuroscience* 22 (5–6): 429–36. https://doi.org/10.1159/000017472.

Rash, J. E., T. Yasumura, K. G.V. Davidson, C. S. Furman, F. E. Dudek, and J. I. Nagy. 2001. "Identification of Cells Expressing Cx43, Cx30, Cx26, Cx32 and Cx36 in Gap Junctions of Rat Brain and Spinal Cord." *Cell Communication and Adhesion* 8 (4–6): 315–20. https://doi.org/10.3109/15419060109080745.

Rash, John E., Heather S. Duffy, F. Edward Dudek, Brent L. Bilhartz, L. Ray Whalen, and Thomas Yasumura. 1997. "Grid-Mapped Freeze-Fracture Analysis of Gap Junctions in Gray and White Matter of Adult Rat Central Nervous System, with Evidence for a 'panglial Syncytium' That Is Not Coupled to Neurons." *Journal of Comparative Neurology* 388 (2): 265–92. https://doi.org/10.1002/(sici)1096-9861(19971117)388:2<265::aid-cne6>3.0.co;2-%23.

Ratté, Stéphanie, and Steven A. Prescott. 2011. "CLC-2 Channels Regulate Neuronal Excitability, Not Intracellular Chloride Levels." *Journal of Neuroscience* 31 (44): 15838–43. https://doi.org/10.1523/JNEUROSCI.2748-11.2011.

*Ratti, Antonia, and Emanuele Buratti. 2016. "Physiological Functions and Pathobiology of TDP-43 and FUS/TLS Proteins." *Journal of Neurochemistry*. https://doi.org/10.1111/jnc.13625.

Re, Diane B., Virginia Le Verche, Changhao Yu, Mackenzie W. Amoroso, Kristin A. Politi, Sudarshan Phani, Burcin Ikiz, et al. 2014. "Necroptosis Drives Motor Neuron Death in Models of Both Sporadic and Familial ALS." *Neuron* 81 (5): 1001–8. https://doi.org/10.1016/j.neuron.2014.01.011.

Redman, Patrick T., Kai He, Karen A. Hartnett, Bahiyya S. Jefferson, Linda Hu, Paul A. Rosenberg, Edwin S. Levitan, and Elias Aizenman. 2007. "Apoptotic Surge of Potassium Currents Is Mediated by P38 Phosphorylation of Kv2.1." *Proceedings of the National Academy of Sciences of the United States of America* 104 (9): 3568–73. https://doi.org/10.1073/pnas.0610159104.

Renton, Alan E., Elisa Majounie, Adrian Waite, Javier Simón-Sánchez, Sara Rollinson, J. Raphael Gibbs, Jennifer C. Schymick, et al. 2011. "A Hexanucleotide Repeat Expansion in C9ORF72 Is the Cause of Chromosome 9p21-Linked ALS-FTD." *Neuron* 72 (2): 257–68. https://doi.org/10.1016/j.neuron.2011.09.010.

Ringel, Florian, and Nikolaus Plesnila. 2008. "Expression and Functional Role of Potassium-Chloride Cotransporters (KCC) in Astrocytes and C6 Glioma Cells." *Neuroscience Letters* 442 (3): 219–23. https://doi.org/10.1016/j.neulet.2008.07.017.

Rinke, Ilka, Judith Artmann, and Valentin Stein. 2010. "ClC-2 Voltage-Gated Channels Constitute Part of the Background Conductance and Assist Chloride Extrusion." *Journal of Neuroscience* 30 (13): 4776–86. https://doi.org/10.1523/JNEUROSCI.6299-09.2010.

Rinné, Susanne, Vijay Renigunta, Günter Schlichthörl, Marylou Zuzarte, Stefan Bittner, Sven G. Meuth, Niels Decher, Jürgen Daut, and Regina Preisig-Müller. 2014. "A Splice Variant of the Two-Pore Domain Potassium Channel TREK-1 with Only One Pore Domain Reduces the Surface Expression of Full-Length TREK-1 Channels." *Pflugers Archiv European Journal of Physiology* 466 (8):

1559–70. https://doi.org/10.1007/s00424-013-1384-z.

*Robberecht, Wim, and Thomas Philips. 2013. “The Changing Scene of Amyotrophic Lateral Sclerosis.” *Nature Reviews Neuroscience*. https://doi.org/10.1038/nrn3430.

Robinson, Hannah K., Alexey V. Deykin, Evgeny V. Bronovitsky, Ruslan K. Ovchinnikov, Alexey A. Ustyugov, Tatyana A. Shelkovnikova, Michail S. Kukharsky, et al. 2015. “Early Lethality and Neuronal Proteinopathy in Mice Expressing Cytoplasm-Targeted FUS That Lacks the RNA Recognition Motif.” *Amyotrophic Lateral Sclerosis and Frontotemporal Degeneration* 16 (5–6): 402–9. https://doi.org/10.3109/21678421.2015.1040994.

Rosen, D R, T Siddique, D Patterson, D A Figlewicz, P Sapp, A Hentati, D Donaldson, J Goto, J P O’Regan, and H X Deng. 1993. “Mutations in Cu/Zn Superoxide Dismutase Gene Are Associated with Familial Amyotrophic Lateral Sclerosis.” *Nature* 362 (6415): 59–62. https://doi.org/10.1038/362059a0.

Rothstein, Jeffrey D., Margaret Dykes-Hoberg, Carlos A. Pardo, Lynn A. Bristol, Lin Jin, Ralph W. Kuncl, Yoshikatsu Kanai, et al. 1996. “Knockout of Glutamate Transporters Reveals a Major Role for Astroglial Transport in Excitotoxicity and Clearance of Glutamate.” *Neuron* 16 (3): 675–86. https://doi.org/10.1016/S0896-6273(00)80086-0.

Scekic-Zahirovic, Jelena, Oliver Sendscheid, Hajer El Oussini, Mélanie Jambeau, Ying Sun, Sina Mersmann, Marina Wagner, et al. 2016. “Toxic Gain of Function from Mutant FUS Protein Is Crucial to Trigger Cell Autonomous Motor Neuron Loss.” *The EMBO Journal* 35 (10): 1077–97. https://doi.org/10.15252/embj.201592559.

Schauwecker, P. E. 2002. “Modulation of Cell Death by Mouse Genotype: Differential Vulnerability to Excitatory Amino Acid-Induced Lesions.” *Experimental Neurology* 178 (2): 219–35. https://doi.org/10.1006/exnr.2002.8038.

Schauwecker, P. E., and O. Steward. 1997. “Genetic Determinants of Susceptibility to Excitotoxic Cell Death: Implications for Gene Targeting Approaches.” *Proceedings of the National Academy of Sciences of the United States of America* 94 (8): 4103–8. https://doi.org/10.1073/pnas.94.8.4103.

Schmitt, Angelika, Esther Asan, Bernd Püschel, and Peter Kugler. 1997. “Cellular and Regional Distribution of the Glutamate Transporter GLAST in the CNS of Rats: Nonradioactive in Situ Hybridization and Comparative Immunocytochemistry.” *Journal of Neuroscience* 17 (1): 1–10. https://doi.org/10.1523/jneurosci.17-01-00001.1997.

Schools, Gary P., Min Zhou, and Harold K. Kimelberg. 2006. “Development of Gap Junctions in Hippocampal Astrocytes: Evidence That Whole Cell Electrophysiological Phenotype Is an Intrinsic Property of the Individual Cell.” *Journal of Neurophysiology* 96 (3): 1383–92. https://doi.org/10.1152/jn.00449.2006.

Sellers, R. S., C. B. Clifford, P. M. Treuting, and C. Brayton. 2012. “Immunological Variation between Inbred Laboratory Mouse Strains: Points to Consider in Phenotyping Genetically Immunomodified Mice.” *Veterinary Pathology* 49 (1): 32–43. https://doi.org/10.1177/0300985811429314.

*Shah, Niyathi Hegde, and Elias Aizenman. 2014. “Voltage-Gated Potassium Channels at the Crossroads of Neuronal Function, Ischemic Tolerance, and Neurodegeneration.” *Translational Stroke Research* 5 (1): 38–58. https://doi.org/10.1007/s12975-013-0297-7.

Sharma, Aarti, Alexander K. Lyashchenko, Lei Lu, Sara Ebrahimi Nasrabady, Margot Elmaleh, Monica Mendelsohn, Adriana Nemes, Juan Carlos Tapia, George Z. Mentis, and Neil A. Shneider. 2016. “ALS-Associated Mutant FUS Induces Selective Motor Neuron Degeneration through Toxic Gain

of Function." *Nature Communications* 7 (1): 1–14. https://doi.org/10.1038/ncomms10465.

Shelkovnikova, Tatyana A., Owen M. Peters, Alexey V. Deykin, Natalie Connor-Robson, Hannah Robinson, Alexey A. Ustyugov, Sergey O. Bachurin, et al. 2013. "Fused in Sarcoma (FUS) Protein Lacking Nuclear Localization Signal (NLS) and Major RNA Binding Motifs Triggers Proteinopathy and Severe Motor Phenotype in Transgenic Mice." *Journal of Biological Chemistry* 288 (35): 25266–74. https://doi.org/10.1074/jbc.M113.492017.

Sík, A., R. L. Smith, and T. F. Freund. 2000. "Distribution of Chloride Channel-2-Immunoreactive Neuronal and Astrocytic Processes in the Hippocampus." *Neuroscience* 101 (1): 51–65. https://doi.org/10.1016/S0306-4522(00)00360-2.

Singer-Lahat, Dafna, Anton Sheinin, Dodo Chikvashvili, Sharon Tsuk, Dafna Greitzer, Reut Friedrich, Lori Feinshreiber, et al. 2007. "K+ Channel Facilitation of Exocytosis by Dynamic Interaction with Syntaxin." *Journal of Neuroscience* 27 (7): 1651–58. https://doi.org/10.1523/JNEUROSCI.4006-06.2007.

Sontheimer, H, E Fernandez-Marques, N. Ullrich, C A Pappas, and S. G. Waxman. 1994. "Astrocyte Na+ Channels Are Required for Maintenance of Na+/K+-ATPase Activity." *Journal of Neuroscience* 14 (5 I): 2464–75. https://doi.org/10.1523/jneurosci.14-05-02464.1994.

Stallings, Nancy R., Krishna Puttaparthi, Christina M. Luther, Dennis K. Burns, and Jeffrey L. Elliott. 2010. "Progressive Motor Weakness in Transgenic Mice Expressing Human TDP-43." *Neurobiology of Disease* 40 (2): 404–14. https://doi.org/10.1016/j.nbd.2010.06.017.

Stevens, Beth, Nicola J. Allen, Luis E. Vazquez, Gareth R. Howell, Karen S. Christopherson, Navid Nouri, Kristina D. Micheva, et al. 2007. "The Classical Complement Cascade Mediates CNS Synapse Elimination." *Cell* 131 (6): 1164–78. https://doi.org/10.1016/j.cell.2007.10.036.

Sufit, Robert L, Senda Ajroud-Driss, Patricia Casey, and John A Kessler. 2017. "Open Label Study to Assess the Safety of VM202 in Subjects with Amyotrophic Lateral Sclerosis." *Amyotrophic Lateral Sclerosis & Frontotemporal Degeneration* 18 (3–4): 269–78. https://doi.org/10.1080/21678421.2016.1259334.

Szade, Agata, Witold N Nowak, Krzysztof Szade, Anna Gese, Ryszard Czypicki, Halina Wav, Józef Dulak, and Alicja Józkowicz. 2015. "Effect of Crossing C57BL/6 and FVB Mouse Strains on Basal Cytokine Expression." https://doi.org/10.1155/2015/762419.

Takeuchi, Ryoko, Mari Tada, Atsushi Shiga, Yasuko Toyoshima, Takuya Konno, Tomoe Sato, Hiroaki Nozaki, et al. 2016. "Heterogeneity of Cerebral TDP-43 Pathology in Sporadic Amyotrophic Lateral Sclerosis: Evidence for Clinico-Pathologic Subtypes." *Acta Neuropathologica Communications* 4 (1): 61. https://doi.org/10.1186/s40478-016-0335-2.

Tanemoto, Masayuki, Nobuyoshi Kittaka, Atsushi Inanobe, and Yoshihisa Kurachi. 2000. "In Vivo Formation of a Proton-Sensitive K+ Channel by Heteromeric Subunit Assembly of Kir5.1 with Kir4.1." *Journal of Physiology* 525 (3): 587–92. https://doi.org/10.1111/j.1469-7793.2000.00587.x.

Taylor, J Paul, Robert H. Brown, and Don W Cleveland. 2017. "Decoding ALS: From Genes to Mechanism" 539 (7628): 197–206. https://doi.org/10.1038/nature20413.

Thiemann, Astrid, Stefan Gründer, Michael Pusch, and Thomas J. Jentsch. 1992. "A Chloride Channel Widely Expressed in Epithelial and Non-Epithelial Cells." *Nature* 356 (6364): 57–60. https://doi.org/10.1038/356057a0.

*Todd, Tiffany W., and Leonard Petrucelli. 2016. "Insights into the Pathogenic Mechanisms of Chromosome 9 Open Reading Frame 72 (C9orf72) Repeat Expansions." *Journal of Neurochemistry*

138 (August): 145–62. https://doi.org/10.1111/jnc.13623.

Tollervey, James R., Tomaž Curk, Boris Rogelj, Michael Briese, Matteo Cereda, Melis Kayikci, Julian König, et al. 2011. "Characterizing the RNA Targets and Position-Dependent Splicing Regulation by TDP-43." *Nature Neuroscience* 14 (4): 452–58. https://doi.org/10.1038/nn.2778.

Toomey, Russell B, and Kimberly J Mitchell. 2016. "Large-Scale Analysis of CRISPR/Cas9 Cell-Cycle Knockouts Reveals the Diversity of P53-Dependent Responses to Cell-Cycle Defects." *Developmental Cell* 51 (1): 87–100. https://doi.org/10.1037/a0038432.Latino.

Tu, Pang Hsien, Pramod Raju, Kathryn A Robinson, Mark E Gurney, John Q Trojanowski, and Virginia M.Y. Lee. 1996. "Transgenic Mice Carrying a Human Mutant Superoxide Dismutase Transgene Develop Neuronal Cytoskeletal Pathology Resembling Human Amyotrophic Lateral Sclerosis Lesions." *Proceedings of the National Academy of Sciences of the United States of America* 93 (7): 3155–60. https://doi.org/10.1073/pnas.93.7.3155.

Valiunas, V., Y. Y. Polosina, Holly Miller, I. A. Potapova, L. Valiuniene, S. Doronin, R. T. Mathias, et al. 2005. "Connexin-Specific Cell-to-Cell Transfer of Short Interfering RNA by Gap Junctions." *Journal of Physiology* 568 (2): 459–68. https://doi.org/10.1113/jphysiol.2005.090985.

Vance, Caroline, Boris Rogelj, Tibor Hortobágyi, Kurt J. De Vos, Agnes Lumi Nishimura, Jemeen Sreedharan, Xun Hu, et al. 2009. "Mutations in FUS, an RNA Processing Protein, Cause Familial Amyotrophic Lateral Sclerosis Type 6." *Science* 323 (5918): 1208–11. https://doi.org/10.1126/science.1165942.

Vance, Caroline, Emma L. Scotter, Agnes L. Nishimura, Claire Troakes, Jacqueline C. Mitchell, Claudia Kathe, Hazel Urwin, et al. 2013. "ALS Mutant FUS Disrupts Nuclear Localization and Sequesters Wild-Type FUS within Cytoplasmic Stress Granules." *Human Molecular Genetics* 22 (13): 2676–88. https://doi.org/10.1093/hmg/ddt117.

Verkhratsky, Alexei, and Maiken Nedergaard. 2018. "Physiology of Astroglia." *Physiological Reviews* 98 (1): 239–389. https://doi.org/10.1152/physrev.00042.2016.

Verkhratsky, Alexei, and Vladimir Parpura. 2015. "Physiology of Astroglia: Channels, Receptors, Transporters, Ion Signaling and Gliotransmission." *Colloquium Series on Neuroglia in Biology and Medicine: From Physiology to Disease* 2 (2): 1–172. https://doi.org/10.4199/C00123ED1V01Y201501NGL004.

*Verkhratsky, Alexei, Reno C. Reyes, and Vladimir Parpura. 2014. "TRP Channels Coordinate Ion Signalling in Astroglia." *Reviews of Physiology, Biochemistry and Pharmacology* 166 (June): 1–22. https://doi.org/10.1007/112_2013_15.

*Verkhratsky, Alexei, José J. Rodríguez, and Vladimir Parpura. 2012. "Calcium Signalling in Astroglia." *Molecular and Cellular Endocrinology*. https://doi.org/10.1016/j.mce.2011.08.039.

Võikar, Vootele, Sulev Kõks, Eero Vasar, and Heikki Rauvala. 2001. "Strain and Gender Differences in the Behavior of Mouse Lines Commonly Used in Transgenic Studies." *Physiology and Behavior* 72 (1–2): 271–81. https://doi.org/10.1016/S0031-9384(00)00405-4.

Walz, Wolfgang, and Melody K. Lang. 1998. "Immunocytochemical Evidence for a Distinct GFAP-Negative Subpopulation of Astrocytes in the Adult Rat Hippocampus." *Neuroscience Letters* 257 (3): 127–30. https://doi.org/10.1016/S0304-3940(98)00813-1.

Wang, Lijun, David H. Gutmann, and Raymond P. Roos. 2011. "Astrocyte Loss of Mutant SOD1 Delays ALS Disease Onset and Progression in G85R Transgenic Mice." *Human Molecular Genetics* 20 (2): 286–93. https://doi.org/10.1093/hmg/ddq463.

Wang, Wen Yuan, Ling Pan, Susan C. Su, Emma J. Quinn, Megumi Sasaki, Jessica C. Jimenez, Ian R.A. MacKenzie, Eric J. Huang, and Li Huei Tsai. 2013. "Interaction of FUS and HDAC1 Regulates DNA Damage Response and Repair in Neurons." *Nature Neuroscience* 16 (10): 1383–91. https://doi.org/10.1038/nn.3514.

Webster, Christopher P, Emma F Smith, Claudia S Bauer, Annekathrin Moller, Guillaume M Hautbergue, Laura Ferraiuolo, Monika A Myszczynska, et al. 2016. " The C9orf72 Protein Interacts with Rab1a and the ULK 1 Complex to Regulate Initiation of Autophagy ." *The EMBO Journal* 35 (15): 1656–76. https://doi.org/10.15252/embj.201694401.

Wilhelmsson, Ulrika, Eric A. Bushong, Diana L. Price, Benjamin L. Smarr, Van Phung, Masako Terada, Mark H. Ellisman, and Milos Pekny. 2006. "Redefining the Concept of Reactive Astrocytes as Cells That Remain within Their Unique Domains upon Reaction to Injury." *Proceedings of the National Academy of Sciences of the United States of America* 103 (46): 17513–18. https://doi.org/10.1073/pnas.0602841103.

Williams, Susan M., Robert K.P. Sullivan, Heather L. Scott, David I. Finkelstein, Paul B. Colditz, Barbara E. Lingwood, Peter R. Dodd, and David V. Pow. 2005. "Glial Glutamate Transporter Expression Patterns in Brains from Multiple Mammalian Species." *Glia* 49 (4): 520–41. https://doi.org/10.1002/glia.20139.

Woo, Dong Ho, Kyung Seok Han, Jae Wan Shim, Bo Eun Yoon, Eunju Kim, Jin Young Bae, Soo Jin Oh, et al. 2012. "TREK-1 and Best1 Channels Mediate Fast and Slow Glutamate Release in Astrocytes upon GPCR Activation." *Cell* 151 (1): 25–40. https://doi.org/10.1016/j.cell.2012.09.005.

Woo, Junsung, Joo Ok Min, Dae Si Kang, Yoo Sung Kim, Guk Hwa Jung, Hyun Jung Park, Sunpil Kim, et al. 2018. "Control of Motor Coordination by Astrocytic Tonic GABA Release through Modulation of Excitation/Inhibition Balance in Cerebellum." *Proceedings of the National Academy of Sciences of the United States of America* 115 (19): 5004–9. https://doi.org/10.1073/pnas.1721187115.

Wooley, Christine M, Roger B Sher, Ajit Kale, Wayne N Frankel, Gregory A Cox, and Kevin L Seburn. 2005. "Gait Analysis Detects Early Changes in Transgenic SOD1(G93A) Mice." *Muscle and Nerve* 32 (1): 43–50. https://doi.org/10.1002/mus.20228.

Wu, King Chuen, Chang Shin Kuo, Chia Chia Chao, Chieh Chen Huang, Yuan Kun Tu, Paul Chan, and Yuk Man Leung. 2015. "Role of Voltage-Gated K+ Channels in Regulating Ca2+ Entry in Rat Cortical Astrocytes." *Journal of Physiological Sciences* 65 (2): 171–77. https://doi.org/10.1007/s12576-015-0356-9.

Wu, Lien Szu, Wei-Cheng Cheng, Shin Chen Hou, Yu Ting Yan, Si Tse Jiang, and C.-K. K.James Shen. 2010. "TDP-43, a Neuro-Pathosignature Factor, Is Essential for Early Mouse Embryogenesis." *Genesis* 48 (1): 56–62. https://doi.org/10.1002/dvg.20584.

Xu, Ya Fei, Yong Jie Zhang, Wen Lang Lin, Xiangkun Cao, Caroline Stetler, Dennis W. Dickson, Jada Lewis, and Leonard Petrucelli. 2011. "Expression of Mutant TDP-43 Induces Neuronal Dysfunction in Transgenic Mice." *Molecular Neurodegeneration* 6 (1): 73. https://doi.org/10.1186/1750-1326-6-73.

Yamamoto, Y., T. Kuwahara, K. Watanabe, and K. Watanabe. 1996. "Antioxidant Activity of 3-Methyl-1-Phenyl-2-Pyrazolin-5-One." *Redox Report* 2 (5): 333–38. https://doi.org/10.1080/13510002.1996.11747069.

Yamanaka, Koji, Severine Boillee, Elizabeth A. Roberts, Michael L. Garcia, Melissa McAlonis-Downes, Oliver R. Mikse, Don W. Cleveland, and Lawrence S.B. Goldstein. 2008a. "Mutant SOD1 in Cell

Types Other than Motor Neurons and Oligodendrocytes Accelerates Onset of Disease in ALS Mice." *Proceedings of the National Academy of Sciences of the United States of America* 105 (21): 7594–99. https://doi.org/10.1073/pnas.0802556105.

Yamanaka, Koji, Seung Joo Chun, Severine Boillee, Noriko Fujimori-Tonou, Hirofumi Yamashita, David H. Gutmann, Ryosuke Takahashi, Hidemi Misawa, and Don W. Cleveland. 2008b. "Astrocytes as Determinants of Disease Progression in Inherited Amyotrophic Lateral Sclerosis." *Nature Neuroscience* 11 (3): 251–53. https://doi.org/10.1038/nn2047.

Yan, Yiping, Robert J. Dempsey, and Dandan Sun. 2001. "Expression of Na+-K+-Cl- Cotransporter in Rat Brain during Development and Its Localization in Mature Astrocytes." *Brain Research* 911 (1): 43–55. https://doi.org/10.1016/S0006-8993(01)02649-X.

Yang, Fan, and Jie Zheng. 2014. "High Temperature Sensitivity Is Intrinsic to Voltage-Gated Potassium Channels." *ELife* 3: e03255. https://doi.org/10.7554/eLife.03255.

Yang, Jehoon, Charles Q. Li, and Jun Shen. 2005. "In Vivo Detection of Cortical GABA Turnover from Intravenously Infused [1-13C]D-Glucose." *Magnetic Resonance in Medicine* 53 (6): 1258–67. https://doi.org/10.1002/mrm.20473.

Yoshida, Toru, Sara K. Goldsmith, Todd E. Morgan, David J. Stone, and Caleb E. Finch. 1996. "Transcription Supports Age-Related Increases of GFAP Gene Expression in the Male Rat Brain." *Neuroscience Letters* 215 (2): 107–10. https://doi.org/10.1016/0304-3940(96)12966-9.

Yu, A. C.H., J. Drejer, L. Hertz, and A. Schousboe. 1983. "Pyruvate Carboxylase Activity in Primary Cultures of Astrocytes and Neurons." *Journal of Neurochemistry* 41 (5): 1484–87. https://doi.org/10.1111/j.1471-4159.1983.tb00849.x.

Zhou, Chang, Cui Ping Zhao, Cheng Zhang, Guo Yong Wu, Fu Xiong, and Cheng Zhang. 2007. "A Method Comparison in Monitoring Disease Progression of G93A Mouse Model of ALS." *Amyotrophic Lateral Sclerosis* 8 (6): 366–72. https://doi.org/10.1080/17482960701538759.

Zhou, Min, and Harold K. Kimelberg. 2000. "Freshly Isolated Astrocytes from Rat Hippocampus Show Two Distinct Current Patterns and Different [K+](O) Uptake Capabilities." *Journal of Neurophysiology* 84 (6): 2746–57. https://doi.org/10.1152/jn.2000.84.6.2746.

Zhou, Min, Gary P. Schools, and Harold K. Kimelberg. 2006. "Development of GLAST(+) Astrocytes and NG2(+) Glia in Rat Hippocampus CA1: Mature Astrocytes Are Electrophysiologically Passive." *Journal of Neurophysiology* 95 (1): 134–43. https://doi.org/10.1152/jn.00570.2005.

Zinszner, Helene, John Sok, David Immanuel, Yin Yin, and David Ron. 1997. "TLS (FUS) Binds RNA in Vivo and Engages in Nucleo-Cytoplasmic Shuttling." *Journal of Cell Science* 110 (15): 1741–50.